RIEGO DEFICITARIO CONTROLADO DEL OLIVAR DE ALTA DENSIDAD:

PROGRAMACIÓN AUTOMÁTICA BASADA EN LA FISIOLOGÍA DE LA PLANTA.

Regulated deficit irrigation in a super high density olive orchard:
automatic scheduling based on the plant physiology.

Carmen M. Padilla Díaz

2018

TESIS DOCTORAL

Riego deficitario controlado del olivar de alta densidad: programación automática basada en la fisiología de la planta

Memoria que presenta

Dña. Carmen María Padilla Díaz

Para optar al título de Doctora por la Universidad de Sevilla

Sevilla, abril 2018

Universidad de Sevilla

Departamento de Cristalografía, Mineralogía y Química Agrícola

Programa de Doctorado Recursos Naturales y Medio Ambiente

Instituto de Recursos Naturales y Agrobiología de Sevilla (IRNAS-CSIC)

Universidad de Sevilla

Departamento de Cristalografía, Mineralogía y Química Agrícola

Programa de Doctorado Recursos Naturales y Medio Ambiente

Tesis Doctoral

Riego deficitario controlado del olivar de alta densidad: programación automática basada en la fisiología de la planta

Tesis Doctoral presentada por Dña. Carmen María Padilla Díaz, en satisfacción de los requisitos necesarios para optar al grado de Doctora en Biología, dirigida por Dr. José Enrique Fernández Luque y Dr. María Victoria Cuevas Sánchez (Instituto de Recursos Naturales y Agrobiología de Sevilla) y tutorada por Dr. Isabel González Díez (Dpto. Cristalografía, Mineralogía y Química Agrícola, Universidad de Sevilla).

LOS DIRECTORES

Dr. José Enrique Fernández Luque

Dr. María Victoria Cuevas Sánchez

EL TUTOR

Dr. Isabel González Díez

EL DOCTORANDO

Dña. Carmen María Padilla Díaz

University of Seville

Department of Crystallography, Mineralogy and Agricultural Chemistry
Doctoral Program in Natural Resources and Environment

Ph.D. Dissertation

Regulated deficit irrigation in a super high density olive orchard: automatic scheduling based on the plant physiology

Ph.D. Dissertation presented by Carmen María Padilla Díaz to fulfill the necessary requirements of the Doctor of Philosophy degree of Biology under the supervision of Dr. José Enrique Fernández Luque and Dr. María Victoria Cuevas Sánchez (Institute of Natural Resources and Agrobiology of Seville), and being advised by Dr. Isabel González Díez (Department of Crystallography, Mineralogy and Agricultural Chemistry, University of Seville).

THESIS SUPERVISORS

Dr. José Enrique Fernández Luque

Dr. María Victoria Cuevas Sánchez

THESIS ADVISOR

Dr. Isabel González Díez

Ph.D. CANDIDATE

Dña. Carmen María Padilla Díaz

FACULTAD DE QUÍMICA
Departamento de Cristalografía, Mineralogía y Química Agrícola

DRA. ISABEL GONZÁLEZ DÍEZ, DIRECTORA DEL PROGRAMA DE DOCTORADO EN RECURSOS NATURALES Y MEDIO AMBIENTE DE LA UNIVERSIDAD DE SEVILLA,

Certifica: que la presente Memoria de Investigación titulada "Riego deficitario controlado del olivar de alta densidad: programación automática basada en la fisiología de la planta", presentada por Dña. Carmen María Padilla Díaz para optar al grado de Doctora por la Universidad de Sevilla, ha sido realizada en el marco del Programa de Doctorado en Recursos Naturales y Medio Ambiente del Departamento de Cristalografía, Mineralogía y Química Agrícola.

En Sevilla, a 11 de abril de 2018.

DOCTOR JOSÉ ENRIQUE FERNÁNDEZ LUQUE, DIRECTOR DEL INSTITUTO DE RECURSOS NATURALES Y AGROBIOLOGÍA DE SEVILLA, DEL CONSEJO SUPERIOR DE INVESTIGACIONES CIENTÍFICAS,

Certifica: que la presente Memoria de Investigación titulada "Riego deficitario controlado del olivar de alta densidad: programación automática basada en la fisiología de la planta", presentada por Dña. Carmen María Padilla Díaz para optar al grado de Doctora por la Universidad de Sevilla, ha sido realizada en el Instituto de Recursos Naturales y Agrobiología de Sevilla (IRNAS-CSIC), bajo la dirección de los Drs. José Enrique Fernández Luque y María Victoria Cuevas Sánchez, reuniendo todas las condiciones exigidas a los trabajos de Tesis Doctoral.

En Sevilla, a 11 de abril de 2018.

Ms. Carmen María Padilla Díaz obtained a scholarship (BES-2013-065380) from the Spanish Ministry of Economy and Competitiveness for making her Ph.D. Thesis. The experimental part of this Thesis was made at the Institute of Natural Resources and Agrobiology of Seville, Spanish National Research Council (IRNAS-CSIC), within the frame of the Projects "*Regulated deficit irrigation of high density olive orchards: automatic scheduling based on plant physiology and the economics of the crop management*" and "*Physiological bases of the balance between the fruit load and the leaf area in olive hedgerow orchards*", a research projects of the Spanish Ministry of Economy and Competitiveness (references AGL2012-34544 and AGL2015-71585-R, respectively).

NOTE: The entire Thesis is written in English. The summary and the conclusions are also written in Spanish to fulfill the necessary requirements to obtain the "International Doctor" degree, under the Agreement 99/2011 (7.2/CG 17-6-11).

LIST OF WORKS DERIVED FROM THIS Ph.D. THESIS

Fernández, J.E., Diaz-Espejo, A., Romero, R., Hernandez-Santana, V., García, J.M., **Padilla-Díaz, C.M**., Cuevas, M.V., (2017) Precision irrigation in olive (*Olea europaea* L.) tree orchards. In: (I.F. García-Tejero and V-H. Durán, Eds.) Water Scarcity and Sustainable Agriculture in Semiarid Environment: Tools, Strategies, and Challenges for Woody Crops. *Elsevier*.

Padilla-Díaz C.M., Rodriguez-Dominguez C.M., Hernandez-Santana, V.,Perez-Martin A., Fernandes R.D.M., Montero A, García J.M., Fernández J.E. (2018) Water status, gas exchange and crop performance in a super high density olive orchard irrigated from leaf turgor measurements. *Agricultural Water Management*. 202, 241–252.

Padilla-Díaz C.M., Rodriguez-Dominguez C.M., Perez-Martin A., Montero A, García J.M., Fernández J.E. (2018) Scheduling a deficit irrigation strategy from leaf turgor measurements: impact on water status, gas exchange and oil yield. Acta Horticulturae. **Accepted**.

Fernandes, R.D.M., Cuevas, M.V., Hernandez-Santana, V., Rodriguez-Dominguez, C.M., **Padilla-Díaz, C.M.**, Fernández, J.E., (2017). Classification models for automatic identification of daily states from leaf turgor related measurements in olive. *Computers and Electronics in Agriculture*.

Fernández J.E., Cuevas M.V., Perez-Martin A., Rodriguez-Dominguez C.M., Hernandez-Santana V., Romero R., García J.M., Montero A., **Padilla-Díaz C.M**., Egea G., Alcon F., Pérez Ruiz M., I.F. García-Tejero, Diaz-Espejo A. (2017). New approaches for precise irrigation in hedgerow olive orchards. *Acta Horticulturae* **Accepted**.

Egea G**., Padilla-Díaz C.M.,** Martínez J., Fernández J.E., Pérez-Ruiz M. (2017). Assessing a crop water stress index derived from aerial termal imaging and infrared thermometry in super-high density olive orchards. *Agricultural Water Management*. 187: 210–221.

García-Tejero I.F., Hernández A., **Padilla-Díaz C.M**., Díaz-Espejo A., Fernández J.E. (2017) Assessing plant water status in an hedgerow olive orchard from thermography at plant level. Agricultural Water Management. 188: 50–60.

Padilla-Díaz C.M., Rodriguez-Dominguez C.M., Hernandez-Santana V., Perez-Martin A., Fernández J.E. (2016) Scheduling regulated deficit

irrigation in a hedgerow olive orchard from leaf turgor pressure related measurements. *Agricultural Water Management.* 164:28-37.

OTHER WORKS PUBLISHED DURING THIS PhD

De Baerdemaeker N.J.F., Ubeau, M. Szanne Degraeve, S., **Padilla-Díaz, C. M.,** […] Steppe K. 2018. The trident of xylem vulnerability to drought-induced cavitation: acoustic vulnerability, hydraulic capacitance and xylem anatomy. Tree Physiology. (Under review).

Torres-Ruiz J.M., Cochard H. , Choat B., Jansen S. , López R. ,Tomášková I. , **Padilla-Díaz C.M.** , Badel E., Burlett R., King A., Lenoir N., Martin-StPaul N.K., Delzon S. (2017) Xylem resistance to embolism: presenting a simple diagnostic test for the open vessel artefact. *New Phytologist*. 215: 489–499. Doi: 10.1111/nph.14589

Koenig W.D., Alejano R., Carbonero M.D., Fernández-Rebollo P., Knops J.M.H., Marañón T., **Padilla-Díaz C.M.**, Pearse I.S., Pérez-Ramos I.M., Vázquez-Piqué J., Pesendorfer M.B. (2016) Is the relationship between mast-seeding and weather in oaks related to their life-history or phylogeny? *Ecology,* 0(0), 2016, pp. 1–13 DOI: 10.1002/ecy.1490

Pérez-Ramos IM, **Padilla-Díaz CM**, Koenig W, Marañón T (2015) Environmental drivers of mast-seeding in Mediterranean oak species. Does leaf habit matter? *Journal of Ecology.* 103(3): 691–700. Doi: 10.1111/1365-2745.12400.

Marañón T, **Padilla-Díaz CM,** Pérez-Ramos IM, Villar R (2014) Investigación sobre ecología y gestión de las especies de *Quercus* frente al cambio global. *Ecosistemas 23*(2): 124-129 [Mayo-Agosto 2014] Doi.: 10.7818/ECOS.2014.23-2.16

Pérez-Ramos IM, Aponte C, García LV, **Padilla-Díaz CM**, Marañón T (2014) Why is seed production so variable among individuals? A ten-year study with oaks. *PLoS ONE* 9(12): e115371. doi:10.1371/journal.pone.0115371

SCIENTIFIC AWARDS DERIVED FROM THIS Ph.D. THESIS

Egea G, **Padilla-Díaz CM**, Martínez J, Fernández JE, Pérez-Ruiz M. Scientific Award Accesit, IV Premio José Humanes para el Desarrollo del Sector Oleícola y del Aceite [IV Award José Humanes for the development of the olive oil sector and industry] bestowed by Editorial Agrícola 2017, 23rd February 2017, Seville (Spain). Title of the award "Desarrollo de una metodología de Apoyo al Riego de Precisión del Olivar, basada en el Uso de la Termometría Infrarroja y Drones Agrícolas" [Development of a Methodology to Support Precision Irrigation of the Olive Orchard, based on the Use of Infrared Thermometry and Agricultural Drones]. Our work, developed during my PhD, was selected as the best cutting-edge technique for its application in a close future in irrigation scheduling of olive orchards.

Photographic Award "images for Science", ASECIC award. Title of photography "Haz de luz para el agua" [Light beam for water]. University of Cordoba (Spain). 6th April, 2015 (Scientific Photography). My awarded photography consisted in a microphotography of a xylem cross section of the olive tree taken with a light microscope during my short research-stay at University of Bordeaux (France).

He reducido el mundo a mi jardín,
y ahora veo la inmensidad
de todo lo que existe.

José Ortega y Gasset

A mi familia

CONTENTS

Chapter 1: Summary, Resumen, Introduction and Objectives 1

1. Summary 3
2. Resumen 7
3. Introduction 10
4. Objectives 12

Chapter 2: Scheduling regulated deficit irrigation in a hedgerow olive orchard from leaf turgor pressure related measurements 13

1. Introduction 15
2. Materials and methods Materials and methods 17
   2.1. Orchard characteristics and irrigation management 17
   2.2. Soil, plant and weather measurements 18
   2.3. Statistical analysis 20
3. Results 20
4. Discussion 29
5. Conclusions 31

Chapter 3: Water status, gas exchange and crop performance in a super high density olive orchard under deficit irrigation scheduled from leaf turgor measurements 33

1. Introduction 3
2. Materials and methods 37
   2.1. Orchard characteristics and irrigation management 37
   2.2. Soil, plant and weather measurements 39
   2.3. Growth and production measurements 40
   2.4. Statistical analysis 40
3. Results 41
   3.1. Water supplies, atmospheric demand and soil water content 41
   3.2. Plant water status versus leaf turgor related measurements 45
   3.3. Gas exchange, growth and production 49
4. Discussion 55
   4.1. Impact of the scheduling irrigation approach on crop physiology and crop performance 55

4.2. Suitability of the scheduling irrigation approach for commercial orchards 57
5. Conclusions 58

Chapter 4: Effect of fruit development on turgor related measurements in olive leaves 61
1. Introduction 63
2. Materials and methods 65
2.1. Orchard characteristics and irrigation management 65
2.2. Experimental setup and maximum turgor related measurements 66
2.3. Leaf-water relations 67
2.4. Pressure-volume curves 67
2.5. Leaf gas exchange measurements 68
2.6. Fruit dry weight and colour index 68
2.7. Statistical analysis 69
3. Results 70
3.1. Maximum turgor related measurements and the influence of fruit presence 70
3.2. Relationship between maximum turgor and environmental variables 70
3.3. Relationship between of maximum turgor and fruit development 73
3.4. Leaf-water relations and the influence of fruit presence 76
4. Discussion 79
4.1. Daily variations on maximum turgor: environmental components 79
4.2. Seasonal variations on maximum turgor: fruit influences 80
4.3. Future challenges 82
5. Conclusions 82
6. Supplementary material 83

Chapter 5: Leaf turgor under drought stress and leaf growth in olive 87
1. Introduction 89
2. Materials and methods 91
2.1. Plant material and experimental setup 91
2.2. Soil and meteorological measurements 91

2.3. Turgor and leaf thickness measurements....92
2.4. Plant-water relations and concomitant measurements....93
2.5. Pressure-volume curves....94
2.6. Statistical analysis....95
3. Results....95
3.1. Tree water deficit induced changes in leaf thickness and turgor measurements....95
3.2. Environmental drivers of turgor, leaf thickness and plant water status....98
3.3. Plant water relations as drivers of turgor and leaf thickness....102
4. Discussion....107
4.1. Environmental drivers of leaf growth and turgor....107
4.2. Internal plant water relations as drivers of turgor....108
4.3. Meaning of turgor in the plant water relations as drivers of growth 110
4.4. Future perspectives....110
5. Conclusions....112
6. Supplementary material....113

Chapter 6: General discussion....115

Chapter 7: Conclusions....121
Conclusions....123
Conclusiones....125

References....127

Chapter 1

Summary, Resumen, Introduction and Objectives

1. SUMMARY

The geographical distribution of olive (*Olea europaea* L.) is mainly in areas of Mediterranean climate, where arid and semi-areas are common. Although olive trees are well adapted to dry conditions, their response to water supply is remarkable. This explains that ca. 20% of the olive cropped area is irrigated. Also, and as for many other fruit tree species, management systems with high plant densities are becoming common. Those changes are justified by the economic value of olive products. Both agronomical approaches have the advantage of contributing to facing the challenge of producing olive fruits and olive oil for the increasing global population. This is particularly important in olive growing areas, for which rising temperatures and lower precipitations are forecasted. Increasing crop water productivity per unit of cropped land is, in fact, a main challenge to olive growers. In this context, one of the most effective responses of the scientific community is the development of new irrigation strategies and reliable tools for monitoring plant water stress and scheduling irrigation. Hedgerow olive orchards with high plant densities (from 1.500 trees ha^{-1}), or super high density (SHD) olive orchards, are considered to be among the most productive management systems for olive. On the other hand, irrigation supplies are required for an acceptable profitability in those orchards, precisely because of the high plant densities. One of the most promising irrigation strategies for SHD olive orchards is regulated deficit irrigation (RDI), which leads to significant water savings at the same time that episodes of excessive water stress are avoided when the crop is most sensitive to drought.

In 2014 and 2015, the first two years of this Ph.D. work, we focused on the feasibility of scheduling a RDI strategy supplying 45% of the crop irrigation needs (45RDI), designed for SHD olive orchards, from the shape of the daily curves recorded with ZIM sensors. These curves are related to leaf turgor pressure. We worked in a commercial, fully productive 'Arbequina' olive orchard with 1667 trees ha^{-1}. In addition to a treatment consisting on applying the mentioned 45RDI strategy, we had a 45RDI treatment scheduled by the crop coefficient approach and a full irrigation treatment (FI), consisting on daily irrigation to replace the crop water needs. Our results show that we were able to schedule irrigation just from the visual analysis of the curves derived from ZIM outputs (i.e. P_p values), without any further data processing. A comparison with the crop coefficient approach showed that, on the tree water status, maximum daily values of gas exchange, number of internodes in current-year shoots, leaf area, oil accumulation in the fruits, growth, fruit and oil yield were similar between treatments. With our approach also, we achieved over 50 % water savings with a negligible impact on yields, as compared to the FI treatment. However, caution must be taken when extrapolating our findings, since there is evidence from the literature on the relations between the tree water status and the shape of the daily curves recorded with the ZIM probes, depending on cultivar and main orchard conditions.

The second two years, 2016 and 2017, we carried out two experiments to increase our understanding of the interaction between the environmental conditions and plant mechanisms influencing turgor related measurements from the ZIM probes. Our purpose was to unravel the plant-based responses of the ZIM probes readings, with the aim of deriving new indicators for scheduling irrigation from the ZIM records. We explored the suitability of using the maximum daily turgor (P_{pmin}) for irrigation scheduling, as a reliable indicator that could be independent from both the cultivar and orchard conditions. The experiment was made in the same orchard mentioned above, but with FI trees only. Basically, we explored the influence of the proximity of fruits to leaves instrumented with ZIM probes, as well as the effect of leaf ageing, soil water availability and vapour pressure deficit. Our data showed no influence of the proximity of fruits on P_{pmin} records, suggesting that P_{pmin} readings can be made in any leaf regardless of being close or far from a cluster of fruits. Moreover, the increase on the elastic modulus with leaf ageing did not have an influence on P_{pmin} either. However, there was a clear effect of two main drivers of transpiration. Thus, daily patterns of P_{pmin} were mainly influenced by the atmospheric demand followed, to a lesser extent, by the available soil water. The pattern of P_{pmin} changed depending on the fruit developmental stage. Two stages were found to have a clearer influence: maximum rate of pit hardening and rapid fruit growth after the midsummer period. Out data supports P_{pmin} being a sensitive and reliable water stress indicator on those periods when the plant water status may have a marked effect on fruit production.

Plant-based sensors have the advantage of using the tree as a biosensor. i.e. their records inform on the plant response to the soil and atmospheric water status. Thus, those sensors are particularly useful for irrigation scheduling. However, their records are not always easy to interpret, due to both the complexity of the soil-water-plant-atmosphere relationships and the adaptive responses of the species to water stress. Therefore, a greater understanding of the actual meaning of plant-based measurements for assessing water stress is needed, to increase the acceptance of plant-based measurements in commercial orchards. The fourth experiment of this doctoral thesis was made with that aim. We used 2-year old, potted olive plants growing in a greenhouse in which climate conditions mimicked those typical of Mediterranean areas. We installed ZIM probes and leaf thickness sensors in representative plants with the aim of determining the threshold levels of main water-environmental drivers of leaf turgor and leaf thickness. In our experiments we considered plants under water-stress and recovery cycles, and fully irrigated plants for control. We also studied changes in cell wall properties, from pressure-volume curves. The hydraulic processes that evolve the combination of leaf turgor, thickness and plant water status along the continuum soil-plant-atmosphere were dependent on field capacity, as a threshold of soil water availability and, to a lesser extent, on the vapour pressure deficit of the air. Under severe drought stress the properties of the cell walls changes and the inversion of the daily P_p curve occurred. The latter, attributed to the accumulation of air in the leaf tissues, had similar dynamics as the leaf thickness measurements. This suggests that the ZIM probe measures a variable related to leaf thickness during the inversion of the

daily P_p curve. This finding opens new possibilities for improving irrigation scheduling in periods when the olive tree is less sensitive to drought stress. This fills a gap previously identified by our own results, on the reliability of using ZIM records to schedule irrigation in periods of the growing cycle when the 45RDI strategy advices for reducing water supplies below the crop water requirements.

2. RESUMEN

La distribución geográfica del olivo (*Olea europaea* L.) se encuentra principalmente en áreas con clima Mediterráneo donde áreas áridas y semiáridas son bastante frecuentes. A pesar de que el olivo es una especie que está bien adaptada a condiciones de escasez hídrica, su respuesta ante aportaciones de riego es destacable. Esto explica por qué ca. 20% de los olivares cultivados son de regadío. Del mismo modo que ocurre para muchas otras especies frutales, son cada vez más frecuentes los marcos de plantación con una densidad de árboles elevada. Estos cambios se justifican por el valor económico de los productos derivados del olivo. Ambas estrategias agronómicas contribuyen a hacer frente al reto de obtener una mayor producción de aceitunas y aceite de oliva de cara al aumento de la población mundial. Esto es particularmente importante en las áreas de cultivo del olivo, en las cuales se prevé un incremento de las temperaturas junto a una disminución en las precipitaciones. De hecho, el incremento de la productividad del agua por unidad de área cultivada es uno de los mayores retos a los que se enfrentan los olivicultores. En este contexto, una de las respuestas más efectivas de la comunidad científica ha sido el desarrollo de nuevas estrategias de riego y de herramientas fiables tanto para la programación del riego como para la monitorización del estrés hídrico en plantas. Los olivares en seto con alta densidad de plantas (a partir de 1.500 árboles ha^{-1}), también llamados olivares en seto de alta densidad, son considerados como los más productivos entre los distintos tipos de manejo que existen en el cultivo del olivar. Por otro lado, precisamente porque son de elevada densidad, se requieren aportes de riego para que estas plantaciones tengan una rentabilidad aceptable. Una de las estrategias de riego más prometedoras para este tipo de plantaciones es la aplicación del riego deficitario controlado (RDC), que permite ahorros de agua considerables al mismo tiempo que se evitan episodios de estrés hídrico excesivo en los momentos en los que el cultivo es más sensible a la sequía.

En 2014 y 2015, los dos primeros años de esta tesis doctoral, nos centramos en el estudio de la idoneidad de la estrategia de RDC aplicando un 45% de las necesidades de riego del cultivo (45RDC; 45RDI a lo largo de esta tesis en inglés), estrategia especialmente diseñada para olivares en seto de alta densidad, basada en la forma de las curvas diarias registradas con las sondas ZIM. Estas curvas están relacionadas con la presión de turgencia de la hoja. Trabajamos en una finca comercial y totalmente productiva de la variedad Arbequina con 1667 árboles ha^{-1}. Además de este tratamiento consistente en la aplicación de la mencionada estrategia 45RDC, tuvimos un tratamiento 45RDC programado mediante el coeficiente del cultivo junto a otro tratamiento donde las plantas se encontraban bien regadas (FI, del inglés *full irrigated*), el cual consistió en un riego diario que reemplazaba las necesidades de hídricas del cultivo. Nuestros resultados muestran que fuimos capaces de programar el riego tan solo con el análisis visual de las curvas derivadas de las lecturas de las sondas ZIM (i.e. valores de P_p) sin ningún tipo de tratamiento de datos posterior. Una comparativa de nuestra aproximación con la aproximación del método del coeficiente del cultivo mostró que, tanto el estado hídrico de

la planta, como valores máximos diarios de intercambio gaseoso, número de entrenudos en los ramos de años, área foliar, acumulación de aceite en los frutos, crecimiento y producción tanto de aceitunas como de aceite fueron similares entre tratamientos. Con nuestra estrategia 45RDC obtuvimos ahorros de agua de más del 50%, con un descartable impacto en la producción comparado con el tratamiento FI. Sin embargo, se debe tener precaución al extrapolar nuestros resultados, ya que hay evidencias en la literatura de que las relaciones entre el estado hídrico de la planta y la forma de las curvas diarias registradas por las sondas ZIM dependen de la variedad del cultivo y de las condiciones de la plantación.

En los dos segundos años, 2016 y 2017, llevamos a cabo dos experimentos para profundizar en el conocimiento sobre las interacciones que se dan entre las condiciones ambientales y los mecanismos de las plantas que influyen en la turgencia y que están relacionados con las medidas de las sondas ZIM. Nuestro propósito fue desentrañar las respuestas basadas en la planta de las lecturas de las sondas ZIM, con el propósito de derivar nuevos indicadores para la programación del riego desde dichas lecturas. Exploramos la idoneidad del uso de la máxima turgencia (P_{pmin}) para la programación del riego, como un indicador fiable que pudiera ser interpretado independientemente de la variedad de cultivo y de las condiciones de cada finca. El experimento se llevó a cabo en la finca mencionada anteriormente, pero únicamente bajo el tratamiento FI. Básicamente, exploramos la influencia de la proximidad de frutos a hojas instrumentadas con las sondas ZIM, así como también el efecto del envejecimiento de la hoja, la disponibilidad de agua en el suelo y el déficit de presión de vapor. Nuestros datos mostraron que no hubo una influencia en la proximidad de frutos sobre las lecturas de P_{pmin} sugiriendo que éstas podrían ser usadas para cualquier hoja independientemente de si está cerca o lejos de un racimo de frutos. Además, el incremento del módulo de elasticidad con la edad de la hoja tampoco tuvo ninguna influencia en la lectura de P_{pmin}. Sin embargo, sí hubo un claro efecto de las dos principales variables motoras de la transpiración. De este modo, los patrones diarios de P_{pmin} estuvieron principalmente influenciados por la demanda atmosférica seguidos, en menor medida, de la disponibilidad hídrica en el suelo. El patrón de P_{pmin} cambió dependiendo del estadío de desarrollo del fruto. Se encontraron dos fases del desarrollo que tuvieron una influencia más evidente: la tasa máxima de endurecimiento del hueso y el de rápido crecimiento del fruto que se produce a fínales de la segunda mitad del verano. Nuestros datos apoyan al P_{pmin} como un indicador sensible y fiable del estrés hídrico en aquellos periodos en los que el estado hídrico de la planta puede tener una marcada influencia en la producción del fruto.

Los sensores basados en medidas directas sobre la planta (*plant-based methods*, en inglés) tienen la ventaja de usar la propia planta como un biosensor, es decir, con sus registros informan de la respuesta de la planta al estado hídrico atmosférico y del suelo al mismo tiempo. Por tanto, estos sensores son particularmente útiles en la programación del riego. No obstante, los registros no son siempre fáciles de interpretar debido a la complejidad de las relaciones suelo-agua-planta-atmósfera y a la respuesta adaptativa de las especies al estrés hídrico. Así mismo, se necesita una mejor comprensión del

significado real de las medidas en planta para evaluar el estrés hídrico y así aumentar la aceptación del uso de este tipo de medidas para la gestión del riego en fincas comerciales El cuarto experimento de esta tesis doctoral se llevó a cabo con este propósito. Para ello usamos plantones de dos años de edad cultivados en invernadero, imitando las condiciones típicas de áreas mediterráneas. Se instalaron sensores ZIM y sensores de grosor de hoja en plantas representativas con el objeto de determinar los valores umbrales de las principales variables ambientales hídricas como motores de la turgencia y del grosor de la hoja. En nuestros experimentos, consideramos plantas sometidas a estrés hídrico con ciclos de recuperación y plantas bien regadas como control. También, estudiamos los cambios en las propiedades hídricas de la pared celular de la hoja a partir de curvas de presión-volumen. Los procesos hidráulicos que envuelven la combinación de la turgencia de la hoja, el grosor de la misma y el estado hídrico de la planta a lo largo del continuo suelo-planta-atmósfera dependieron de la capacidad de campo, siendo esta última un umbral de la disponibilidad hídrica del suelo y, en menor medida, el déficit de presión de vapor del aire. Bajo estrés hídrico severo, las propiedades de las paredes celulares de la hoja cambiaron y tuvo lugar la inversión de la curva P_p diaria. Esta última, atribuida a la acumulación de aire en los tejidos de la hoja, presentó una dinámica similar a las medidas del grosor de la hoja. Esto sugiere que la sonda ZIM mide una variable relacionada con el grosor de la hoja durante la inversión de la curva diaria de P_p. Estos resultados, por tanto, abren nuevas posibilidades para la mejora en la programación del riego en los periodos en los que el olivo es menos sensible al estrés hídrico. Esto, resuelve las carencias en el conocimiento previamente identificadas en nuestros resultados, con la fiabilidad de usar los registros por las sondas ZIM para la programación del riego a lo largo de todo el periodo de crecimiento del olivo siguiendo las recomendaciones de la estrategia 45RDC, reduciendo las cantidades de riego aplicadas por debajo de las necesidades hídricas del cultivo.

3. INTRODUCTION

It is widely recognized that the olive tree (*Olea europaea* L.) is one the most symbolic species of the Mediterranean Basin due to its ecological, cultural, and economical relevance (Kaniewski et al., 2012). The native or wild distribution of olive is concentred around Mediterranean Basin. In the eastern of Mediterranean Basin, about 6,000 years ago the domestication or cultivation of the olive tree (Zohary et al.; 2012) was being developed and spreading either from Cyprus, Anatolia, Crete and Egypt towards the western of Mediterranean by Phoenicians, Greeks and later by Romans (Baldoni et al., 2006; Breton et al., 2006). Nowadays, Spain, Tunisia, Italy and Morocco are the largest areas in the world dedicated for its growing (Data from FAO, 2016; http://faostat.fao.org) and also, most of the total olive oil is being produced in such areas. However, currently it is widely spread around the world too but particularly in areas with Mediterranean climate, i.e. mild winters with torrential precipitations and hottest summers with scant and irregular precipitations, as the best growing conditions for the olive.

Although olive trees are well adapted to Mediterranean drought conditions (Fernández 2014a), their response to water supply is remarkable. Nowadays there is an ongoing replacement of the traditional rainfed olive-groves by orchards with irrigation systems as well as a higher number of trees per hectare. Arguably, those changes were due to modernisation of agricultural machinery and are justified by the high economic value of the olive products. These explain that ca. 20% of the olive cropped area is irrigated.

In addition, the world population is expected to increase 1:3 before 2050 (FAO 2009). In this period, rising temperatures and lower precipitation is forecasted for Mediterranean areas (IPCC, 2014). Both agronomical approaches (i.e. irrigation and high plant densities) have the advantage of contributing to facing the challenge of producing olive fruits and olive oil for the increasing global population. This is particularly important in olive growing areas, for which rising temperatures and lower precipitations are forecasted. Increasing crop water productivity per unit of cropped land is, in fact, a main challenge to olive growers. In this context, one of the most effective responses of the scientific community is the development of new irrigation strategies and reliable tools for monitoring plant water stress and scheduling irrigation (Iniesta et al., 2009; Martín-Vertedor et al., 2011; Gomez-del-Campo, 2013; Fernández 2014a).

Among the tools for monitoring the plant water stress are plant-based sensors which also are widely used for irrigation scheduling. Plant-based sensors are located directly on the plant and have the advantage of using the tree as a biosensor. i.e. their records inform on the plant response to the soil and atmospheric water status. Thus, those sensors are particularly useful for irrigation scheduling. However, their records are not always easy to interpret, due to both the complexity of the soil-water-plant-atmosphere relationships and the adaptive responses of the species to water stress. Therefore, a greater understanding of the actual meaning of plant-based measurements for assessing water stress is needed, to increase the acceptance of plant-based measurements in commercial orchards. There is needed to carry on experiments under controlled climatic conditions

which allow us to comprehend the physiological mechanisms that are under the signals of the sensors for its implementation in the olive orchards.

The most suitable irrigation strategies for arid and semi-arid areas are deficit irrigation (DI) strategies designed for the crop and environment conditions. These are widely used in olive, a typical crop in these areas (Rallo et al. 2016). Hedgerow olive orchards with high plant densities (from 1.500 trees ha^{-1}), or super high density (SHD) olive orchards, are considered to be among the most productive management systems for olive. On the other hand, irrigation supplies are required for an acceptable profitability in those orchards, precisely because of the high plant densities. To control the frequency and irrigation amounts, i.e. irrigation strategies, according to plant water needs in SHD olive orchards is needed to extend the timespan at the fully productive and also to enable water savings (Fernandez 2014b). Deficit irrigation is specially required in hedgerow orchards with high plant densities, or super high density (SHD) orchards, where excessive growth must be avoided by controlling water and fertilizer supplies. For those orchards, regulated deficit irrigation (RDI) has been reported as one of the best DI strategies (Fernández et al. 2013; Fernández 2014b).

After several experiments at the Sanabria orchard, a commercial SHD 'Arbequina' orchard near Seville, southwest Spain (Fernández et al., 2013, 2017), our group recommends the 45RDI strategy for SHD olive orchards in the area, and in many other olive growing areas of similar characteristics. The 45RDI strategy consists on irrigating daily with to replace 100% of irrigation needs (IN) in three periods of the annual growing cycle. These periods, named as Periods 1, 2 and 3, are those in which olive is most sensitive to water stress. In between those periods, one or two irrigation events per week are applied, with a total water supply, for the considered period, from 15 to 30% of IN, depending of the time of the year. The total water supply, for the whole season, in this 45RDI strategy is aimed at 45% of IN. The successful application of any RDI strategy requires effective irrigation scheduling. In our group we have tested different water stress indicators and related systems to schedule irrigation, based on sap flow, trunk diameter variations and leaf turgor related measurements (Fernández 2014a). Among them, the ZIM system, which uses the leaf patch clamp pressure probe (LPCP probe) (Zimmermann et al., 2008**)** has been proved to be useful to schedule the 45RDI irrigation strategy in our SHD olive orchard (Fernández et al., 2011; Fernández 2014a).

To these reasons the main purpose of this PhD was to validate of the use of the indicators for irrigation scheduling derived from the turgor related measurements in a commercial olive orchard under a 45RDI along two years of experiment that will be described in the Chapters 2 and 3. Moreover, to getting deeper in the fundamental understanding of the interaction between the environmental and plant mechanisms that drive turgor measurements to implement new indicators for irrigation scheduling will be further developed in the Chapters 4 and 5.

4. OBJECTIVES

- To validate and corroborate the usefulness of the methodology based on ZIM system of two years of the irrigation scheduling
- To test the influence among two years in plant water status (water potential, stomatal conductance and net photosynthesis) as well as vegetative growth (number of internodes and leaf area) and production. We found that no differences between $45RDI_{CC}$ and $45RDI_{TP}$ for any variable studied of both years.
- To unravel the role of the proximity of fruits to the leaf on the maximum daily turgor.
- Due to the complex relations between leaves and fruits, acting this last one as sinks and sources of water and carbon, and their potential effect on the maximum turgor, the aim was to test the influence of the location of the fruit as well as its development on the leaf monitored by ZIM probe
- To determine, from the combined use of ZIM probes and LS sensors, the threshold level of leaf turgor that is driving leaf thickness growth and changes in cell wall properties using pressure-volume curves under the influence of drought stress.
- To determine the threshold levels of water-environmental drivers, and the impact of drought stress, of leaf turgor, and leaf turgor as a driver of leaf growth.

Chapter 2

Scheduling regulated deficit irrigation in a hedgerow olive orchard from leaf turgor pressure related measurements

1. INTRODUCTION

In most olive orchards irrigation is required to achieve an acceptable profitability (Gucci et al., 2012). When the purpose of supplying water is not only to increase yield, but also to raise water productivity, to control vigour and to improve fruit and oil quality, irrigation scheduling becomes a challenge. In addition to a deep knowledge of the crop physiology related to water use, precise irrigation requires effective tools for monitoring water stress. Our understanding of both the olive adaptation to water stress and its response to irrigation has improved substantially in the last decades, as summarized in reviews such as those by Connor and Fereres (2005), Sanzani et al. (2012) and Fernández (2014a). In parallel, advances on electronics and data transmission have allowed a development of systems for the automatic and continuous monitoring of water stress in fruit tree orchards, including olive (Zimmermann et al., 2008; Fernández et al., 2008; Ortuño et al., 2010). Combined with remote imagery of the whole orchard (Zarco-Tejada et al., 2009; Gonzalez-Dugo et al., 2013), some of these systems have proven to possess a high potential for scheduling irrigation in commercial orchards (Fernández 2014b).

Olive orchards with plant densities over 1500 trees ha^{-1}, also called super-high-density (SHD) olive orchards (Vossen et al., 2004), are especially sensitive to irrigation supplies. If those are too low, not only crop performance but also the productive life of the orchard can be reduced. If irrigation supplies are too high, tree vigour can be excessive, making mechanical harvesting difficult (León et al., 2007) and decreasing the long-term crop performance from heterogeneous light distribution around the canopy (Connor et al., 2009; Gómez-del-Campo et al., 2009). In addition, both fruit and oil quality are affected by irrigation management (Morales-Sillero et al., 2008; Gomez-Rico et al., 2009; García et al., 2013). Current knowledge shows that a regulated deficit irrigation (RDI) strategy together with an effective system to monitor the tree water stress could be the best approach for an effective irrigation management in SHD olive orchards (Gómez-del-Campo, 2013; Fernández et al., 2013).

The suitability of different irrigation strategies for olive orchards, including RDI, has been addressed by various authors (Grattan et al., 2006; Pastor et al., 2007; Proietti et al., 2012; Fernández et al., 2013). For the monitoring of water stress, recent efforts have focused mainly on plant-based sensors with data transmission systems that allow automatic and continuous recording of main physiological variables related to the tree water status. This is the case for sap flow (Fernández et al., 2008; Ramos and Santos, 2009; Rousseaux et al., 2009), trunk diameter (Pérez-López et al., 2008; Moriana et al., 2010; Cuevas et al., 2010) and leaf turgor (Zimmermann et al., 2008; Ache et al., 2010; Fernández et al., 2011). Details on the required characteristics of any plant-based sensor to schedule irrigation are given in Fernández and Cuevas (2010). Recently, Fernández (2014b) assessed the applicability of systems based on sap flow, trunk diameter and leaf turgor related measurements to monitor water stress and to schedule irrigation in commercial orchards. They concluded that the success of any of these methods relies, among other things, on the possibility of deriving a user-friendly water stress index from the collected records.

In the assessment by Fernández (2014b), the ZIM system (YARA ZIM Plant Technology, Hennigsdorf, Germany), which provides information on the leaf turgor pressure (P_c), was considered as one of the most promising systems to schedule irrigation in commercial olive orchards. In addition to being sensitive and reliable, as well as robust enough for working under field conditions for long periods, the ZIM system provides a user friendly water stress index, suitable for deriving irrigation decisions just from the visual analysis of the raw outputs. The potential of the index to schedule irrigation in a SHD olive orchard was first tested by Fernández et al. (2011). Basically, the ZIM system uses the leaf patch clamp pressure probe, or ZIM probe (Zimmermann et al., 2008), together with transmission data systems for the user to access to the collected information through any computer, tablet or smartphone connected to the Internet.

The ZIM probe measures the leaf patch output pressure (P_p), which is inversely coupled with P_c. For trees with abundant water supply, daily P_p curves show maximum values during the day, when P_c decreases because of transpiration, and minimum values at night, during leaf rehydration after stomatal closure. For trees under water stress conditions, however, the shape of the curve changes. Fernández et al. (2011) observed, in 'Arbequina' olive trees, half-inversed and completely inversed diurnal P_p curves when values of midday stem water potential (Ψ_{stem}) dropped below *ca.* −1.7 MPa. The shape of the curves became back to normal a few days after rewatering, the number depending on the level of water stress previously reached. Fernández et al. (2011) made concomitant measurements of P_p and leaf and stem water potential (Ψ_{stem}) recorded with a Scholander-type pressure chamber, and mentioned three States, 1 to 3, according to the shape of the diurnal P_p curve recorded in olive trees under increasing water stress. In a joint work between the research groups of Zimmermann and Fernández, the three States were further defined for olive (Ehrenberger et al., 2012). In State 1 (low stress) the P_p curve showed maximum values during the day and minimum values at night. This was typical of leaves close to maximum turgor ($P_c >> 50$ kPa), in trees with $\Psi_{stem} > -1.2$ MPa. In State 2 (moderate water stress, $P_c \approx 50$ kPa, -1.2 MPa $> \Psi_{stem} > -1.7$ MPa) P_p values started to increase from early morning, decreased for some time on the central hours of the day and recovered in the afternoon. In State 3 (severe water stress, $P_c << 50$ kPa, $\Psi_{stem} < -1.7$ MPa) the P_p curve was fully inversed, with minimum values during the day and maximum values at night. The work of Fernández et al. (2011) refers, however, to a single year, and measurements were made on young trees (4 years old) only. That by Ehrenberger et al. (2012) was also made with young olive plants, in this case potted plants. Our first hypothesis is that the relation between the State shown by P_p curves and the ranges of tree water stress established according to Ψ_{stem} values also holds for mature, fully productive olive trees. Taking into account that the water stress levels at which the P_p curve changes from State 1 to Sate 2 (-1.2 MPa) and from State 2 to State 3 (-1.7 MPa) are close to reference threshold levels of water stress in olive (Moriana et al., 2010; 2012), and that the change in State is a visual indicator, easy to use by farmers without specific training, our second hypothesis is that such indicator can be used to schedule regulated deficit irrigation in commercial SHD olive orchards.

The aims of this work were (i) to prove whether the correspondence between States 1, 2 and 3 of the P_p curves and the Ψ_{stem} threshold levels reported by Fernández et al. (2011) and Ehrenberger et al. (2012) holds for mature, fully productive olive trees, and (ii) to evaluate the suitability of an irrigation scheduling approach based on changes among States 1 and 3 to schedule regulated deficit irrigation in a super-high-density olive orchard.

2. MATERIALS AND METHODS

2.1. Orchard characteristics and irrigation management

The experiments were made in 2013 and 2014, in the same super-high-density olive (*Olea europaea* L., cv Arbequina) orchard where Fernández et al. (2011, 2013) made their experiments. The orchard, located at 25 km to the east of Seville (37° 15' N, −5° 48' W), had trees at the top of 0.4 m high ridges, planted at 4 m × 1.5 m (1,667 trees ha^{-1}), with tree rows oriented N-NE to S-SW. Climate in the area is Mediterranean with mild, wet winters and hot, dry summers. The rainy period is between September and May, being dry for the rest of the year. Average values of precipitation (P) and potential evapotranspiration (ET_o) in the area are 540 mm and 1,528 mm, respectively (period 2002-2014). In the hottest months, July and August, maximum values of air temperature were over 40 °C and rarely over 45 °C. In the coldest months, December and January, minimum values of air temperature were seldom below 0 °C and very rarely below −5 °C. Additional details on the trees, environmental characteristics and orchard management are given by Fernández et al. (2011, 2013).

In 2013, when the trees were 7 years old, we had a full irrigation (FI) treatment in which trees were daily irrigated for the whole irrigation season to replace 100% of the irrigation needs (IN), and a regulated deficit irrigation treatment (45RDI) for which the total water supplied along the season was aimed to replace 45% of IN. The irrigation strategy for this 45RDI treatment is shown in Fig. 1. Basically, the irrigation amounts (IA) must be equal or close to IN in three periods of the year when the crop is most sensitive to water stress (Fernández 2014a). For the rest of the year just one or two irrigation events per week are applied. In our area, period 1 (around bloom) falls into the rainy season, so irrigation is usually required in periods 2 and 3 only. In 2013 we used the crop coefficient approach (Allen et al., 1998) to schedule irrigation. This is why we named $45RDI_{cc}$ the 45RDI treatment applied this year. Every Monday of the irrigation season the irrigation needs were calculated as $IN = ET_c - P_e$, being ET_c the crop evapotranspiration estimated by the crop coefficient approach and P_e the effective precipitation, assumed to be 75% of the precipitation recorded by the weather station in the orchard. The calculated IN values were applied daily to the FI trees. For the $45RDI_{CC}$ trees irrigation was reduced according to Fig. 1. Thus, the $45RDI_{CC}$ trees were irrigated daily in periods 2 and 3, but for the rest of the irrigation season water was supplied just once or twice per week. The crop coefficient (K_c) values were adjusted for the orchard conditions from measurements made from 2010 to 2012 by Fernández et al. (2013). The resulting K_c values were 0.60 in May, 0.63 in June,

0.57 in July and August, 0.65 in September and 0.69 in October. The calculated irrigation doses were input in an irrigation controller (Agronic 2000, Sistemes Electrònics PROGRÉS, S.A., Lleida, Spain) and water was applied through a pipe per tree row with three 2 L $hour^{-1}$ drippers per tree, 0.5 m apart. Fertilizers were injected into the irrigation system once a week during the whole irrigation season, to match the tree requirements (Fernández et al., 2013). All treatments received the same amounts of fertilizers. We used a randomized block design with four 12 m × 6 m plots per treatment. Each plot contained 24 trees, and measurements were made in the central 8 trees.

In 2014 we had the FI and the $45RDI_{CC}$ treatments, both scheduled with the crop coefficient approach. In addition, we had a $45RDI_{TP}$ treatment, for which we also used the 45RDI strategy depicted in Fig. 1 but scheduled from outputs of the ZIM system. As detailed in Section 2.2, we instrumented with ZIM probes one tree per plot, in three plots out of the four $45RDI_{TP}$ plots. At the beginning of both period 2 and period 3, all RDI trees showed moderate to severe levels of water stress, because of the lack of water in the soil caused by the reduced irrigation applied on the weeks before. We then supplied daily IA values amounting to 120% IN on the first three days of both period 2 and 3. This was enough for the daily P_p curves recorded in those trees to change from State 2 or 3 to State 1. For the rest of the period, every morning we visualized the three P_p curves recorded the day before, one from each of the three trees instrumented with ZIM sensors, and adjusted irrigation to the $45RDI_{TP}$ trees according to the State of the P_p curves and the 3-day weather forecast given through Internet. Thus, when one out of the three P_p curves changes from State 1 to State 2 and the weather forecast announced increasing atmospheric demand, the IA value for the $45RDI_{TP}$ treatment was increased by 15%. If atmospheric demand was expected to decrease, or the most sensitive instrumented $45RDI_{TP}$ tree did not show a change from State 2 to State 3, IA was not modified. In case of a change from State 2 to State 3, or a second tree changing from State 1 to State 2, IA was increased by 15%. When the State shown by the P_p curves indicated a recovery of the tree water status, IA was decreased, again by 15%. Outside of periods 2 and 3, when irrigation is applied just once or twice per week, IA values were applied according to Fig. 1. In our case, and because we were using the crop coefficient approach to schedule irrigation both in the FI and $45RDI_{CC}$ treatments, we used the calculated IN values to derived the IA values for the $45RDI_{TP}$ trees on the weeks before, in between, and after periods 2 and 3.

2.2. Soil, plant and weather measurements

Soil water status was monitored as detailed in Fernández et al. (2013). Basically, a Profile probe (Delta-T Devices Ltd, Cambridge, UK) was used to record volumetric soil water content (θ_v) values in the root zones of three trees per treatment, and the values used to calculate changes on the relative extractable water (REW) along the two irrigation seasons, for all treatments. Previous work in the orchard showed that records in three trees per treatment were enough to derive reliable REW values (Fernández et al., 2011, 2013).

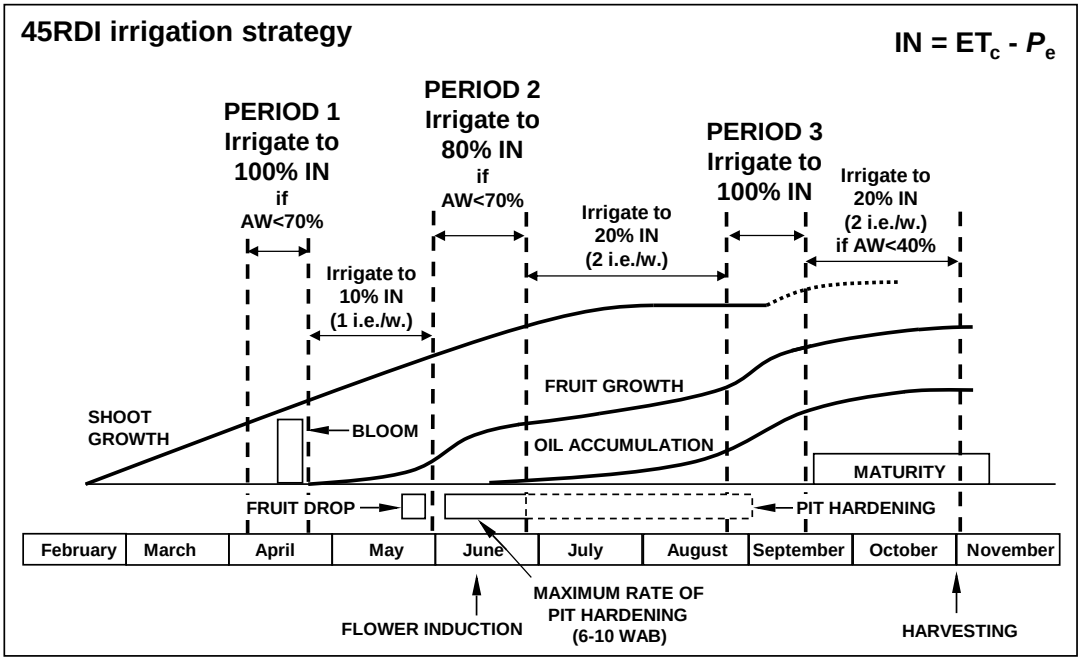

Fig. 1. Regulated deficit irrigation strategy applied in the orchard for the 45RDI treatments. In the three periods of high crop sensitivity to water stress (periods 1 to 3), irrigation is applied daily. For the rest of the year just one or two irrigation events per week (i.e./w.) are applied, replacing 10% or 20% of the total irrigation needs (IN) in the period. AW is the available water in the soil. Both the double sigmoidal curve for growth and the sigmoidal curve for oil accumulation are observed in years with very hot and dry summers. In years with less demanding conditions, both variables show a linear increase along the summer. ET_c = crop evapotranspiration; P_e = effective precipitation, assumed to be 75% of the precipitation recorded by a weather station in the orchard; WAB = weeks after bloom. After Fernández et al. (2013).

Both in the FI and 45RDI treatments, and before the beginning of the 2013 and 2014 irrigation seasons, one central tree per plot was instrumented, in three of the four plots, with ZIM probes (YARA ZIM Plant Technology, Hennigsdorf, Germany). The instrumented trees were representative of those in the treatment, in terms of size, leaf area, water status and gas exchange. As for the REW values, records from three trees per treatment were enough to monitor the tree water status variability within each treatment, according to the findings by Fernández et al. (2011). In each instrumented tree, a ZIM probe was clamped on a leaf of the east side of the canopy, at *ca*. 1.5 m above ground. Once every 5 min the output of the probe was sent via radio to a datalogger with a GPRS modem for data transfer to a server own by ZIM Plant Technology GmbH, to which we accessed via Internet. The ZIM probes were left working until the end of the irrigation seasons.

Measurements of both predawn (Ψ_{pd}) and midday stem water potential (Ψ_{stem}) were made with a Scholander-type pressure chamber (PMS Instrument Company, Albany, Oregon, USA). Once every other week during the entire irrigation seasons, one leaf per

tree from two representative trees per plot (n = 8) were sampled. For Ψ_{stem} we selected leaves close to a main branch and wrap them in aluminium foil ca. 2 h before measurements. These leaves were sampled from 11.30 GMT to 12.30 GMT. Both for Ψ_{pd} and Ψ_{stem}, the sampled leaves were put into an aluminium canister with wet filter paper inside and taken to the pressure chamber within a maximum of 3 min after sampling. Sampled leaves were taken from trees next to those instrumented with ZIM probes, such that leaf sampling did not affect P_p outputs.

Main weather conditions in the orchard were recorded every 30 min with a Campbell weather station (Campbell Scientific Ltd., Shepshed, UK). In addition, weather records required to calculate ET_o for the crop coefficient approach were collected from a standard weather station of public access through the Internet, belonging to the local government (Fernández et al., 2013).

Harvesting was made on October 29th 2013, day of year (DOY) 302 and on November 21st 2014 (DOY 325). The trees were manually harvested and total fruits per plot were weighted separately. From the recorded fruit yields and the total IA per treatment we calculated the irrigation water productivity (WP) as the amount of marketable product per hectare and unit of supplied water.

2.3. Statistical analysis

Data shown are mean ± standard error. For the statistical analysis we used linear mixed models (LMM) with Tukey's all-pair comparisons to analyse the differences between irrigation treatments (fixed factor) statistically significant at $p < 0.05$. These analyses were performed by R software (R Core Team, 2012) with R packages 'nlme R' (Pinheiro et al., 2011) and 'multcomp R' (Hothorn et al., 2008).

3. RESULTS

Total IA applied in 2013 to the FI treatment was lower than expected because of malfunctioning of the irrigation pump at the beginning of the irrigation season. This explains the lack of irrigation until June 18th, DOY 169 (Fig. 2A) and the decrease on REW values on those days (Fig. 2C). For the rest of the 2013 irrigation season, and also for the 2014 irrigation season, IA ≈ IN in the FI treatment and REW values were close to 1, suggesting non-limiting soil water conditions (Figs. 2C,D). In the 45RDI treatments, however, the REW dynamics agreed with changes on IA established by the applied RDI strategy. Thus, in periods 2 (June) and 3 (late August – mid September), REW values of *ca.* 0.8, were recorded, while in between periods 2 and 3 (July-August) and after period 3 (from mid September), REW values were lower, due to the low IA applied on those weeks to the 45RDI trees. Data of 2014 shows that in period 2 (DOY 154-185), IA values amounted to 72.2 mm in $45RDI_{CC}$ and to 61.5 mm in $45RDI_{TP}$. In period 3 (DOY 238-259) these values were 66.8 mm in $45RDI_{CC}$ and 67.1 mm in $45RDI_{TP}$. For the FI treatment, IA

values were 93.1 mm in period 2 and 69.7 mm in period 3. Differences in IA between treatments had little impact on REW values in those two periods (Fig. 2D). Consequently, similar water stress levels were found in trees of all treatments, for both period 2 and 3, as Ψ_{pd} (Figs. 3A,C) and Ψ_{stem} (Figs. 3B,D) values show. In between those periods the trees' water stress increased considerably in the 45RDI treatments, as expected. After period 3 the autumn rainfall (Figs. 2A,B) contributed to keeping low values of water stress (Fig. 3).

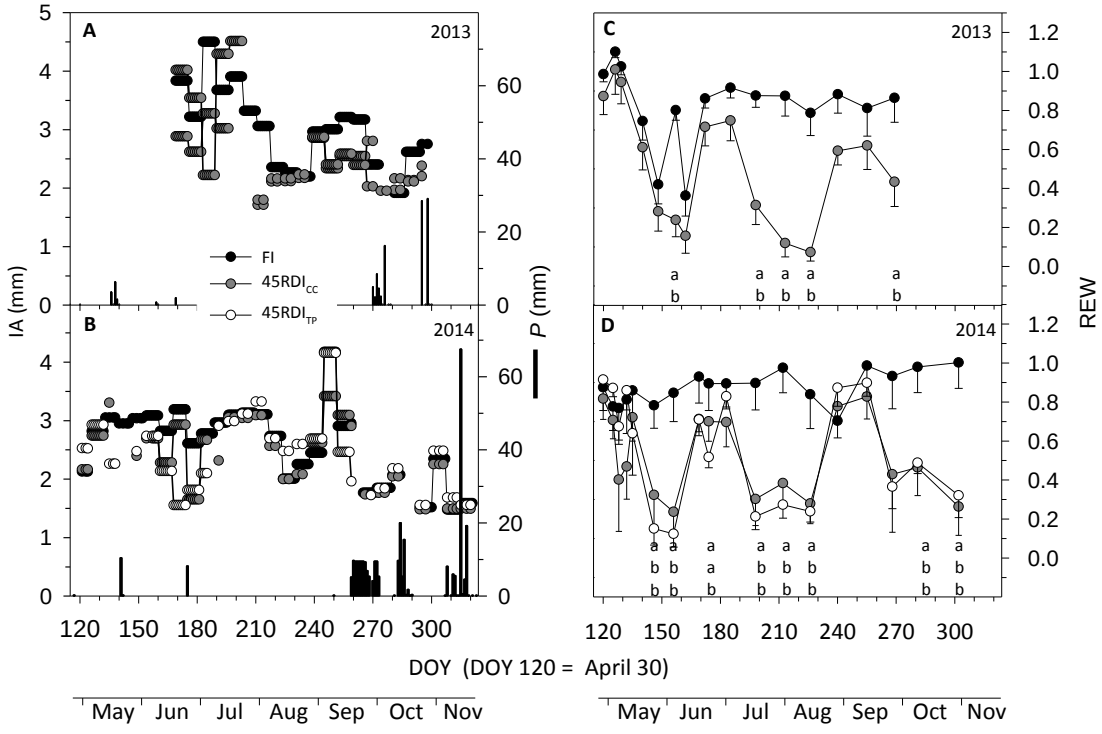

Fig. 2. Seasonal courses of both the irrigation amounts (IA) supplied to each treatment and the precipitation (*P*) collected in the orchard (A,B), and the values of relative extractable water (REW) derived from the soil water contents (avg – SE) measured in the plots of each treatment (C,D). Measurements were made on the irrigation seasons of 2013 and 2014. Different letters indicate significant differences between treatments, at $p < 0.05$. Letters are not shown when no differences were found. DOY = day of year.

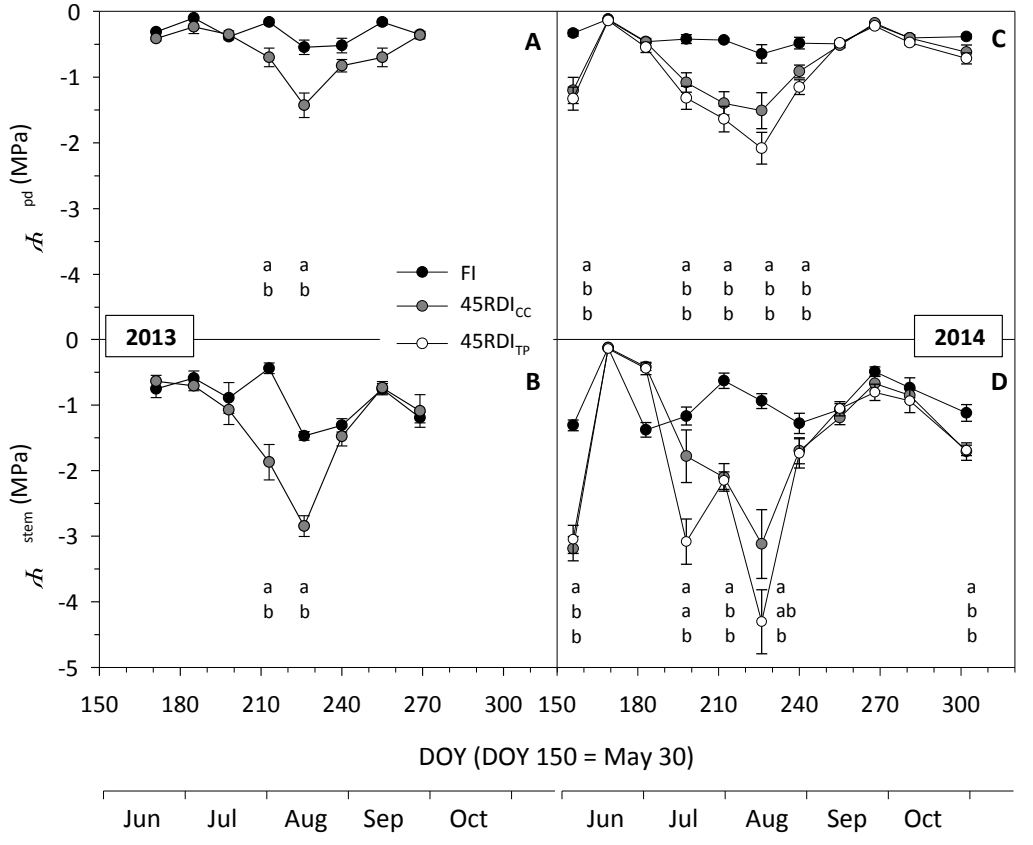

Fig. 3. Seasonal courses of predawn water potential (Ψ_{pd}, avg ± SE) and midday stem water potential (Ψ_{stem}, avg ± SE) measured in 2013 (A, B) and 2014 (C, D) in FI, 45RDI$_{cc}$ and 45RDI$_{TP}$ trees. Different letters indicate significant differences between treatments at $p < 0.05$. Letters are not shown when no differences were found. DOY = Day of year.

Since our irrigation scheduling approach was based on outputs of the ZIM probe, we wanted to compare those outputs with measurements with the Scholander-type pressure chamber, a widely used instrument to monitor olive water stress (Moriana et al., 2012; Naor et al., 2013). In Fig. 4 we show data from both methods, collected in May and September, i.e. before and after the highly demanding mid-summer period. The shown P_p curves correspond to a 45RD$_{CC}$ tree (Fig. 4A) and a FI tree (Fig. 4B). All the other instrumented trees showed a similar behaviour. Values of Ψ_{pd} and Ψ_{stem} showed that trees of both treatments had similar water stress levels in May and in September. Values of P_p, however, were greater in September than in May, for both the 45RDI$_{CC}$ and the FI trees. Results in Fig. 4, therefore, suggest that water stress monitoring should not rely on absolute P_p values, at least for our orchard conditions.

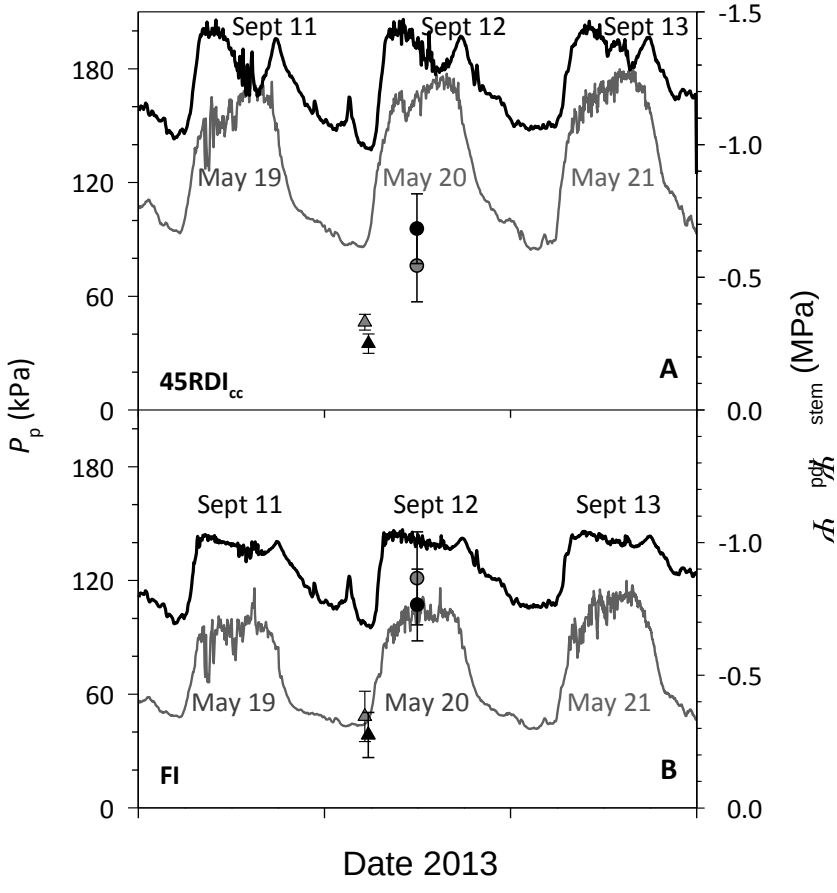

Fig. 4. Daily curves of the ZIM probe outputs (P_p) installed in a representative tree of the 45RDI$_{CC}$ (A) and FI (B) treatments applied in 2013. The shown curves correspond to days prior (May) and after (September) the most demanding, in terms of water stress, mid-summer period. Also shown are predawn (Ψ_{pd}, avg ± SE, triangles) and midday stem water potential (Ψ_{stem}, avg ± SE, circles) values measured with a Scholander-type pressure chamber in trees next to the trees instrumented with ZIM probes, also in May and September. Both for the curves and symbols, the grey and black colours mean measurements in May and the September, respectively.

Our irrigation scheduling approach, however, relies on the State shown by the P_p curves, and not on absolute values. As mentioned in the Introduction, Fernández et al. (2011) and Ehrenberger et al. (2012) found that State 1 was observed in olive trees with $\Psi_{stem} > -1.2$ MPa, Sate 2 in trees with -1.2 MPa $< \Psi_{stem} < -1.7$ MPa and State 3 in trees with $\Psi_{stem} < -1.7$ MPa. But they both worked with young trees only. To test the suitability of our irrigation scheduling approach for olive trees of any age, from young to fully mature, highly productive trees, we made Fig. 5. In this figure Ψ_{stem} values measured in trees of all treatments are plotted against the State shown by the P_p curves collected on the same days. The figure shows the data we collected in 2013 and 2014, and also data collected by our team from 2010 in the same orchard, when we began this set of studies on scheduling regulated deficit irrigation in super-high-density olive orchards. Including data from our previous work allows for a more robust assessment on the relation between Ψ_{stem} values and the State shown by P_p curves. Measurement details for the 2010-2013 period can be seen in Fernández et al. (2011, 2013) and Diaz-Espejo et al. (2012). Figure 5 shows data collected in 4 to 8-year-old trees, under a wide range of both soil water conditions and atmospheric demand. In the 68.3% of the cases in which P_p curves were in State 1 we found Ψ_{stem} values to be > -1.2 MPa, and in the 81.8% of the cases in which P_p curves were in State 3, $\Psi_{stem} < -1.7$ MPa. Thus, both for States 1 and 3 we got similar results, in most cases, than those reported by Fernández et al. (2011) and Ehrenberger et al. (2012). However, about one third only of the trees in which P_p records showed State 2 had Ψ_{stem} values in between -1.2 and -1.7 MPa, as previously reported by those authors. This lack of agreement can be explained, at least in part, by State 2 being not always easy to identify. Both States 1 and 3 can be clearly identified from the shape of the P_p curves. However, at moderate levels of water stress typical of State 2, decreases in the P_p values collected at the central hours of the day were highly variable, being not always easy to identify whether the shape of the P_p curve suggested State 2 or it was just noise caused by changing atmospheric conditions.

Changes among States observed in 2014 in each of the trees instruments with ZIM probes, as well as the average Ψ_{stem} values for each treatment, are shown in Fig. 6. This figure illustrates, in fact, the tree-to-tree variability of the State shown by the P_p curves collected in our orchard. Trees of the FI treatment always showed State 1, except for days of sudden increase in ET_o, such as DOY 242-244. The $45RDI_{TP}$ trees showed State 1 for most days of periods 2 and 3. An exception was at the beginning of period 3, when the available water in the soil was very low after the mid-summer period of reduced irrigation. State 2 was also observed on some days of Period 2, likely because of the reduced IA, which amounted to 0.68% of IN only (Fig. 7). In between periods 2 and 3, all $45RDI_{TP}$ trees showed State 2 or 3, as expected. In the autumn irrigation was also reduced, but the total water supplied by irrigation and precipitation (Fig. 2B) was enough to avoid severe water stress, as commented when reporting findings shown in Fig. 3. The $45RDI_{CC}$ trees showed a similar behaviour than the $45RDI_{TP}$ trees, with the difference of a lower recovery from water stress after the beginning of both periods 2 and 3. This can be explained by the fact that $45RDI_{TP}$ trees were irrigated with IA = 120% IN on the first three days of each period, as explained in Section 2.1.

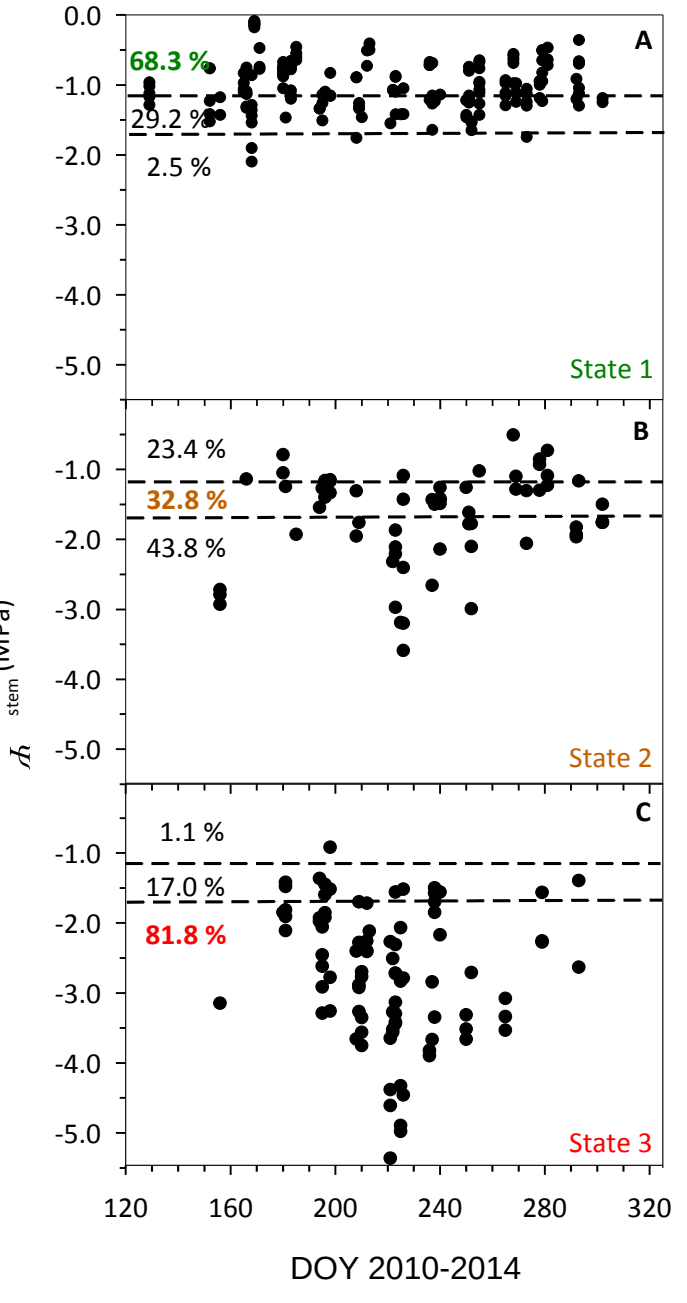

Fig. 5. Midday stem water potential (Ψ_{stem}) values measured in representative trees of all the irrigation treatments at the Sanabria orchard during the irrigation seasons of 2010 to 2014. Each data point corresponds to a single measurement with a Scholander-type pressure chamber. Dashed lines represent the midday stem water potential values values identified by Fernández et al. (2011a) and Ehrenberger et al. (2012) as typical of State 1 (Ψ_{stem} > -1.2 MPa) (A), State 2 (-1.2 MPa > Ψ_{stem} > -1.7 MPa) (B) and State 3 (Ψ_{stem} < -1.7 MPa) (C). The State is given by the shape of the daily leaf patch clamp pressure curve, as described by Ehrenberger et al. (2012). DOY = Day of year.

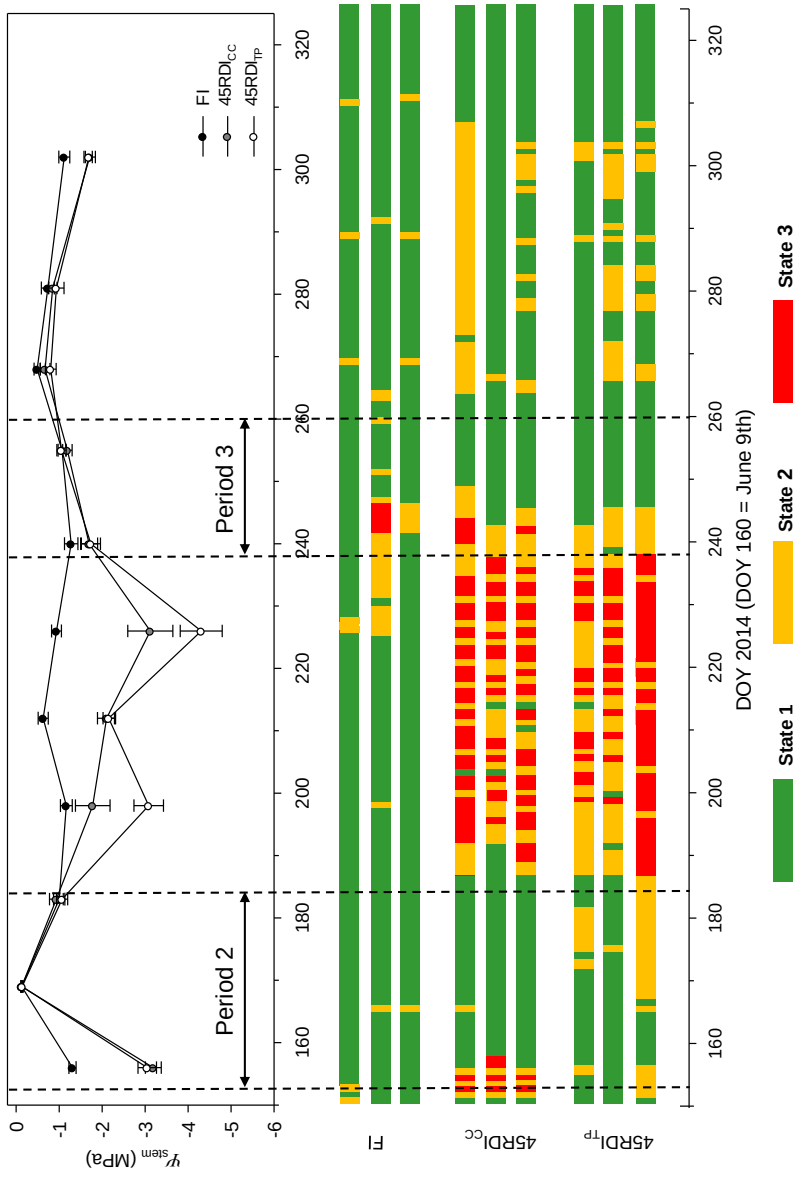

Fig. 6. Seasonal courses of midday stem water potential (Ψ_{stem}, avg. ± SE) measured in FI, 45RDI$_{CC}$ and 45RDI$_{TP}$ trees of the Sanabria orchard during the whole irrigation season of 2014. P_n curves were collected by three ZIM probes per treatment and shown here through State 1 (low water stress), State 2 (moderate stress) and State 3 (severe stress) by horizontal colour bars. Periods 2 and 3 shown in Fig. 1, as observed in this year 2014, are represented. DOY = Day of year.

Figure 7 shows the results from applying our irrigation approach to schedule the 45RDI$_{TP}$ treatment. Figures 7A and 7C show the P_p curves collected in a 45RDI$_{TP}$ tree, for periods 2 and 3, respectively. We chose the tree in which State 2 appeared earlier. The other two trees showed similar behaviour, although signs of water stress appear one or two days later than in the tree used for Fig. 7. A certain tree-to-tree variability in fruit tree orchards can be expected, due to spatio-temporal variations of soil and plant conditions (Fernández and Cuevas, 2010). Arrows in Fig. 7 show the days on which we increased or decreased irrigation according to the State shown by the P_p curve. Figures 7B (period 2) and 7D (period 3) show differences in the daily IA values when estimated with the crop coefficient approach (45RDI$_{CC}$) as compared to our irrigation scheduling approach based on the ZIM system (45RDI$_{TP}$). Also shown are the total IA applied for both treatments in each period, expressed as a percentage of the IN calculated for the period. These data show that in period 2 the amount of water supplied by irrigation was lower in 45RDI$_{TP}$ than in 45RDI$_{CC}$ (Fig. 7B). In period 3, when irrigation demands were lower, IA values in 45RDI$_{TP}$ and in 45RDI$_{CC}$ were similar (Fig. 7D).

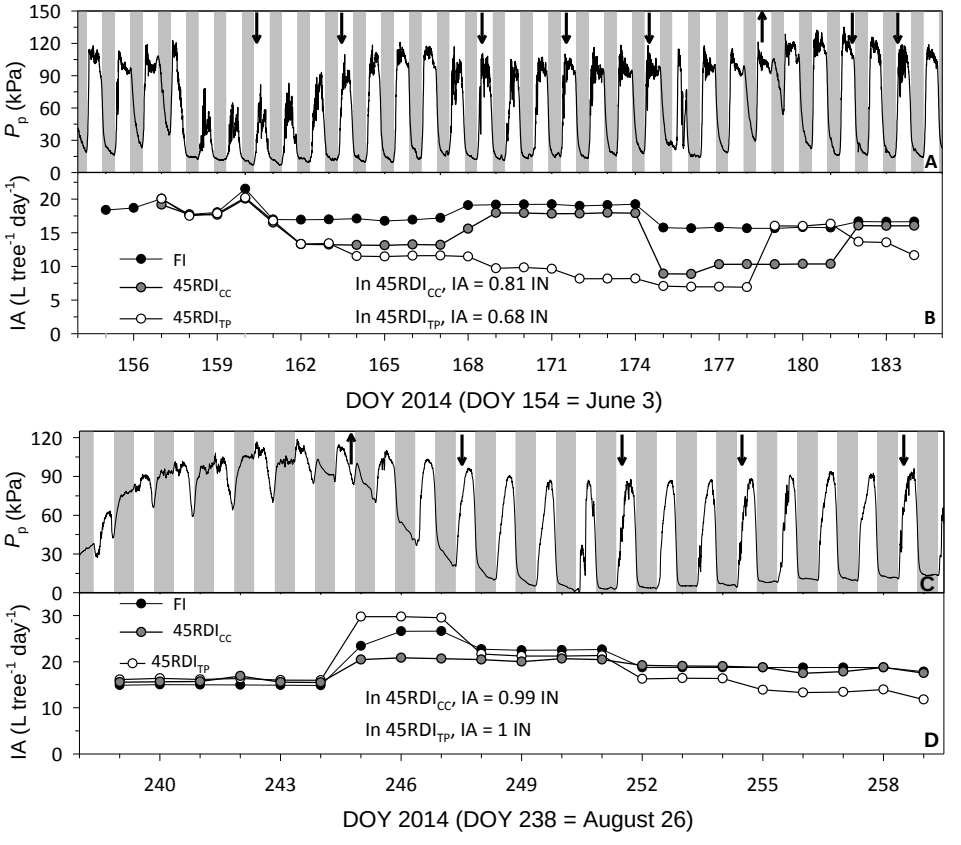

Fig. 7. Time courses of the P_p values recorded on a 45RDI$_{TP}$ representative tree in period 2 (A) and period 3 (C) of the 2014 irrigation season (see Fig. 1 to identify the periods). Also shown are the irrigation amounts (IA) supplied to each treatment in each period (B,D), expressed as a fraction of the calculated irrigation needs (IN) for the period. IA was increased (arrows up) or decreased (arrows down) according to changes in the State of the daily P_p curves (see the irrigation approach described in Section 2.1). DOY = Day of year.

The crop response to the irrigation treatments in terms of fruit yield and irrigation water productivity (WP) is shown in Table 2. The trees were already fully productive in 2013 and 2014, as expected for their age (7 and 8 years old, respectively). Considering data of both years, and averaging results from the $45RDI_{CC}$ and $45RDI_{TP}$ treatments, the 45RDI trees, which received 53.9% of the total IA supplied to the FI trees (Table 1), had a fruit yield of 72.4% of that in FI (Table 2). Values of WP increased with RDI in 30.2%, on average. For 2013, however, WP data are not reliable, because of the problem with the irrigation pump we had at the beginning of the 2013 irrigation season (Section 3). Data from 2014 show that differences in fruit yield between $45RDI_{TP}$ and $45RDI_{CC}$ were not significant ($p = 0.54$ and $p = 0.22$, respectively). Still, data of one year only is not enough to evaluate the impact of the irrigation treatment on production.

Table 1. Water supplies (IA = irrigation amounts; *P* = precipitation) and potential evapotranspiration (ET_o) in the experimental orchard for the two irrigation seasons. All values are in millimeters. Values of IA are also expressed as percentages of irrigation needs (% IN). DOY = day of year.

	2013		2014	
	Whole year	Irrigation period (DOY 133–301)	Whole year	Irrigation period (DOY 116–324)
ET_o	1464.3	1000.3	1437.6	1110.1
P	476.4	112.5	549.4	317.6
IA in FI		367.6 (80.0% IN)		462.9 (87.1% IN)
IA in $45RDI_{CC}$		197.9 (43.1% IN)		238.2 (44.8% IN)
IA in $45RDI_{TP}$				235.9 (44.4% IN)

Data with * were affected by reduced water supply at the beginning of the irrigation season (see Section 3 for details).

Table 2. Fruit yield (n = 4) and water productivity values for each treatment and experimental year. Different letters indicate significant differences between treatments at $p < 0.05$.

Year	Treatment	Fruit yield (kg ha^{-1})	Irrigation water productivity (kg ha^{-1} mm^{-1})
2013	FI	22559.8 ± 1453.1 a	61.4* ± 3.9 a
	45RDI$_{CC}$	14952.1 ± 873.0 b	75.6* ± 4.4 b
2014	FI	19283.0 ± 2708.5 a	41.6 ± 5.9 a
	45RDI$_{CC}$	13443.0 ± 2847.9 a	53.4 ± 12.0 a
	45RDI$_{TP}$	17025.6 ± 2077.0 a	72.2 ± 8.8 a

4. DISCUSSION

As mentioned above, our group began in 2010 a set of studies to identify both a suitable RDI strategy for hedgerow olive orchards with high tree densities (SHD olive orchards) and a reliable, user-friendly water stress indicator to schedule irrigation. In a first set of experiments made from 2010 to 2102, Fernández et al. (2013) evaluated the impact on crop performance of an earlier version of the RDI strategy, with two irrigation levels (30% and 60% of IN). Experiments were run in parallel to assess the performance of different water stress indicators, from the conventional leaf and stem water potential, and stomatal conductance, to new plant-based methods for automatic and continuous monitoring of water stress. These experiments with concomitant measurements of a wide range of variables related to the water status in the soil, plant and surrounding atmosphere, provided insight into the links between physiological processes in olive trees under water stress and outputs from sap flow, trunk diameter variations and leaf turgor related measurements (Fernández et al., 2011; Diaz-Espejo et al., 2012; Rodriguez-Dominguez et al., 2012; Cuevas et al., 2013). Those findings, together with contributions from other authors on the usefulness of those plant-based sensors to monitor water stress in fruit trees, allowed for detailed assessments on the potential of each method for monitoring water stress and schedule irrigation. The work by Fernández et al. (2008), Ramos and Santos (2009) and Rousseaux et al. (2009) show, to a good extent, the advantages and disadvantages of sap flow measurements to improve water management in olive and other fruit trees. The same can be said for trunk diameter variations on the work by Pérez-López et al. (2008), Moriana et al. (2010) and Cuevas et al. (2010). And the potential of using leaf turgor related measurements with that purpose was evaluated by Ben-Gal et al. (2010), Rüger et al. (2010) and Zimmermann et al. (2010, 2013). Knowledge from these and other

publications was collected by Fernández (2014b) in a review on the applicability of those methods to schedule irrigation in commercial orchards. He concluded that the ZIM system was one of the most promising systems for commercial olive orchards. The system is easier to install and use than those of sap flow and trunk diameter variation, and as robust as those two when working under field conditions for the long irrigation seasons common in most olive growing areas. On the outputs, Fernández (2014b) showed that both sap flow and trunk diameter related measurements require high training both to process the collected data and to understand their physiological meaning. For the leaf turgor related measurements, he stated that, although we are still far from fully understanding the physiological meaning of the ZIM probe readings, there was a potential for scheduling irrigation based just on the visual analysis of the P_p daily curves. This is crucial for the acceptance of any method to schedule irrigation by farmers and orchardists without specific training, as previously stated by Naor (2006 and Fernández and Cuevas (2010), among others.

Our results suggest that we cannot expect a robust correlation between the tree water status and P_p values for the whole irrigation season (Fig. 4). This is not surprising, since aging induces structural and mechanical changes in the olive leaf that could easily affect the outputs of the ZIM probes. Thus, the water stress history of the leaf can affect the palisade parenchyma (Chartzoulakis et al., 1999; Bacelar et al., 2004), as well as the density and thickness of the leaf (Centritto, 2002). The seasonal course of the Ψ_{stem} *vs*. P_p relationship can also be affected by changes in the elastic modulus (ε) of the leaf cells. It has been observed that, in olive, ε tends to increase with leaf age (Bongi and Palliotti, 1994) and drought (Dichio et al., 2003). All these changes, together with others on leaf response to environmental stimuli (Marchi et al., 2008) can affect the Ψ_{stem} *vs*. P_p relationship along the season. The fact that, at least for olive, the Ψ_{stem} *vs*. P_p relationship changes with time must be taken into account when P_p values are used to derive water stress indices requiring normalization, as for the case described by Bramley et al. (2013). Figure 4, in fact, suggests that establishing an effective normalization procedure of the P_p records is not straightforward.

Our irrigation approach (Section 2.1), however, does not rely on absolute P_p values, but on changes between States, which it does not require normalization. Our hypothesis was that findings by Fernández et al. (2011) and Ehrenberger et al. (2012) reported for young trees, also holds for mature, fully productive trees. This is, in fact, supported by Fig. 5, which shows that the relation between the State of the P_p curve and the ranges of tree water status defined by Fernández et al. (2011) and Ehrenberger et al. (2012) holds reasonably well for olive trees of different age growing under a wide range of environmental variables. This supports the potential of the change in the State of the daily P_p curve as a user-friendly, visual indicator for irrigation scheduling. Such potential was confirmed in 2014, when we used our irrigation approach to schedule irrigation of treatment 45RDI$_{TP}$. In period 2 the IA values derived from our approach were lower than those calculated from the crop coefficient approach, i.e. those of the 45RDI$_{CC}$ treatment (Figs. 7A,B). For that period, the reduced irrigation in 45RDI$_{TP}$ as compared to that in 45RDI$_{CC}$ did not lead to differences in plant water status (Fig. 3), despite of the greater

water savings achieved with our irrigation approach. In period 3 differences between our approach and that of the crop coefficient were less evident (Figs. 7C,D). Results from a single year, however, might not be enough to reliably state differences between both approaches.

With our irrigation approach we managed to keep similar stress levels in the $45RDI_{TP}$ trees than in the FI trees, during the sensitive periods 2 and 3 (Fig. 3). As compared to the $45RDI_{CC}$ treatment, our irrigation approach showed similar results in terms of tree water stress level, and greater water savings. In addition to that, yield and irrigation water productivity values were similar in $45RDI_{TP}$ than in $45RDI_{CC}$. Although more years are required to evaluate the impact of these two approaches on crop performance and water productivity, these results suggest that our irrigation scheduling approach leads to similar values of both variables, if not better, than the crop coefficient approach.

The reported advantages of $45RDI_{TP}$ as compared to $45RDI_{CC}$ might not be enough to recommend adopting our irrigation approach in all cases. If both reliable K_c values and a nearby weather station are available, the crop coefficient approach can be a good option to apply the 45RDI strategy (Fig. 1) in hedgerow olive orchards with high plant densities. Those conditions, however, are not accomplished in most olive orchards. Then, our irrigation scheduling approach based on the ZIM system can be used with confidence to schedule irrigation. Still, there are empirical aspects in our approach that must be further addressed. These refer to increasing or decreasing IA by 15% in periods 2 and 3, and to using IA = 120% IN on the first three days of those periods. Such values are purely empirical and require further attention. In addition, our irrigation scheduling approach based on the ZIM system does not provide information to estimate IA in between periods 1 and 2, 2 and 3, and after period 3. On those days IA must be based on whatever knowledge the farmer has on the orchard water needs, which may led to imprecise results. Still, the advantage of our irrigation scheduling approach, as compared to the crop coefficient approach, can be especially remarkable in large orchards where soil, plant and atmospheric conditions are highly variable. In those cases the crop coefficient approach can led to large errors, at least for certain parts of the orchard where the used K_c values fit worst. In those orchards is where the use of ZIM sensors, combined with remote infrared images for selecting the trees to instrument (Zarco-Tejada et al., 2009; Gonzalez-Dugo et al., 2013), could show a better performance.

5. CONCLUSIONS

Our irrigation scheduling approach, based on the use of the ZIM system, allowed for an effective application of regulated deficit irrigation in a hedgerow olive orchard with high plant density. Our irrigation scheduling approach can be used by farmers without specific training, since it is based on the State shown by the outputs from the ZIM sensors. The State can be easily identified, just by visualising the daily curves derived from the raw outputs collected by ZIM sensors, without any further data processing. Our results proved

a robust enough relation between States 1 to 3 shown by the P_p curves and water stress levels in olive trees. This relation, previously established for young trees by our group and by the group that developed the ZIM system, also holds for mature, fully productive olive trees growing under a wide range of environmental conditions. Our irrigation scheduling approach showed a performance as good as that of the crop coefficient approach, and can led to a more precise irrigation scheduling in large, highly variable orchards. There is still room, however, for further elucidating aspects of our approach that, in its current state, are purely empirical.

Chapter 3

Water status, gas exchange and crop performance in a super high density olive orchard under deficit irrigation scheduled from leaf turgor measurements

1. INTRODUCTION

The world population is expected to increase 1:3 before 2050 (FAO, 2009). In this period, rising temperatures and lower precipitation is forecasted for Mediterranean areas (IPCC, 2014). We are facing the challenge, therefore, of producing more food, fibber and biofuel with less water and greater atmospheric demand. Among the responses of the scientific community to that challenge are the development of new irrigation strategies and effective tools for monitoring plant water stress and scheduling irrigation. Concerning the irrigation strategy, that can vary from full irrigation (irrigating with enough water to replace 100% of the crop water needs) to supplementary, or complementary, irrigation (just one or very few irrigation events supplying a small fraction of the crop water needs). Between both, the user can choose among a variety of deficit irrigation strategies (Fereres and Soriano, 2007; Iniesta et al., 2009; Ruiz-Sanchez et al., 2010; Martín-Vertedor et al., 2011; Gomez-del-Campo, 2013; Fernández 2014a). For assessing water stress and scheduling irrigation, the user can choose among different methods based on soil, atmosphere or plant measurements. The latter are widely used in fruit trees, including olive. In fact, a variety of methods are available, from the conventional, non-automated methods for assessing leaf or stem water status and stomatal conductance or photosynthesis, to methods with systems that run continuously and automatically, based on measurements related to sap flow, trunk diameter and leaf turgor pressure, among other plant variables (Jones, 2004, 2007; Ben-Gal et al., 2010; Fernández, 2014b). Many of those methods, apart from running automatically and being easily implemented with data transmission systems for a remote access to the recorded data through the internet, can be combined with remote imagery for a precise irrigation of large orchards (Gonzalez-Dugo et al., 2015; Gago et al., 2015; Bellvert et al., 2016; Fernández 2017).

The most suitable irrigation strategies for fruit trees orchards in arid and semi-arid areas are deficit irrigation strategies specifically designed to match both the crop characteristics and main environment conditions (Rallo et al., 2016). Deficit irrigation is especially suitable to hedgerow orchards with high tree densities, also called super high density (SHD) orchards, where excessive growth must be avoided by controlling water and fertilizer supplies. For SHD olive orchards, regulated deficit irrigation (RDI) has been reported as one of the best deficit irrigation strategies (Fernández et al., 2013; Fernández, 2014b). Several experiments at the Sanabria orchard, a commercial SHD 'Arbequina' orchard near Seville, southwest Spain, representative of those in many other Mediterranean olive growing areas, proved the suitability of the 45RDI strategy for SHD olive orchards (Fernández et al., 2013, 2017; Hernandez-Santana et al., 2017). The 45RDI strategy consists in irrigating daily to replace 100% of irrigation needs in three periods of the annual growing cycle. These periods, named as periods 1, 2 and 3, are those in which olive is most sensitive to water stress (Fernández et al., 2013; Fernández et al., 2014a). In between those periods, one or two irrigation events per week are recommended. As reported by Fernández et al. (2013) and Padilla-Diaz et al. (2016), the total water supplies in between the three mentioned periods amounted to 15-30% of the irrigation needs,

depending of the time of the year. The total water supply for the whole irrigation season in this 45RDI strategy aims at 45% of the irrigation needs.

The successful application of any RDI strategy requires effective irrigation scheduling. For olive, different water stress indicators and related systems to schedule irrigation based on sap flow, trunk diameter variations and leaf turgor related measurements have been assessed (Fernández, 2014a). Among them, the ZIM system, which uses the leaf patch clamp pressure (LPCP or also called ZIM) probe (Zimmermann et al., 2008), has been proved to be useful to assess water stress in commercial orchards (Fernández et al., 2011; Fernández, 2014a). The ZIM probe records the output pressure (P_p), a variable inversely correlated with the leaf turgor pressure (Zimmermann et al., 2008), a variable closely related to water stress (Fernández, 2014b). Egea et al. (2017) analysed the financial feasibility of scheduling irrigation at the Sanabria orchard from the three mentioned plant-based type of measurements, and concluded that the ZIM system is the best approach. To evaluate the potential of the ZIM system to assess water stress and to schedule irrigation, Fernández et al. (2011) and Ehrenberger et al. (2012) analysed the relationship between midday stem water potential (Ψ_{stem}), a variable widely accepted as a reliable indicator of plant water status, and the P_p values recorded with the ZIM probe in olive trees. They found that the shape of the daily P_p curve changes dramatically with the level of water stress, and defined three different "States" or shapes of the curve typical of certain Ψ_{stem} levels: State 1, for $\Psi_{stem} > -1.2$ MPa, State 2 for $-1.2 < \Psi_{stem} < -1.7$ MPa and State 3 for $\Psi_{stem} < -1.7$ MPa. Similar studies has been made for other olive cultivars and environments (Marino et al., 2016), and for other species (Martínez-Gimeno et al., 2017). The potential for scheduling irrigation from a visual analysis of the curve, from which the orchardist easily identifies the State of the P_p daily curve and, therefore, the level of water stress of the trees, was already suggested by Fernández et al. (2011) and Ehrenberger et al. (2012). This was used by Padilla et al. (2016) to derive an irrigation scheduling approach for the Sanabria olive orchard, and to run preliminary evaluation measurements during the irrigation season of 2014. They had two regulated deficit irrigation treatments, $45RDI_{CC}$ and $45RDI_{TP}$. In both of them they applied the regulated deficit irrigation strategy proposed for SHD olive orchards by Fernández et al. (2013) and Fernández (2014a). For $45RDI_{CC}$, they scheduled irrigation with the crop coefficient approach, while for the $45RDI_{TP}$ they designed and applied an irrigation scheduling approach based on the visualization of the daily P_p curves recorded with ZIM sensors (see Section 2.1 for details). They evaluated the performance of their irrigation scheduling approach by comparing $45RDI_{CC}$ versus $45RDI_{TP}$, in terms of the irrigation amounts, relative extractable water in the soil, stem water potential at both predawn and midday, and fruit yield. Padilla-Diaz et al. (2016) confirmed the relationships between the level of plant water stress and the shape (States) of the daily P_p curves first reported by Fernández et al. (2011) and Ehrenberger et al. (2012), and concluded that the irrigation scheduling approach applied to the $45RDI_{TP}$ treatment showed a performance as good as that of the crop coefficient approach, allowing for precise irrigation scheduling in orchards for which the crop coefficient values were unknown. They, however, were concerned on the empirical assumptions of their irrigation scheduling approach, e.g. changing the irrigation amount by 15%, as well on their

evaluation relying on a reduced number of variables monitored for a single irrigation season.

The aim of this work was to apply the irrigations scheduling approach proposed by Padilla-Diaz et al. (2016) for two consecutive years at the Sanabria orchard, and to study a wider range of variables with the aim of further assessing the advantages and limitations of the irrigations scheduling approach based on leaf turgor related measurements as compared to the crop coefficient approach. We applied the same $45RDI_{TP}$ and $45RDI_{cc}$ treatments they used, and stem water potential, stomatal conductance and CO_2 net assimilation, as well as the number of internodes in shoots of the current year, leaf area, fruit yield, and seasonal oil accumulation in the fruit and total oil yield, were monitored on representative trees of each treatment, both in 2014 and 2015. We also had a fully irrigated treatment as a control (FI treatment), in which the trees were daily irrigated for the whole irrigation season to replace 100% of the irrigation needs.

2. MATERIAL AND METHODS

2.1. Orchard characteristics and irrigation management

The orchard, located at 25 km to the east of Seville (37° 15' N, −5° 48' W), was planted in 2007 with one-year-old 'Arbequina' trees. The trees were at the top of 0.4 m high ridges and at 4 m × 1.5 m (1667 trees ha^{-1}). Measurements described below were made during the irrigation seasons of 2014 and 2015, when the trees were 8 and 9 years old, respectively. The hedgerows were kept ca. 2.10 m wide and ca. 2.5 m high by pruning in January. We applied the same irrigation treatments described by Padilla-Díaz et al. (2016), i.e. FI, $45RDI_{cc}$ and $45RDI_{TP}$, and with the same layout: four 12 m × 6 m plots per treatment, in a randomized block design. Basically, daily irrigation was applied to the full irrigation (FI) trees during the whole irrigation season, aimed to replace 100% of the irrigation needs. Every Monday of the irrigation seasons the irrigation needs (IN) were calculated as $IN = ET_c - P_e$, being ET_c the crop evapotranspiration estimated from the crop coefficient approach, and P_e the effective precipitation, estimated as 75% of precipitation recorded by the weather station in the orchard (see Padilla et al., 2016, for details on the K_c and potential evapotranspiration values). For the 45RDI trees, we applied a regulated deficit irrigation strategy consisting on daily irrigation to replace 100% of the irrigation needs on the periods when the crop is most sensitive to water stress (periods 1, 2 and 3 shown in Fig. 1 of Padilla et al., 2016), while reducing to one or two irrigation events per week in between those periods. For both 45RDI treatments, the irrigation supply for the whole irrigation season aimed to 45% of the irrigation needs.

The difference between $45RDI_{CC}$ and $45RDI_{TP}$ was that in the $45RDI_{CC}$ treatment irrigation was scheduled from the crop coefficient approach, while in the $45RDI_{TP}$ treatment irrigation was scheduled from the State of the daily P_p curves recorded with ZIM sensors in representative $45RDI_{TP}$ trees, according to the irrigation scheduling approach

proposed by Padilla et al. (2016). Basically, we clamped a ZIM probe in three $45RDI_{TP}$ trees, one per plot in three plots out of the four $45RDI_{TP}$ plots. In 2014 we did not irrigate on period 1, because rainfall was enough, at that time of the year, to replace the crop water needs. In 2015, however, we had to irrigate on that period. Still, the irrigations amounts in on period 1 in 2015 were calculated with the crop coefficient approach for both the $45RDI_{CC}$ and $45RDI_{TP}$ treatments, because at that time we were still installing and checking the ZIM probes and related system. At the beginning of both period 2 and period 3, all the $45RDI_{TP}$ trees showed moderate to severe levels of water stress because of the lack of rain and the reduced irrigation applied on the weeks before each period. Consequently, most ZIM probes were in State 3. We then supplied daily irrigation amounts of 120% of the irrigation needs, on the first three days of both period 2 and 3. This was enough for the daily P_p curves recorded in those trees to change from State 2 or 3 to State 1. For the rest of the period, we adjusted irrigation to the $45RDI_{TP}$ trees according to the State of the P_p curves and the 3-day weather forecast given through Internet. Thus, when one out of the three P_p curves changed from State 1 to State 2 and the weather forecast announced increasing atmospheric demand, irrigation was increased by 15%. If atmospheric demand was expected to decrease, or the most sensitive instrumented $45RDI_{TP}$ tree did not show a change from State 2 to State 3, the irrigation dose was not modified. In case of a change from State 2 to State 3, or a second tree changing from State 1 to State 2, irrigation was increased by 15%. When the State shown by the P_p curves indicated a recovery of the tree water status, irrigation was decreased, also by 15%. Outside of periods 2 and 3, when irrigation was applied just once or twice per week, irrigation amounts were applied according to Fig. 1 in Padilla et al., (2016). On those days, i.e. on the weeks before, in between, and after periods 2 and 3, we used the irrigation needs calculated for the FI treatments with the crop coefficient approach, to derive the required irrigation amounts for the $45RDI_{TP}$ trees.

In 2014 the irrigation season started on April 26th, day of year (DOY) 116, and ended on November 20th (DOY 324). In 2015 the irrigation season lasted from April 8th (DOY 98) to October 25th (DOY 298). The calculated irrigation doses were input in an irrigation controller (Agronic 2000, Sistemes Electrònics PRO-GRÉS, S.A., Lleida, Spain) and water was applied through a single pipe per tree row with three 2 L h^{-1} drippers per tree, 0.5 m apart. Fertilizers were injected once per week into the irrigation system to match the tree requirements (Fernández et al., 2013). All treatments received the same amounts of fertilizers. Climate in the area is typically Mediterranean, with mild, wet winters and little precipitation during the irrigation season (May to October). Average values of precipitation (P) and potential evapotranspiration (ET_o) in the area are 522.7 mm and 1531.5 mm, respectively (period 2002-2015). The soil had a 0.4 m deep sandy layer over a clayey layer with low conductance. Most roots were in the top sandy layer (Details in Fernández et al., 2013).

2.2. Soil, plant and weather measurements

All measurements described in this section and in Section 2.3 were made on both 2014 and 2015. From the 24 trees of each plot, measurements were made in the central 8 trees to avoid any border effect. Soil water status was assessed as described by Fernández et al. (2013). Basically, we used a Profile probe (Delta-T Devices Ltd., Cambridge,UK) to record volumetric soil water content (θ_v) values in the root zones of one tree per plot in three plots per treatment. The recorded values were used to calculate the seasonal course of the relative extractable water (REW), for all treatments.

One central tree per plot, in three out of the four plots of the all treatments, was instrumented with ZIM probes (also called leaf patch clamp pressure probe and now commercially named Yara Water-Sensors, YARA ZIM Plant Technology, Hennigsdorf, Germany). In each instrumented tree, a ZIM probe was clamped on a leaf of the east side of the canopy, at ca. 1.5 m above ground. Once every 5 min the output of the probe was sent via radio to a datalogger with a GPRS modem for data transfer to a server own by YARA ZIM Plant Technology GmbH to which we accessed via Internet. Details on both the ZIM probes and their performance when used in olive are given elsewhere (see review by Fernández 2017). Basically, the probes were able to measure continuously and automatically for the whole irrigation season, since they are not affected by weather conditions, dust, spraying, etc. (Fernández et al., 2011). Precaution should be taken, however, with traffic in the orchard, since they are magnetic and can be easily removed by tractors and machinery. When that happened, or when the sampled leave was detached from the tree by any reason, reclampling was made. That did not affect the application irrigation scheduling approach, since the State of the daily P_p curve collected before and after reclamplig was the same (reclamping was made on a new leaf of the same tree). Measurements of Ψ_{stem} were made every two weeks, for the entire irrigation seasons, in one leaf per tree sampled from two representative trees per plot and three plots per treatment. The selected leaves were close to a main branch and wrapped in aluminum foil ca. 2 h before measurements. These leaves were sampled from 11.30 GMT to 12.30 GMT and Ψ_{stem} measured with a Scholander-type pressure chamber (see Padilla-Diaz et al., 2016, for details). Leaf gas exchange measurements were made on the same days and trees than Ψ_{stem}. Measurements were made at ambient light and CO_2 conditions. We sampled young but fully developed leaves from the east part of the canopy, at ca. 1.5 m above ground. Measurements were made with a Licor LI-6400 portable photosynthesis system (Li-cor, Lincoln NE, USA), with a 2 cm x 3 cm standard chamber, at 08.00–09.00 GMT, the time for maximum daily stomatal conductance ($g_{s,max}$) and CO_2 net assimilation (A_{max}) in olive (Fernández et al., 1997).

Weather measurements were made as described by Fernández et al. (2013). Basically, main weather variables in the orchard were monitored by a Campbell weather station (Campbell Scientific Ltd., Shepshed, UK) located at the center of the area covered by the experimental plots. For the calculation of potential evapotranspiration values (ET_o) required to schedule irrigation with the crop coefficient approach data were collected from

a nearby standard weather station belonging to the Agroclimatic Information Network of the local government (https://www.juntadeandalucia.es/).

2.3. Growth and production measurements

Shoot growth was assessed by measuring the number of internodes of four current-year shoots per tree, in two trees per plot, each randomly selected from a cardinal point of the canopy and at ca. 1.5 m above ground. Measurements were made once per month from June to November, both in 2014 and 2015. Leaf area (LA) measurements in each plot were made after pruning in January with a LAI-2000 Plant Canopy Analyzer (LI-COR, Lincoln, NE, USA) (see Cuevas et al., 2013, for details) and also during the whole irrigation seasons, one every other week.

Fruit and virgin olive oil (VOO) yields were obtained after manual harvesting of three out of the eight trees in the central area of each plot, from the four plots per treatment. Harvesting was made on November 21st 2014 (DOY 325) and on November 6th 2015 (DOY 310). Total fruits per tree were weighted separately. From each plot we took 2 kg of fruit for the oil physical extraction with the Abencor method (Comercial Abengoa S.A., Seville, Spain), as detailed by Martinez et al. (1975). Fruit water productivity (WP) and oil WP were calculated as kilograms of fruit or oil per cubic meter of applied water. Although the standard definition for WP (Molden et al., 2010; Perry, 2011) considers the amount of water actually consumed by the crop and not the water applied, our soil water measurements suggested that all the water applied was consumed by the crop.

Oil accumulated in the fruits was determined from June to November, both in 2014 and 2015. We collected manually around 100 fruits from ca. 1.5 m high of five out of the eight central trees of each plot (the other three trees were used to determine yield, as described above). After grinding the fruits we obtained ca. 20 g of fresh paste, which was dehydrated at 105 °C. The oil of the dehydrated paste was chemically extracted by using hexane as a solvent (Soxhlet's method, García et al., 2013). Results were expressed as percentage of oil per dry weight.

2.4. Statistical analysis

We used linear mixed models (LMM) with Tukey´s post-hoc comparisons to analyze the effects of the irrigation treatment (fixed factor) on REW, Ψ_{stem}, $g_{s,max}$, $A_{,max}$, number of internodes, leaf area and fruit and VOO yield, as dependent variables at $\alpha < 0.05$. We used leaf identity within plot as the random factor structure in the Ψ_{stem}, $g_{s,max}$, and $A_{,max}$ analyses to describe appropriately our experimental design and deal with the non–independent nature of the spatial experimental design. In the rest of comparisons the random factor was not necessary as we only have one value per plot. When no normal and heterocedastic residuals were obtained, appropriate transformation of the variable was used. Data are shown as mean ± standard error. We used the R software (R Core Team, 2012) to perform

the statistical analysis, with help of 'nlme' packages (Pinheiro et al., 2011) for LMM and for pair comparisons 'multcomp' (Hothorn et al., 2008).

3. RESULTS

3.1. Water supplies, atmospheric demand and soil water content

Results on the irrigation amounts (IA) supplied to each treatment are shown in Table 1. The good agreement between the aimed and the actual doses shows a reasonably good irrigation management. Still, in 2015 total water supplies for the 45RDI treatments were closer to 50% than to 45% of the irrigation needs. That was a year of high atmospheric demand (1581.37 mm) and low precipitation (237.60 mm), so the calculated irrigation needs (5855 m^3 ha^{-1}) were unusually high (Table 1), as compared to previous years in which this amount was usually below 5000 m^3 ha^{-1} (Fernández et al., 2017). The total IA applied in 2015 to both 45RDI treatments was quite similar, although with marked differences on periods 2 and 3 (Table 1). The seasonal courses of IA for the three treatments are displayed in Fig. 1A, together with the collected precipitation.

Values of relative extractable water (REW) calculated from the soil water measurements made in 2015 are shown in Fig. 1B. For the FI treatment they were usually around 0.8, suggesting non-limiting soil water conditions for olive. The low REW value registered in the FI treatment on DOY 225 (Fig. 1B) was probably due to the peak on atmospheric demand registered on the previous days (Fig. 2). For the two 45RDI treatments REW values showed similar trends, with no differences between treatments. Before periods 2 and 3, the soil in the two 45RDI treatments was very dry but recovered quickly after the increase on irrigation of both periods, and hence, no differences in REW were observed among the FI and the 45RDI treatments (Fig. 1B). In between period 2 and period 3, REW values showed severe soil water depletion in the 45RDI treatments, as expected. In the autumn, the rainfall and IA supplied by irrigation avoided the soil becoming so dry. Main features of the REW seasonal courses in 2015 were similar to those in 2014 (see Padilla et al., 2016), with no differences among treatments on periods 2 and 3, for any of the two years.

Table 1. Water supplies (IA = irrigation amounts; P = precipitation) and potential evapotranspiration (ET_o) in the experimental orchard for the two irrigation seasons (2014 and 2015). All values are in millimeters. Values of IA are also expressed as percentages of irrigation needs (% IN). DOY = day of year. Values with an asterisk were published by Padilla-Díaz et al. 2016 and with two asterisks by Hernandez-Santana et al. 2017.

	Whole year	Irrigation period	Period 2	Period 3
2014		DOY 116–324	DOY 154–185	DOY 238–259
P	549.4*	317.6*	8.2	5.3
ET_o	1437.6*	1110.1*	191.3	143.5
IA in FI		462.9 (87.1% IN)*	93.1 (104.3 % IN_{P2})*	69.7 (103.6% IN_{P3})*
IA in $45RDI_{CC}$		238.2 (44.8% IN)*	72.2 (81.0 % IN_{P2})*	66.8 (99.0 % IN_{P3})*
IA in $45RDI_{TP}$		235.9 (44.4% IN)*	61.5 (68.0% IN_{P2})*	67.1 (100.0 % IN_{P3})*
2015		DOY 98-298	DOY 146-173	DOY 237-257
P	237.60**	76.22**	0.00	0.00
ETo	1581.33**	1223.65**	193.48	123.00
IA in FI		585.55 (101.5% IN)**	94.62 (101.7% IN_{P2})	362.16 (105.8% IN_{P3})
IA in $45RDI_{CC}$		286.98 (49.8% IN)**	73.16 (78.6% IN_{P2})	61.21 (107.3% IN_{P3})
IA in $45RDI_{TP}$		290.33 (50.3% IN)	83.79 (90.0% IN_{P2})	50.93 (89.3% IN_{P3})

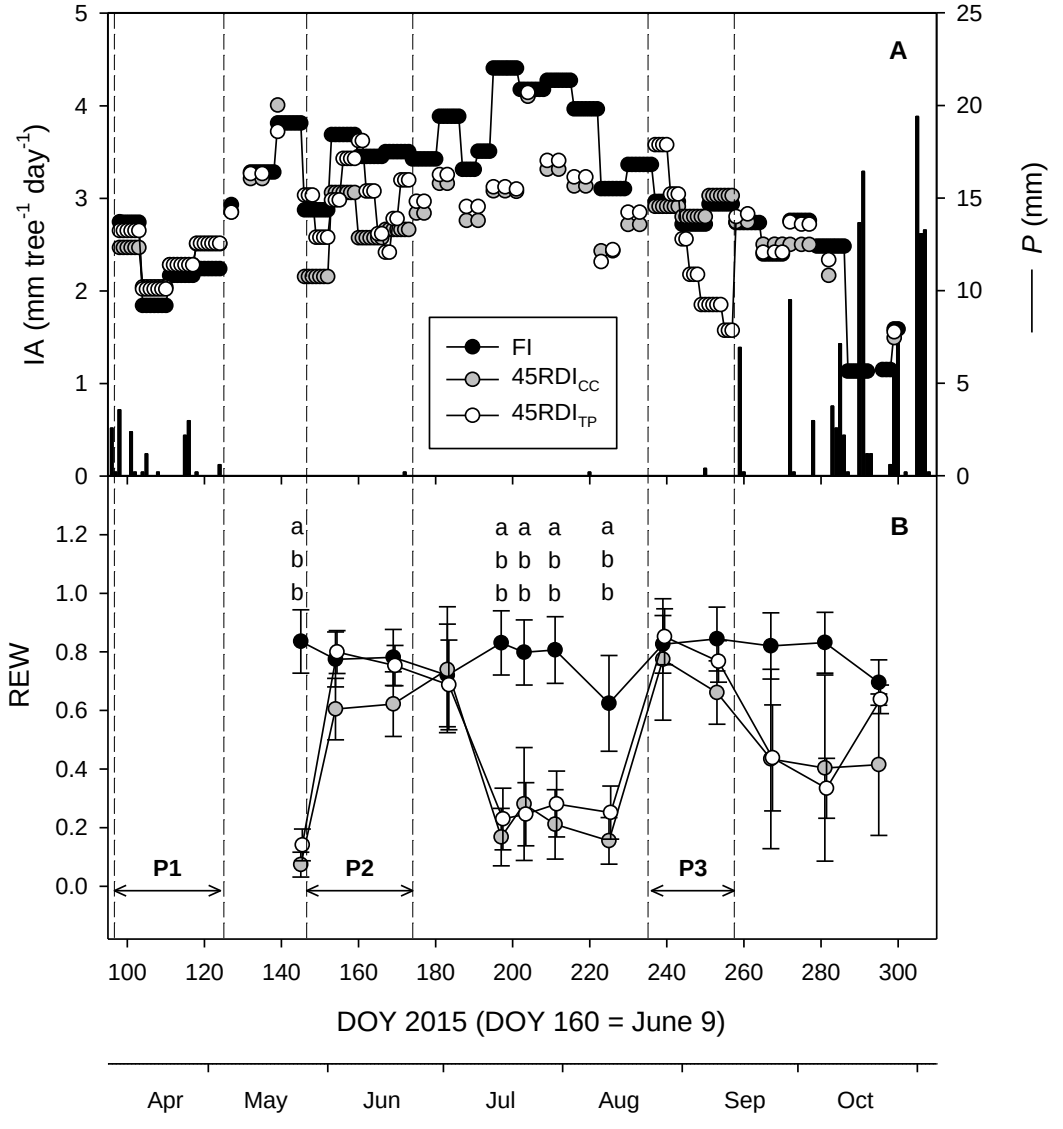

Fig. 1. Seasonal courses of both the irrigation amounts (IA) supplied to each treatment and the precipitation (*P*) collected in the orchard (A), and the values (avg ± SE) of relative extractable water (REW) derived from the soil water contents measured in the plots of each treatment (B). Measurements were made on the irrigation season of 2015. A similar figure but with data of 2014 was published by Padilla et al. (2016). P1, P2 and P3 correspond to the periods 1, 2 and 3 in which olive is most sensitive to water stress (Fernández et al., 2013). Different letters indicate significant differences between treatments at $p < 0.05$. Letters are not shown when no differences were found. DOY = day of year. Part of the data of REW was shown in Hernandez-Santana et al. (2017).

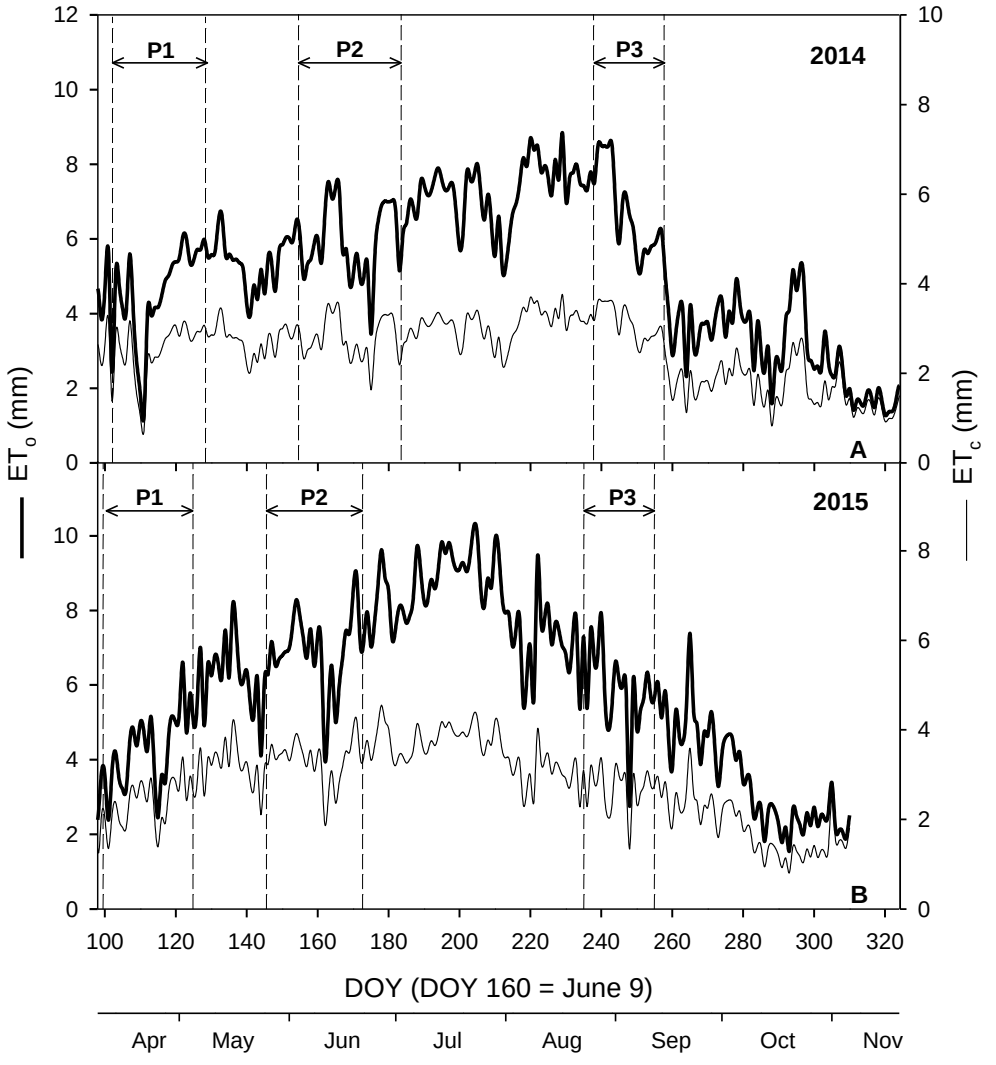

Fig. 2. Seasonal courses, for the irrigation seasons of 2014 (A) and 2015 (B), of both the potential evapotranspiration (ET_o) in the area and the crop evapotranspiration (ET_c) estimated with the crop coefficient approach for the olive orchard at Sanabria. P1, P2 and P3 correspond to the periods 1, 2 and 3 in which olive is most sensitive to water stress (Fernández et al., 2013). DOY = day of year.

One of the concerns of Padilla-Diaz et al. (2016) was the suitability of the 15% value for changing IA. Although percentages ranging from 10 to 20% are common in this type of studies (Goldhamer and Fereres, 2004; Conejero et al., 2007; Velez et al., 2007; Fernández et al., 2008a), they had no evidence on 15% being a proper value. To assess whether that value was appropriate, we determined the coefficient of variation (CV, %) of the daily values of the irrigation needs (IN) calculated at Sanabria with the crop coefficient approach, on periods 2 and 3 of the two experimental years (Table 2). The coefficient of variation was calculated as the ratio of the standard deviation of the daily IN values to the average IN for each period, expressed in percentage. With those values we calculated the

mean of the CV and the standard error for daily changes in IN. As shown in Table 2, the average CV for IN was 15.14%, a value similar to the 15% change in the irrigation amount adopted in our irrigation scheduling approach.

Table 2. Daily variation of the irrigation needs for each Period under our irrigation scheduling approach based on the ZIM system. CV IN (%) values are the coefficient of daily variation of irrigation needs. DOY = day of year.

Year	Period	CV IN (%)
2014	P2 (DOY 154-185)	16.77
	P3 (DOY 238-259)	15.14
2015	P2 (DOY 146-173)	14.58
	P3 (DOY 237-257)	16.78

In addition to the accumulated ET_o values for the two irrigation seasons, Table 1 shows the ET_o values for the whole 2014 and 2015, and for the periods 2 and 3 of each year, and Fig. 2 shows the seasonal ET_o courses for both irrigation seasons. Also shown in that figure are the seasonal courses of the crop evapotranspiration (ET_c) values calculated with the crop coefficient approach (Section 2.1).

3.2. Plant water status versus leaf turgor related measurements

Figure 3 shows the results from applying the Irrigation scheduling approach developed by Padilla-Díaz et al. (2016) to schedule irrigation in the $45RDI_{TP}$ treatment, on periods 2 (Fig. 3A,B) and 3 (Fig. 3C,D) of 2015, as compared to the crop irrigation approach applied. Figures 3A and 3C display the collected P_p curves from the sampled tree that first showed the onset of water stress through the shift from State 1 to State 2. Arrows indicate the days in which the irrigation amount was increased (arrow up) or decreased (arrow down) by 15%, as a response to changes in the State of the daily P_p curve. The resulting irrigation amounts are displayed in Fig. 3B (period 2) and 3D (period 3). On period 2, the total amounts of water supplied to the $45RDI_{CC}$ and $45RDI_s$ treatment amounted to 79% and 90% of the irrigation needs calculated for the FI treatment, respectively (Fig. 3B). On period 3, these values were of 107% and 89%, respectively (Fig. 3D). See Padilla et al., (2016) for a similar figure with data of 2014.

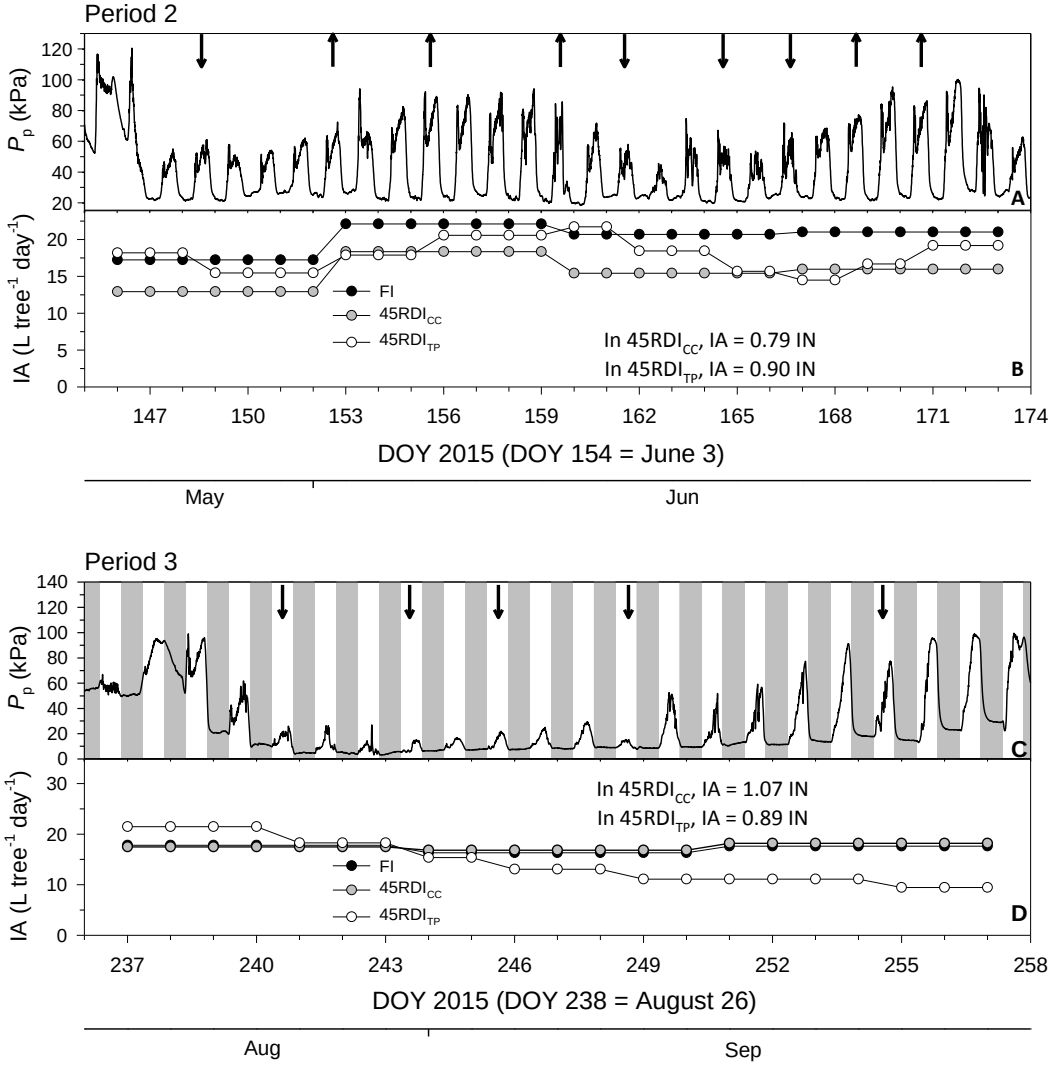

Fig. 3. Time courses of the P_p values recorded on a 45RDI$_{TP}$ representative tree in period 2 (A) and period 3 (C) of the 2015 irrigation season (see Fernández et al., 2013, to identify those periods in which olive is most sensitive to water stress). Also shown are the irrigation amounts (IA) supplied to each treatment in each period, expressed as a fraction of the calculated irrigation needs (IN) for the period (B,D). IA was increased (arrows up) or decreased (arrows down) according to changes in the State of the daily P_p curves and the weather forecast of three days (see the irrigation scheduling approach described in the Introduction section). DOY = Day of year.

For 2015, the tree-to-tree variability in the State of the P_p curves from all trees instrumented with ZIM probes and the seasonal courses of Ψ_{stem} for each treatment are shown in Fig. 4. A similar figure was published by Padilla et al. (2016) with data from 2014. For all treatments, the appearance of State 1, 2 or 3 was in accordance to the plant water status as represented by Ψ_{stem}. Thus, in periods 2 and 3, most trees showed State 1 or 2, while in between the two periods, when the irrigation amounts of the 45RDI trees markedly decreased (Fig. 1), State 3 was common in nearly all 45RDI trees. The same was observed in between period 3 and harvesting, although on this period the number of days in which the 45RDI trees showed State 3 was lower, likely because of the lower atmospheric demand (Fig. 2) and greater water supplies both from irrigation and rainfall (Fig. 1). On these autumn days, the $45RDI_{TP}$ trees showed State 3 on a greater number of days than the $45RDI_{CC}$ trees, despite of both treatments receiving similar amounts of water. Probably, the lower irrigation amounts applied to $45RDI_{TP}$ on period 3, as compared to $45RDI_{CC}$ (Fig. 3D), led to differences on the soil water status between both treatments, which could have caused the observed differences on State. The REW data show no significant differences among treatments for that time of the year, but the variability was very high, as shown by the standard errors shown in the Fig. 1B, such that actual differences in soil water content could have been enough to explain the differences on the State shown in Fig. 4.

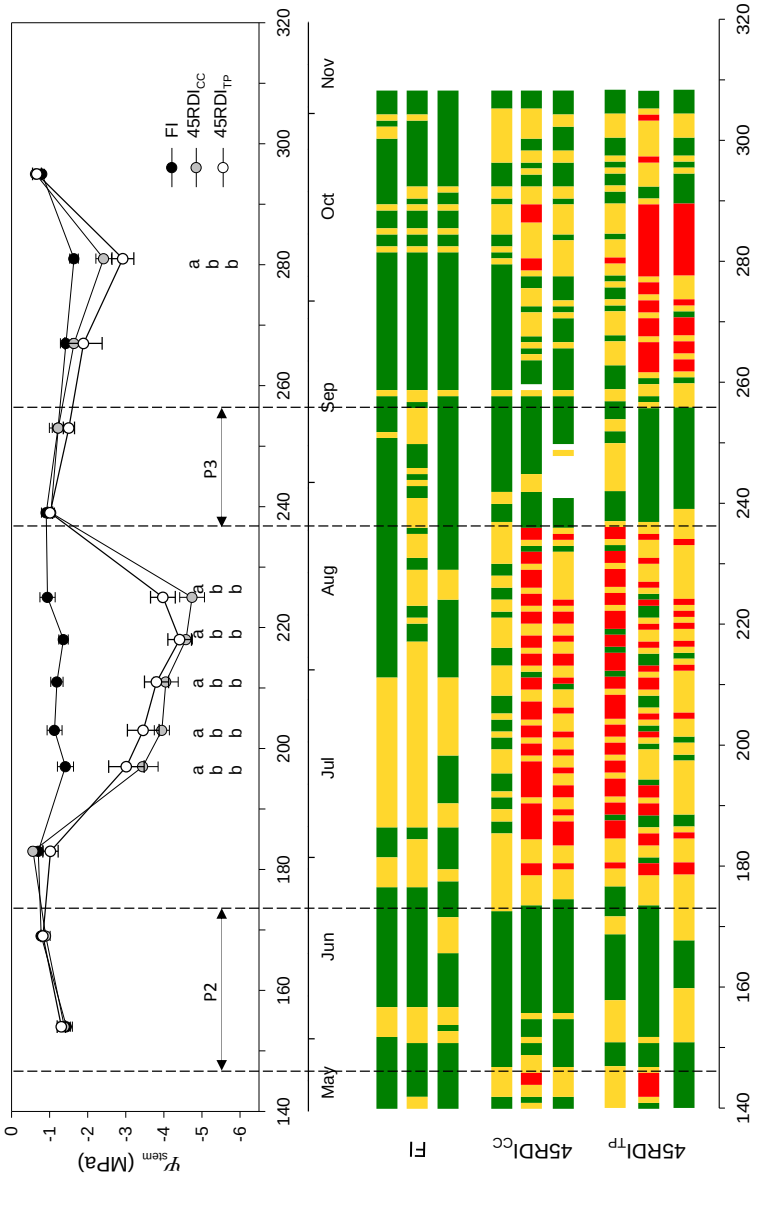

Fig. 4. Seasonal courses of midday stem water potential (Ψ_{stem}, avg. ± SE) measured in FI, 45RDI$_{CC}$ and 45RDI$_{TP}$ trees of the Sanabria orchard during the irrigation season of 2015. Different letters indicate significant differences between treatments, at $p < 0.05$. Letters are not shown when no differences were found. P_p curves were collected by three ZIM probes per treatment and shown here through State 1 (low water stress), State 2 (moderate stress) and State 3 (severe stress) by horizontal colour bars. P2 and P3 correspond to periods 2 and 3 represented in Fig. 3. DOY = Day of year.

3.3. Gas exchange, growth and production

As expected, the 45RDI treatments had a significant influence not only on the plant water status, as described above and in Padilla et al. (2016), but also on gas exchange. Thus, significant differences on $g_{s,max}$ and A_{max} between the FI and the 45RDI treatments were observed not only in between period 2 and 3 and from period 3 to harvest, but also during periods 2 and 3, especially at the beginning of both periods, i.e. on the first days after water recovery (Fig. 5). In 2014, the low $g_{s,max}$ and A_{max} values recorded on DOY 226 and 268 (Fig. 5A,B) were likely due to those days being cloudy, with low radiation levels. Similarly to Ψ_{stem}, there were no differences for $g_{s,max}$ and A_{max} among 45RDI treatments, except in the autumn of 2015, when lower values were sometimes recorded, for both variables, in $45RDI_{TP}$ trees than in $45RDI_{CC}$ trees.

For the two experimental years, the number of internodes in shoots of the year was greater in FI trees than in 45RDI trees (Fig. 6). No differences were detected between the two 45RDI treatments. Similarly, the FI trees showed greater values of leaf area than the 45RDI trees but differences among the two 45RDI treatments were not significant either (Fig. 7).

In Figure 8 we show the percentage of oil accumulated in the fruits of every treatment along the two irrigation seasons. In both years, the synthesis of oil began at the end of June (ca. DOY 180) and the greatest rate of oil synthesis occurred from the second week of October (ca. DOY 280). As compared to the FI treatment, in July and August the two 45RDI trees lagged behind in oil synthesis. During the autumn, however, no differences among treatments were observed, such that, at harvesting, fruits of all treatments showed similar oil content expressed as percentage of dry weight.

Results from 2014 and 2015 shows that, on average, with 45RDI treatments we supplied 47.3%- of IN, and obtained 76.2% of fruit yield and 75.1% of oil yield, as compared to the FI treatment. However, differences among treatments, for both fruit yield or oil yield, were never significant at $\alpha = 0.05$ (Table 3). In 2015, however, the *P* values were close to the standard significant level (0.068 for fruit production and 0.086 for oil production), suggesting an effect of the FI treatment, as compared to the 45RDI treatments, on both production variables. The high standard errors suggest that the number of replications ($n = 4$) was too low to account for the high tree-to-tree variability on production. Results in Table 3 suggest lower differences, for both fruit and oil yield, between the two 45RDI treatments than in between them and the FI treatment. This agrees with results on water productivity (WP). Thus, the values of WP show no statistical differences between FI and 45RDI in 2014, while in 2015 significant differences were detected for WP, both for fruit and oil, between the FI and the 45RDI treatments. Differences for the two 45RDI treatments on WP were negligible.

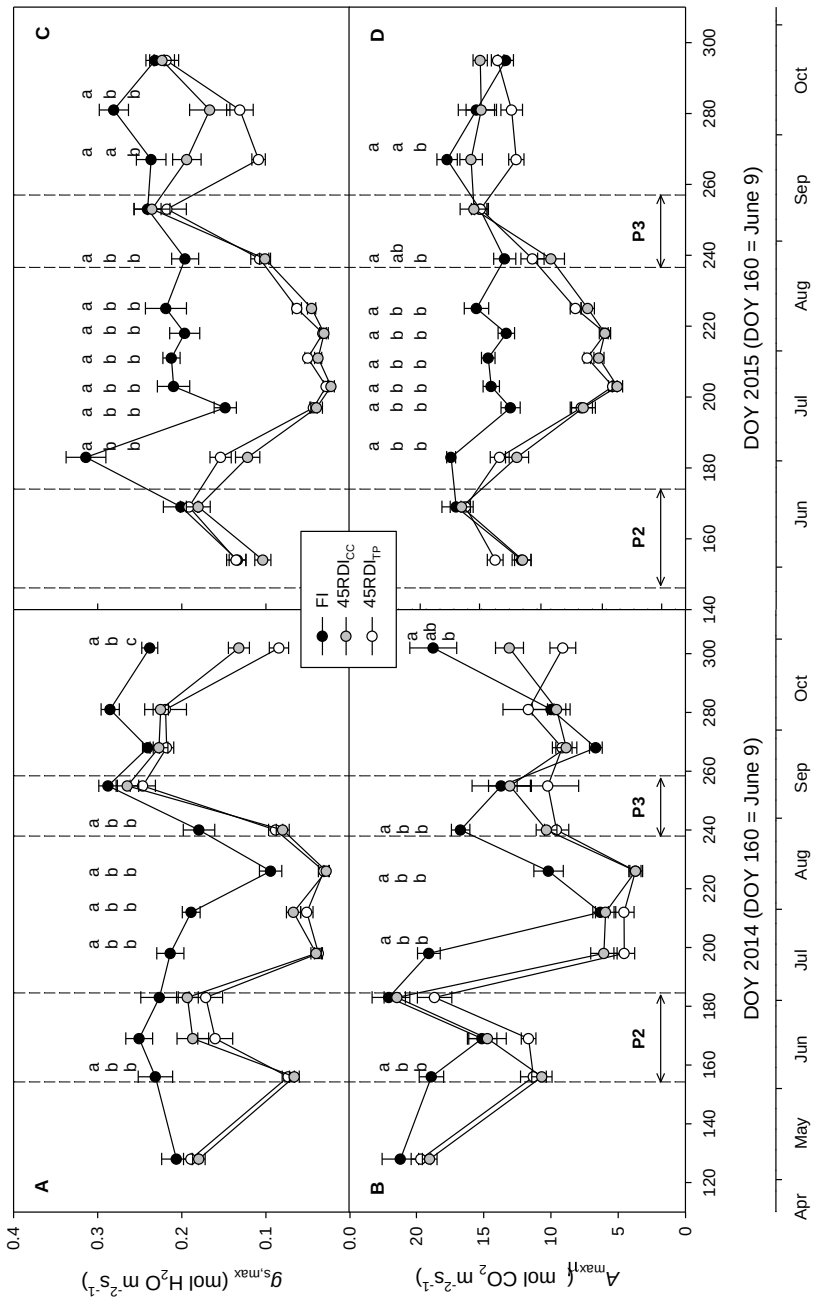

Fig. 5. Seasonal courses of maximum daily stomatal conductance ($g_{s,max}$) (A,C) and and CO_2 net assimilation (A_{max}) (B,D) measured in FI, 45RDI$_{CC}$ and 45RDI$_{TP}$ trees of the Sanabria orchard during the irrigation seasons of 2014 and 2015. Values are avg. ± SE and different letters indicate significant differences between treatments at $p < 0.05$. Letters are not shown when no differences were found. P2 and P3 correspond to periods 2 and 3 represented in Fig. 3. DOY = Day of year. Part of the data of $A_{,max}$ were shown in Hernandez-Santana et al. (2017).

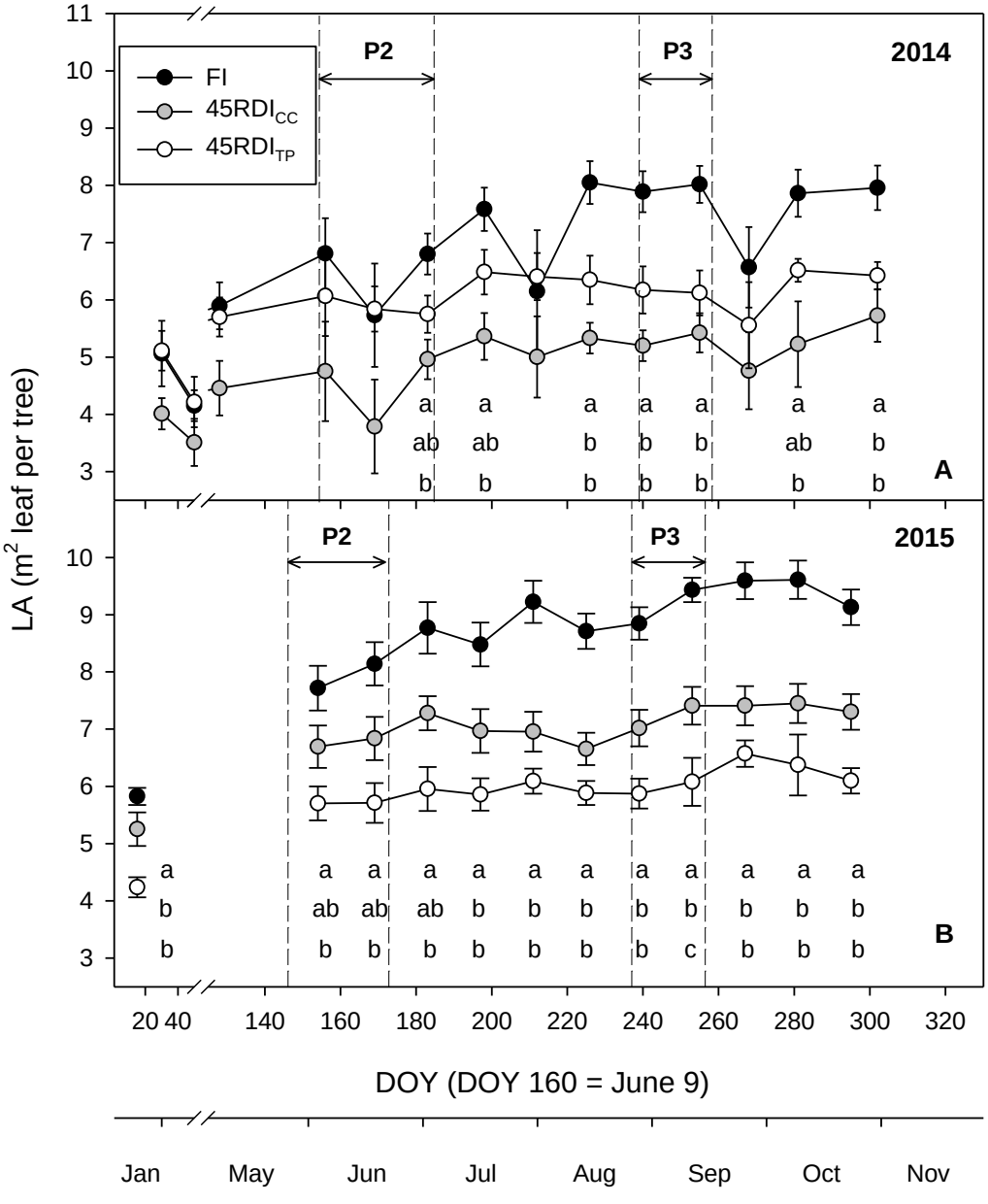

Fig. 6. Seasonal courses of the number of internodes in current-year shoots recorded in 2014 (A) and 2015 (B). Values are avg. ± SE and different letters indicate significant differences between treatments at $p < 0.05$. Letters are not shown when no differences were found. P2 and P3 correspond to periods 2 and 3 represented in Fig. 3. DOY = Day of year.

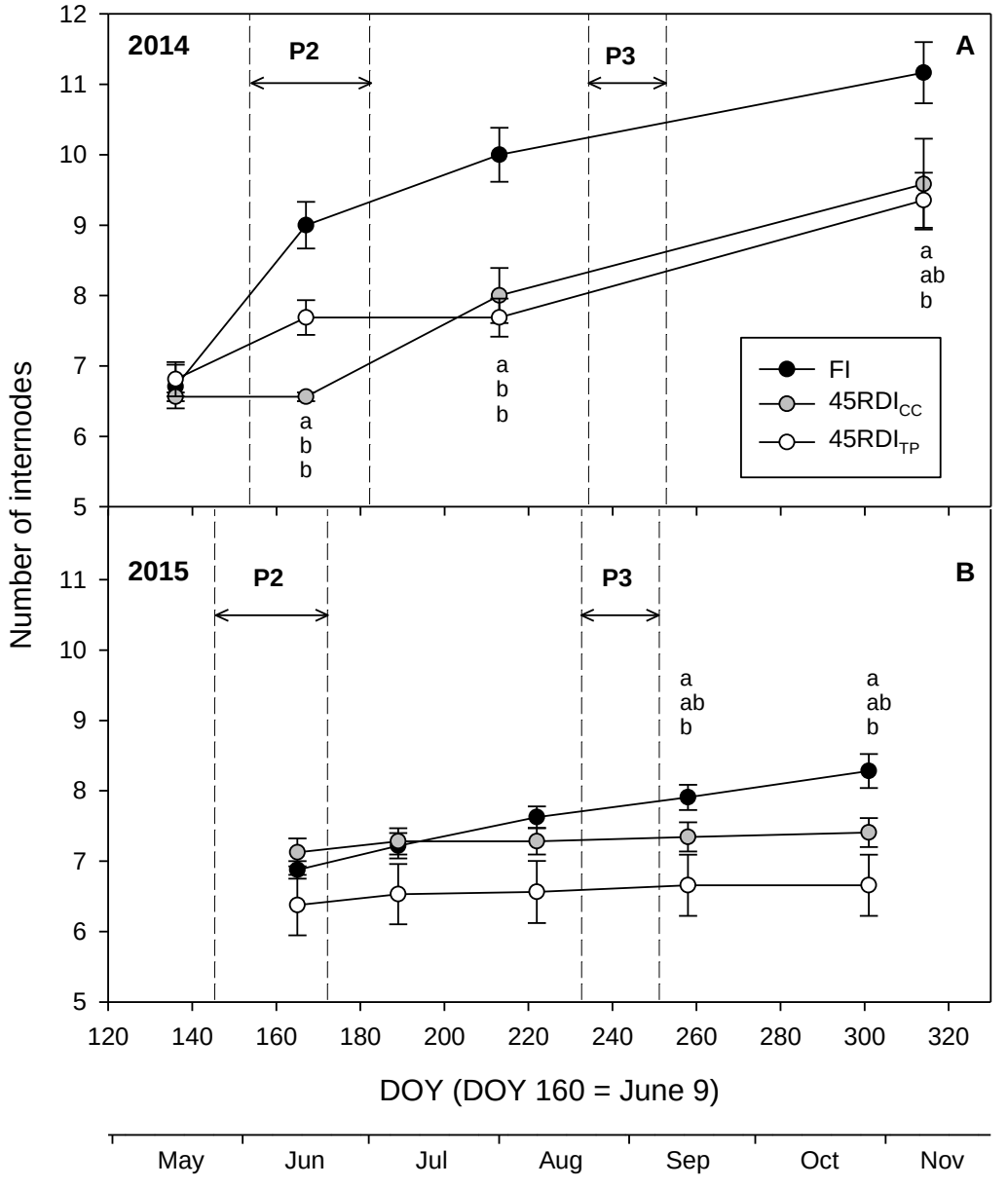

Fig. 7. Seasonal courses of leaf area (LA) recorded in2014 (A) and 2015 (B). Values are avg. ± SE and different letters indicate significant differences between treatments at $p < 0.05$. Letters are not shown when no differences were found. P2 and P3 correspond to periods 2 and 3 represented in Fig. 3. DOY = Day of year.

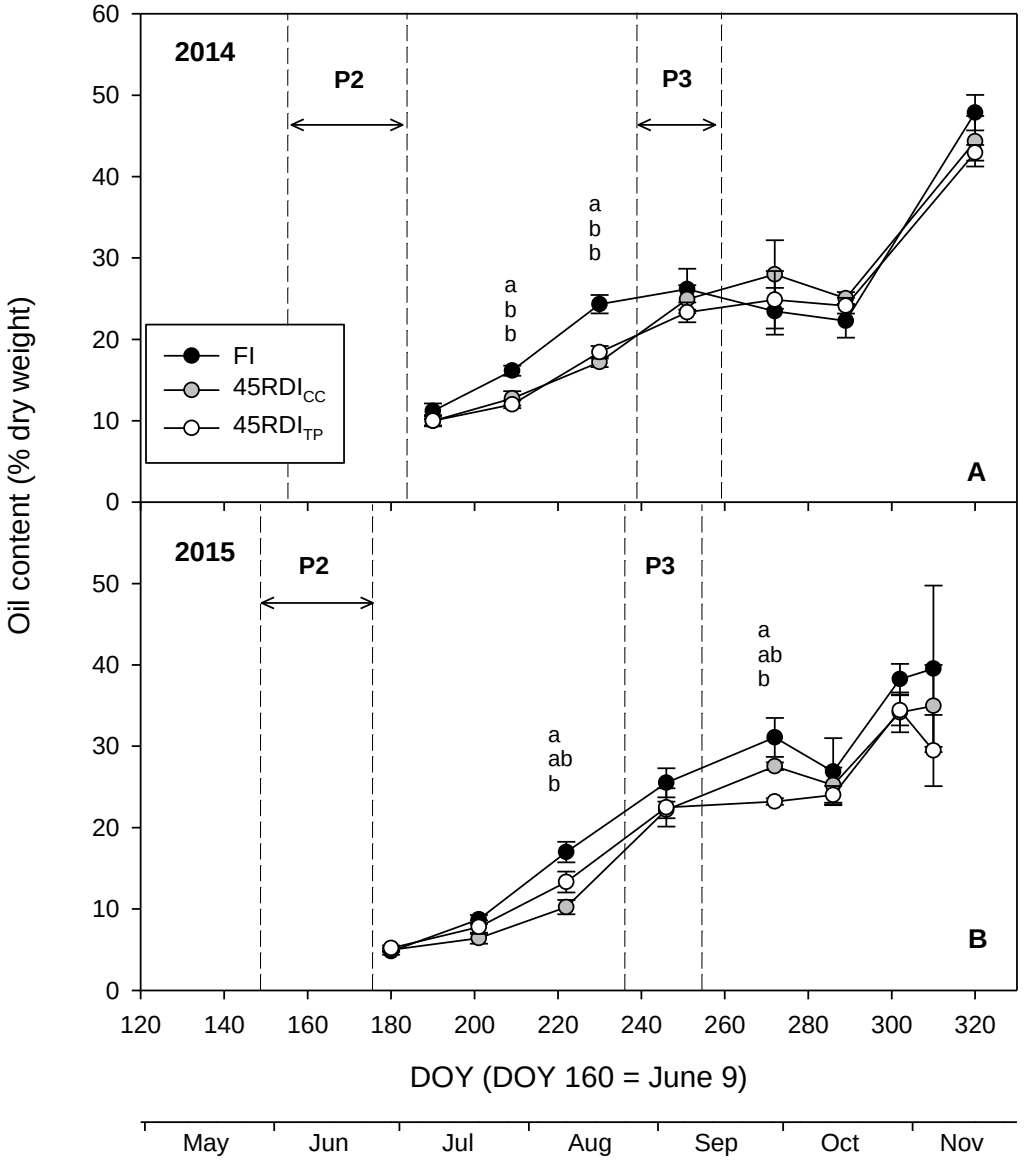

Fig. 8. Seasonal courses of oil accumulation recorded in 2014 and 2015. Values are avg. ± SE and different letters indicate significant differences between treatments at $p < 0.05$. Letters are not shown when no differences were found. P2 and P3 correspond to periods 2 and 3 represented in Fig. 3. DOY = Day of year.

Table 3. Fruit and oil yield, water productivity of fruit and oil for each treatment and experimental years (2014 and 2015). Values for each treatment are in average ± SE, *n* = 4. Different letters indicate significant differences between treatments at $p < 0.05$. Values with an asterisk were published by Padilla-Díaz et al. 2016 and with two asterisks by Hernandez-Santana et al. 2017.

Year	Treatment	Fruit yield (kg ha^{-1})	Oil yield (kg ha^{-1})	WP Fruit (kg ha^{-1} mm^{-1})	WP Oil (kg ha^{-1} mm^{-1})
2014	FI	19283.0 ± 2708.5 a*	1875.8 ± 288.6 a	41.6 ± 5.9 a*	4.1 ± 0.6 a
	$45RDI_{CC}$	13443.0 ± 2847.9 a*	1195.0 ± 258.0 a	53.4 ± 12.0 a*	5.0 ± 1.1 a
	$45RDI_{TP}$	17025.6 ± 2077.0 a*	1641.5 ± 132.4 a	72.2 ± 8.8 a*	7.0 ± 0.6 a
2015	FI	19724.8 ± 1608.28 a**	1957.4 ± 183.7 a**	33.7 ± 2.7 a	3.3 ± 0.3 a
	$45RDI_{CC}$	15073.8 ± 386.04 a**	1387.4 ± 86.1 a**	52.5 ± 1.4 b	4.8 ± 0.3 b
	$45RDI_{TP}$	13865.6 ± 757.15 a	1534.5 ± 130.6 a	47.8 ± 2.6 b	5.3 ± 0.5 b

4. DISSCUSION

4.1. Impact of the scheduling irrigation approach on crop physiology and crop performance

Similarly to 2014 (see Padilla-Díaz et al., 2016, for details), in 2015 no significant differences either on the total irrigation amount applied or on the seasonal course of REW were found between $45RDI_{CC}$ and $45RDI_{TP}$ (Fig. 1). For both period 2 and 3, the irrigation amounts supplied to the $45RDI_{TP}$ trees was ca. 90% of IN (Table 1, Fig. 3), which means that our irrigation scheduling approach based on the use of leaf turgor related measurements was suitable for ensuring non-limiting soil water conditions on these periods of high crop sensitivity to water stress. The water status of the $45RDI_{TP}$ trees showed, in fact, no differences on periods 2 and 3 with the FI trees. Values of Ψ_{stem} values were nearly always above –1.2 MPa, a threshold value for safe hydraulic functioning in olive (Torres-Ruiz et al., 2013; Hernandez-Santana et al., 2016). This agrees with trees of the 45RDI treatments being in State 1 or 2 most of the days on periods 2 and 3. In fact, the number of days in State 2 shown by the 45RDI trees on both periods was similar to that of the FI trees. This suggests that the occurrence of State 2 on those periods was due more to the high atmospheric demand recorded on those days (Fig. 2) than to a lack of water in the root zone.

Values of both $g_{s,max}$ and A_{max} were also similar for all treatments, on periods 2 and 3 (Fig. 5). This is with the exception of the first days of both periods, on which gas exchange was lower in the 45RDI trees than in the FI trees. This was expected, since it is known than in olive, Ψ_{stem} recovers soon after water stress than gas exchange. This, the full recovery of $g_{s,max}$ and A_{max} may take a few days depending on the severity of the water stress suffered before the recovery irrigation (Fereres et al., 1996; Fernández et al., 1997). The mechanisms behind that behaviour has not been clearly stablished yet. Nevertheless, Torres-Ruiz et al. (2013) suggested that this stomatal behaviour during stress and recovery might be due to the ABA synthetized during the water stress period, which controlled stomata opening at the beginning of the recovery period. The 45RDI strategy applied in the orchard implies a period of water stress before periods 2 and 3, in which the soil can become markedly depleted (Fig. 1B). As described above, in our irrigation scheduling approach we irrigated with 120% of the irrigation needs on the first days of both periods, for a quick recovery of the soil water status, aiming to minimise the described delay in the recovery of both $g_{s,max}$ and A_{max}.

Plant growth was reduced by the 45RDI treatments, as expected, but no differences were observed between $45RDI_{CC}$ and $45RDI_{TP}$ either for the number of internodes in the current-year shoots (Fig. 6) or leaf area (Fig. 7). It is well known that growth in olive is very sensitive to water stress, as occurs in other fruit tree species (Fernández, 2014b; Rosecrance et al. 2015; Cajias et al. 2016), so the lower number of internodes and reduced leaf area in the 45RDI trees was expected. This effect of the 45RDI treatments on growth agrees with the lower levels of A_{max} found in these trees (Fig. 5), as compared to the FI trees. The reduction both of $g_{s,max}$ and A_{max} was not necessarily negative. On the one hand,

reducing g_s can improve water use efficiency, since the A vs. g_s relationship in olive shows A becoming asymptotic for g_s values above ca. 0.2 mol m^{-2} s^{-1} (Fernández et al., 2008b). On the other hand, a reduction in A contributes to avoid excessive growth (Hernandez-Santana et al., 2017), which may be an advantage in SHD olive orchards both to facilitate mechanical harvesting with the vineyard type straddle-harvesters normally used in these orchards (León et al., 2007) and to avoid competency for light among trees (Gomez-del-Campo et al., 2009; Connor et al., 2012). Both factors ensure a long productive life of the orchard (Fernández et al., 2017).

In between periods 2 and 3, when REW values ranged most of the time from 0.2 to 0.3 only for the 45RDI treatments (Fig. 1B), and maximum values of atmospheric demand were recorded (Fig. 2), the 45RDI trees became severely stressed. Thus, from mid-July to the end of August the 45RDI trees showed midday Ψ_{stem} values in between ca. –3.0 and –4.7 MPa (Fig. 4), $g_{s,max}$ values of ca. 0.05 mol H_2O m^{-2} s^{-1} and A_{max} values around 4 mol CO_2 μm^{-2} s^{-1}. It is known, however, that the olive tree is quite tolerant to water stress at this time of the year (Moriana et al., 2003; Perez-Martin et al., 2009), and that it is able to recover from severe water stress with a reduced impact on crop performance, providing enough water during both period 3 and ripening is available (Lavee et al., 1990; Lavee and Wodner, 1991). This agrees with the dynamics of oil accumulation observed in our orchard, which showed a recovery of the oil content in the fruits after the beginning of period 3 (Fig. 8).

Concerning production, oil accumulation in the fruits during pit hardening was affected in the 45RDI trees, as compared to the FI trees (Fig. 8). During ripening, however, similar values were observed in all treatments. For fruit and oil yield, our statistical analysis showed no differences between treatments (Table 3). Olive presents a linear increase of production with water supply, until a certain level from which little increase on production, if any, is observed when increasing the water supply (Moriana et al., 2003). Other authors have reported little impact on fruit and oil yields despite significant reductions on water supply (Grattan et al., 2006; Rosecrance et al., 2015). In our case, and as indicated in Section 3.3, the number of replicas we had was too low to properly account for the high tree-to-tree variability on both fruit and oil yield existing in the orchard. It is clear, however, that similar results on fruit and oil yield were obtained independently of the approach used to schedule the 45RDI treatment, which means that, for both production variables, our irrigation scheduling approach based on the use of the ZIM system was as effective as that based on the crop coefficient approach. The same can be said for the water productivity (WP) values (Table 3). In fact, at least in 2015 differences on fruit and oil WP were significant in between the FI and the 45RDI treatments, with no differences between $45RDI_{CC}$ and $45RDI_{TP}$.

4.2. Suitability of the scheduling irrigation approach for commercial orchards

As detailed above, our results suggest similar crop performance for both $45RDI_{CC}$ and $45RDI_{TP}$. Previous results obtained by our group at the Sanabria orchard, with similar irrigation strategies as the 45RDI but with different levels of water stress, all scheduled with the crop coefficient approach, suggested that $45RDI_{CC}$ is a suitable option for SHD olive orchards similar to our experimental orchard (Fernández et al., 2013, 2017; García et al., 2017). However, and as Padilla-Diaz et al. (2016) already pointed out, the required values of both the crop coefficient (K_c) and the potential evapotranspiration (ET_o) in the area are not available for many olive orchards. On the top of that, the crop coefficient approach implies a delay in the scheduling of irrigation, since weather data must be collected prior to the calculation of ET_o. The irrigation scheduling approach proposed by Padilla et al. (2016) and further tested in this work, relies on continuous and automatic leaf turgor related measurements. This real-time data information is suitable for irrigation scheduling in olive (Fernández 2017). Fernández (2014b) made a comparative study on three different methods to schedule irrigation in SHD olive orchards, based, respectively, on sap flow, trunk diameter variations and leaf turgor related measurements. They reported that the ZIM system used for leaf turgor related measurements was the easiest to install and use, and robust enough to withstand field conditions for long irrigation seasons. The potential and limitations of these three plant-based variables to derive suitable plant water stress indicators and to schedule irrigation in commercial orchards was analysed not only by Fernández (2014b), but also by Fernández (2017) and Fernández et al. (2017), and they all agreed on the high potential of leaf turgor related measurements for precision irrigation. Egea et al. (2017) made a financial assessment of the three mentioned methods to schedule regulated deficit irrigation in super high density olive orchards, and concluded that scheduling irrigation with the ZIM method, i.e. from leaf turgor related measurements, was the most profitable one. Our results confirm the advantages of the irrigation scheduling approach proposed by Padilla et al., 2016. Among the main ones is that, contrarily to sap flow and trunk diameter variations records, no data processing is required, because the visual analysis of the P_p daily curves is enough to identify the State, i.e. the level of water stress, of the monitored trees. A procedure for the automatic identification of the State shown by daily P_p curves, based on the use of random forest models, has been recently published by Fernandes et al. (2017), which will facilitate the application of the irrigation scheduling approach to commercial orchards. In addition, the method can be combined with airborne imagery for the zoning or zonification of the orchard. This allows for differential irrigation doses and frequencies depending on the variation in water requirements identified within the orchard. Finally, the combination of leaf turgor related measurements with the 3-day weather forecast allows for an early response of irrigation management to environmental conditions. These features confer our irrigation scheduling approach a high potential for precision irrigation, which may significantly contribute to the rational water use in super high density olive orchards (Fernández, 2017; Fernández et al., 2017).

The irrigation scheduling approach has, however, several limitations. First, caution must be taken when assuming a particular water stress level to the State shown by the P_p curve. Thus, Marino et al. (2016) found lower threshold values of Ψ_{stem} for the olive Sicilian genotypes 'Nocellara del Belice' and 'Olivo di Mandanici' than those reported by Fernández et al. (2011) and Ehrenberger et al. (2012) for 'Arbequina' trees. Further studies are then needed to establish the extent at which the ranges of water stress for States 1 to 3 depend on the cultivar and orchard conditions. Second, neither the 120% increase in the irrigation amount on the first days of periods 1 to 3 nor the 15% change in the irrigation amount made afterwards, have been contrasted against the crop physiology or crop performance. The fact that the average coefficient of variation value of the irrigation needs agrees with the 15% percentage of change on the irrigation amount (Table 2) suggests that this percentage is reasonable. This supports that the use of this percentage recommended for our irrigation scheduling approach is suitable for proper irrigation scheduling in orchards similar to our experimental orchard. In any case, the empirical character of the two percentages adopted in the irrigation scheduling approach may curtail their reliability when applied to other orchards with different conditions. Third, the ZIM probe does not work properly beyond a certain level of water stress which, in our case, was reported to be that occurring at ca. $\Psi_{stem} < -1.7$ MPa. This is not limiting for scheduling irrigation on periods 1, 2 and 3, because Ψ_{stem} is usually greater than –1.7 MPa thanks to the high irrigation amounts applied on those days. Still, State 3 was often found in between periods, when the irrigation amounts are low (Fig. 4) and, as explained by Ehrenberger et al. (2012), the information provided by the ZIM probes on those days is not useful to assess the actual water stress of the trees. Irrigation scheduling in between periods must relay, therefore, on a different method. Padilla et al. (2016) suggested that, on those days, the farmer could use whatever knowledge they have on the orchard water needs. This is a rough solution that may lead to imprecise determinations of the irrigation amounts, but the impact on the overall irrigation management will be low because of the reduced number of irrigation events on those days in between periods (see Fig. 1 in Padilla et al., 2016). In any case, we are already working on new water stress indicators derived from the P_p values recorded at State 3. Any advances on this task, together with the approach derived by Fernandes et al. (2017) for the automatic assessment of the daily P_p curve State, could highly contribute to the use of the proposed irrigation scheduling approach in a context of precision irrigation.

5. **CONCLUSIONS**

Our findings, on a greater number of variables than those monitored by Padilla-Diaz et al. (2016), confirm that the proposed irrigation scheduling approach is suitable to schedule regulated deficit irrigation in hedgerow olive orchards with similar conditions than those used in the present experiments. Both calculating the irrigation amounts at the beginning of the periods of high sensitivity to water stress (periods 1 to 3) as 120% of the irrigation

needs and changing by 15% the irrigation amounts applied for the rest of each period seem to be adequate for keeping non-limiting soil water conditions on those periods. Nonetheless, the fact that the values recorded by the ZIM probes at State 3 are not informative on the actual leaf turgor, curtails the suitability of the proposed irrigations scheduling approach to calculate irrigation amounts in between periods. It is expected that both recent advances for the automatic identification of the daily P_p curve States and further studies on the information provided by the P_p records at State 3 will increase the suitability of the proposed irrigation scheduling approach for precision irrigation of hedgerow olive orchards.

Confirming the scheduling RDI from leaf turgor pressure

Chapter 4

Effect of fruit development on turgor related measurements in olive leaves

1. INTRODUCTION

Irrigation management is required for a better profitability in most olive orchards (Gucci et al., 2012), being super-high density (SHD) olive orchards (from 1.500 trees ha^{-1}) particularly sensitive to irrigation supplies (Vossen et al., 2004). The most suitable irrigation strategy for SHD olive orchards is usually a regulated deficit irrigation (RDI) strategy. With RDI 80–100% of the irrigation needs are applied when the trees are most sensitive to water stress, in contrast of the rest of the growing cycle when one/two irrigation events per week are applied, or even with when irrigation is withheld (Chalmers et al., 1981; Goldhamer, 1999; Fernández et al., 2013; Fernández 2014a; Padilla-Díaz et al., 2016). The periods most sensitive to water stress have been identified as the period from the last stages of floral development to full bloom (P1); the period from week ca. 6 to 10 after full bloom, i.e. at the maximum rate of pit hardening (P2) (this periods ends when the pit offers resistance to the cut with a knife); and a period of ca. 3 weeks prior to ripening, when a marked increase in oil accumulation occurs (P3) (Fernández et al. 2013). In some Mediterranean areas, P1 normally occurs during the rainy season. For the other two, however, irrigation supplies close to crop water needs must be applied.

Both P2 and P3 are key phenological stages for fruit development. The fruit growth (i.e. fresh and dry weight accumulation) normally exhibits a double-sigmoid pattern in which P2 and P3 are coincident with moments of a rapid fruit growth (Lavee, 1986). P2 is defined by a high rate of cell division and cell enlargement (Rallo and Rapoport, 2001; Rapoport et al., 2010, 2013 Hammami et al., 2011, 2013;) while on P3 occurs the veraison (i.e. changes in fruit colour associated to fruit maturation), as well as modifications in the pathways of oil synthesis and cell enlargement (Lavee, 1986). Plant-water relations during fruit development are complex. Most of the time, leaves act as sources of water and carbon and fruits as sinks. The water potential gradient ($\Delta\Psi$) between leaves and the fruits determines the direction of water through the shared xylem (Matthews and Shackel, 2005). Likewise, the carbon allocation from the leaves through the phloem is tightly coordinated with xylem by sharing water potential, which is mainly driven by xylem tension (Diaz-Espejo and Hernandez-Santana, 2017).

On the other hand, it is widely accepted that plant-based methods are highly suitable for precise irrigation scheduling. Basically, they provide valuable information on the response of the plant to the prevailing soil and atmosphere water status (Jones, 2004; Fernández 2014b). Among the existing variety of methods those based on sap flow (SF), trunk diameter variations (TDV) and leaf turgor (LT) related measurements have been widely studied (Jones, 2004, 2007; Ben-Gal et al., 2010; Fernández, 2014b). Although SF is nowadays one of the most promising approaches due to its potential capacity for estimating both plant water consumption and changes in stomatal conductance (Hernández-Santana et al. 2016), its use to assess water stress and schedule irrigation in commercial orchards is not easy. Thus, SF sensors and related systems are complicated to install and maintain, and the collected records are not easy to interpret (Fernández, 2014b).

The same can be said, although to a lesser extent, on TDV. Leaf turgor related measurements, however, are those posing less difficulties for their use in commercial orchards (Padilla-Díaz et al., 2016, 2018; Egea et al., 2017). There is a lack of information on the suitability of those indicators to assess the effect of fruit development stages on the measure variable. This information, however, could be valuable to better schedule irrigation on periods when undesired events of water stress may highly penalize fruit development and, therefore, production.

Field measurements of leaf turgor can be made with the leaf patch turgor pressure probe, or ZIM probe. It records the output pressure (P_p; kPa), a variable inversely correlated with the cell turgor pressure (Zimmermann et al., 2008). Several water stress indices can be derived from the values and shape of the daily P_p curve. Among others, the "State" of the curve has been probed to have a potential for irrigation scheduling. The State of the daily P_p curve is related to the stem water potential (Ψ_{stem}; MPa). Thus, Fernández et al. (2011) and Ehrenberger et al. (2012) reported that State 1 was usually recorded when $\Psi_{stem} > -1.2$ MPa (negligible stress), State 2 for $-1.2 < \Psi_{stem} < -1.7$ MPa (moderate stress) and State 3 when $\Psi_{stem} < -1.7$ MPa (severe stress). Each one of these three "States" is characterized by a particular shape of the P_p daily curve. In Sate 3 the curve is inverted and it means that the ZIM probe cannot properly measure the actual leaf turgor pressure, because of air and water vapour accumulation among the mesophyll cells (Ehrenberger et al., 2012).

The mentioned relationships between the States and Ψ_{stem} thresholds were found in 'Arbequina' olive trees of a SDH olive orchard close to Seville. They differ from the Ψ_{stem} thresholds reported by Marino et al. (2016), the discrepancies being due, according to the same authors, to differences on olive cultivar, genotype and the specific environmental characteristics of the orchards. For State 1 they found a variable Ψ_{stem} threshold, varying from Ψ_{stem} -1.5 to -2.5 (MPa); for State 2, they reported values between –1.8 and –2.8 MPa. Scheduling irrigation based on these Ψ_{stem} thresholds is not advisable, because these stress levels are too high for the sensitive periods P2 and P3 in olive. For this reason, Marino et al. (2016) proposed the use of the minimum daily value of P_p (P_{pmin}, the maximum daily turgor), recorded during the last hours of the night, as a new indicator for irrigation scheduling.

Also, Aissaoui et al. (2016) found, for two varieties of Tunisian olive trees under different regimes of soil water availability, that the most sensitive indicator for water stress was, again, P_{pmin}. It has been reported, however, that P_{pmin} values may change along the irrigation season even if the trees are kept under non-limiting soil water conditions. Thus, Fernández et al. (2011) and Padilla-Díaz et al. (2016) observed, in fully irrigated trees, that P_{pmin} was usually closer to zero at the beginning of the irrigation season that at the end. This was attributed to changes in the structural and mechanical characteristics of the olive leaf related to aging (Chartzoulakis et al., 1999; Centritto, 2002; Bacelar et al., 2004; Marchi et al., 2008), as well as changes in the elastic modulus of the leaf cells, which tends

to increase with leaf age (Bongi and Palliotti, 1994) and drought (Dichio et al., 2003). This outlined the need for a better understanding of the potential of P_{pmin} as an effective indicator for irrigation scheduling.

In the present study we aimed to unravel the role of the proximity of fruits to the leaf in which the maximum daily turgor (P_{pmin}) was being recorded. We wanted to know whether the complex relations between leaves and fruits, as sinks and sources of water and carbon, and their potential effect on P_{pmin}, could advice for the sample leaf being chosen close or far from fruits. We monitored both fruit dry weight along most of the growing season, and changes in fruit colour during veraison. Moreover, as it is suggested below, the effect of the leaf structural properties on the leaf-water relations and its impact on P_{pmin} were also tested. With that purpose, we constructed pressure volume curves along the whole growing season, which helped us to understand the variation on the osmotic potential at full turgor, on the elastic modulus, the leaf water potential at turgor loss point and the absolute capacitance at full turgor for leaves both next to a cluster of fruits and relatively far from them. Our sampled trees were under full irrigation conditions because, as mentioned above, ZIM probes do not measure properly in State 3, i.e. under severe water stress. Still, our analyses allowed us to determine the effect of both atmospheric demand and water availability on P_{pmin}. Besides, the predawn water potential, predawn leaf relative water content and maximum stomatal conductance and photosynthesis were also evaluated for leaves close and far from fruit clusters.

2. MATERIALS AND METHODS

2.1. Orchard characteristics, soil and meteorological measurements

The experiment was carried out in 2016 in a 10-year old commercial super high density (1667 trees ha^{-1}) olive orchard (*Olea europaea* L. cv Arbequina), located at 25 km from Seville (37º 15' N, −5º 48' W), Spain. The area has a typical Mediterranean climate (i.e. winters characterized mild and wet, summers hot and dry) with average annual values of precipitation (*P*, period 2002-2016) and evapotranspiration (ET_o) 1531 mm and 509 mm respectively. More details about environmental characteristics and orchard management are given by Fernández et al. (2011, 2013) and Padilla-Díaz et al. (2016).

The experiment was performed with trees that were daily irrigated along the whole irrigation season to replace the 100% of irrigation needs (IN), i.e. under full irrigation conditions. The IN was calculated every week as $IN = ET_c - P_e$, being ET_c the evapotranspiration of the crop estimated from the crop coefficient approach (see Fernández et al., 2013 for details on the coefficients adjusted for the orchard) and P_e the effective precipitation, assumed as the 75% of the precipitation recorded by the weather station of the orchard (Orgaz and Fereres, 2001). The calculated IN values were input every Monday in an irrigation controller (Agronic 2000, Sistemes Electrònics PRO-GRÉS, S.A., Lleida, Spain) and water in the orchard was applied through an irrigation system which consisted

of one pipe per tree row with 2 L h^{-1} drippers every 0.5 m. Fertilizers applied through the irrigation system once per week during the whole irrigation season. Main weather conditions were recorded every 30 minutes by a Campbell weather station (Campbell Scientific Ltd. Shepshed, UK) located in the centre of the experimental plots. ET_o (mm) values were recorded from a standard weather station located close to the orchard, from the RIA network of the Junta de Andalusia. In addition, the three days forecast vapour pressure deficit (VPD; kPa) was calculated through the temperature and humidity predictions made by the official Spanish Meteorology website (AEMET) from records of the mentioned weather station. The soil water status in the root zone of one tree per plot (see below for details about the experimental design) was monitored with a Profile probe (Delta-T Devices Ltd., Cambridge, UK) which recorded volumetric soil water content (θ_v; m^3 m^{-3}) values at 0.1, 0.2, 0.3, 0.4, 0.6 and 1.0 m depth. Two access tubes per plot were installed, at ca. 0.5 m from the tree trunk, one at 0.1 m from a dripper (within the wet bulb), and the other at 0.4 m from the dripper (outside of the wet bulb, i.e. in drying soil). During the irrigation season, measurements of θ_v were made 1-2 times per week. The recorded values were used to calculate the dynamics of the relative extractable water (REW) along the irrigation season. More details about the weather conditions and soil characteristics of the orchard are shown in Fernández et al. (2011, 2013).

2.2. Experimental setup and maximum turgor related measurements

The experiment started on June 4th (day of year, DOY, 156) and finished the day of harvesting on November 8th (DOY 313). Measurements should have started earlier, but the irrigation pump broke down at the beginning of the irrigation season. This experiment was carried out in three plots randomly distributed in the orchard. Each plot contained 24 trees in 2 m × 6 m. Two central trees per plot (n = 6) were sampled. Four branches of similar characteristics per tree, from the east side of the canopy, were selected and marked. Fruits in two out of those four branches were removed on June 1st, before the experiment began. Thus, two treatments per tree were applied: in the F+ treatment, the ZIM probes were clamped in leaves of branches with fruits, at some 4-5 internodes of the closer cluster of fruits. In the F– treatment, the ZIM probes were clamped in leaves from a branch where all the fruits, from the apex to its insertion in the main trunk, were removed prior clamping. On June 4th, four ZIM probes (Yara Water-Sensors, YARA ZIM Plant Technology GmbH, Hennigsdorf, Germany) per tree, in the six trees per treatment, were clamped early in the morning (05.30 – 07.30 GMT), when the leaf turgor were around its maximum. We installed one probe per branch in two F+ and F– branches per tree, amounting to a total of 24 ZIM probes. They were clamped avoiding the central nerve of healthy and fully developed current-year leaves. These leaves were the 6th or 7th leaf from the apex, in twigs at ca. 1.5-1.9 m above ground. The recorded P_p values were sent every 5 min by radio to a datalogger with a GPRS modem which sent the data to a server belonging to YARA ZIM Plant Technology GmbH. The data were on the internet at almost real-time. We did not have to re-clamp any of the probes for the rest of the experiment.

Maximum leaf turgor occurred on the last hours of the night, i.e. before dawn. This was the time of the day when minimum P_p values were recorded. For comparison of the P_{pmin} values among treatments, we normalized the collected values according to the following equation:

$$P_{pmin}\ (\%) = \frac{P_p' - P_{p'min}}{P_{p'max} - P_{p'min}}\ x\ 100 \quad , \qquad (1)$$

where P_p' is the minimum value of P_p achieved on the day, and $P_{p'min}$ and $P_{p'max}$ are the minimum and maximum P_p value, respectively, recorded during the whole experimental period. Thus, the calculated P_{pmin} values represented the percentage of full turgor reached on the day. The normalized P_{pmin} values were averaged first by tree and second by treatment.

2.3. Leaf-water relations

We expected that marked changes in the atmospheric demand along the irrigation season would have an effect on plant-water relations. To monitor them, we measured main physiological variables the day after the weather forecast predicted an abrupt change in VPD.

For the time course of predawn water potential (Ψ_{pd}; MPa; 04.30 – 06.00 GMT), measurements were made with a Scholander-type pressure chamber (PMS Instrument Company, Albany, Oregon, USA) in one leaf per treatment from six trees with ZIM probes. The sampled leaves had similar location and developmental stage as the leaves monitored with the ZIM probes.

At the same time and with the same criteria as for Ψ_{pd}, we sampled one leaf per treatment from the six trees to calculate the relative water content (RWC; %). After sampling, those leaves were immediately introduced in an opaque plastic tube, taken to the laboratory and weighed for fresh weight (FW; g) with a 10^{-5} digital balance (XS105 Dual Range, Mettler Toledo AG, Greifensee, Switzerland). Later, the leaves were rehydrated by standing the petiole in distilled water at 4 ºC during 24 h in darkness, and then weighed by again for the rehydration weight (WW; g). Then, leaves were dried in an oven at 70 ºC during 48 h, and weighed for the dry weight (DW; g). Calculations of RWC were made as follows:

$$\text{RWC}\ (\%) = \frac{\text{FW} - \text{DW}}{\text{WW} - \text{DW}}\ x\ 100 \quad . \qquad (2)$$

2.4. Pressure-volume curves

A single leaf from each tree with ZIM probes (n = 6) was sampled at predawn, in the same days as the other physiological variables mentioned above were measured. Immediately after cutting, the leaves were introduced in opaque plastic tubes with the petiole submerged in distilled water and stored overnight in darkness at 4 ºC, for rehydration. Each sampled leaf was used in the construction of its pressure-volume (P-V) curve, following the leaf bench dehydration method. Basically, a P-V curve consists in relates the loss of leaf water

potential (Ψ_{leaf}) with the loss of water volume along the leaf dehydration. Therefore, in the construction of our P-V curves, the Ψ_{leaf} (MPa) was periodically measured with a Scholander-type pressure chamber and its weight determined with a digital balance, till Ψ_{leaf} ca. –4 MPa was reached. The leaves were scanned (HP Scanjet 3970 Scanner series) for determining their area (S; m^2) with the ImageJ software (*Schneider* et al., 2012). Later, they were oven-dried at 70 ºC during 48 h for getting the dry weight (DW; g). The leaf water potential at turgor loss point (Ψ_{tlp}; MPa) was determined as the first interception point of the linear relationship $-1/\Psi_{leaf}$ (Y axis) vs the leaf relative water content (RWC; %) (X axis) curve, whereas the osmotic potential at full turgor (π_o; MPa) is given by the intercept of that linear relationship with the Y axis. The elastic modulus (ε; MPa) was estimated as the slope of $-1/\Psi_{leaf}$ vs RWC from full turgor till turgor loss point. The absolute capacitance at full turgor (C_{FT}; mol m^{-2} MPa^{-1}) was estimated according to Blackman and Brodribb (2011), i.e. from the slopes of linear regressions of the data fitted till Ψ_{tlp} with the following equation:

$$C_{FT}\,(mol\,m^{-2}\,MPa^{-1}) = \frac{\partial \mathrm{RWC}}{\partial \Psi_{leaf}} \left(\frac{DW}{S}\right)\left(\frac{WW}{DW}\right)\frac{1}{M} \quad , \qquad (3)$$

where DW is the dry weight (g), S is the leaf area (m^2), WW is the mass of water in the leaf at RWC = 100% and M the molar mass of water. These calculations of the parameters derived from the P-V curves were developed using the methodology published by Sack et al., 2011. These derived parameters were averaged by day and treatment.

2.5. Leaf gas exchange measurements

Maximum daily stomatal conductance ($g_{s,max}$; mol H_2O $m^{-2}s^{-1}$) and CO_2 net assimilation (A_{max}; µmol CO_2 $m^{-2}s^{-1}$) were measured on the same days and trees that Ψ_{pd}. For both variables, two leaves were sampled per treatment in the six trees with ZIM probes, following the same criteria as described for Ψ_{pd}. Measurements were made at 08.00 – 09.00 GMT, maximum leaf gas exchange occurs in olive (Fernández et al., 1997). We used a Licor LI-6400 portable photosynthesis system (Li-cor, Lincoln NE, USA), with a 2 cm x 3 cm standard chamber at ambient light and CO_2 conditions. The collected data were averaged firstly by tree and secondly by treatment.

2.6. Fruit dry weight and colour index

Fruit dry weight (g) was determined by random sampling of six fruits in the eight central trees of each plot, every other week along the whole irrigation season. The fruits were dried in an oven 48 h at 70 °C and then weighed with a digital balance. When the fruits were estimated to have 50% of its final size (Sanz-Cortés et al., 2002), 25 fruits per plot were randomly selected on the same sampling days for fruit dry weight, and used for the colour index measurements. The colour parameters of the fruits were measured in the equatorial plane of the fruits by a Chroma Meter (CR-400/410, Konica Minolta, Sensing

Inc., Osaka, Japan). The Chroma Meter was calibrated by a standard white and CIE coordinates (*L*, *a* and *b*). The fruit colour index was determined by the equation

$$\text{Fruit Colour Index} = L\frac{(b-a)}{100} \quad (4)$$

where *L* is the lightness (white = 100, black = 0), *a* is the range red-green (*a* > 0 represents the increasing redness whereas *a* < 0 represents the increasing greenness) and *b* is the range yellow-blue (*b* > 0 represents the increasing yellowness whereas *b* < 0 the increasing blueness). Higher values of colour index mean that the colour of the fruits was shifting from green to yellowish. Lower values correspond to later phases of veraison, when the fruits became purple and black.

2.7. Statistical analysis

Data shown of the all physiological variables including REW are mean ± standard error. We used t-test comparisons of mean to analyse the differences between treatments (here considered $P \leq 0.05$) for all measured physiological variables and for the P_{pmin} values for each treatment. Before each t-test comparison, we tested the normality and homoscedasticity of each variable using a Shapiro-Wilk and Levene's test, respectively. Those variables that were neither adjusted to normality nor homoscedasticity of the variance were transformed prior to apply t-test comparisons. Data from concomitant measurements (i.e. REW, fruit dry weight and fruit colour index) were interpolated assuming linear relationships using the "zoo" package (Zeileis and Grothendieck, 2005).

Principal component analyses (PCA) were carried out to assess the effect of the main environmental variables on P_{pmin}, for each treatment. We developed three PCA tests for the main periods of fruit development with the main daily environmental variables (i.e. maximum VPD, ET_o, maximum solar net radiation, *P*, maximum wind speed, interpolated REW and irrigation amounts applied). This analysis was carried out for each of the three intervals related to olive fruit development (Sanz-Cortés et al., 2002). These intervals are referred to in the literature as period 2 (P2), period 3 (P3) and the period in between (Fernández et al., 2013; Fernández, 2014a; Padilla-Díaz et al., 2016). Both P2 and P3 are considered moments of high sensitivity to water stress (Fernández et al., 2013; Fernández 2014a). Due to the percentage of explanatory variability, two main components of the PCA were taken to perform linear models, using P_{pmin} as response variable to all three periods and treatment. Distribution of normality and homoscedasticity of the residuals of the models were tested prior to transformation of the variable. Pearson's correlation tests were performed to understand the percentage of association between fruit dry weight as well as fruit colour index with P_{pmin}. These analyses were performed using R software (R Core Team, 2012) v. 3.4.2.

3. RESULTS

3.1. Maximum turgor related measurements and the influence of fruit presence

We found that the time courses of normalized maximum turgor related measurements (P_{pmin}) were not affected by the proximity of fruits (Fig. 1A), as shown by theto non-statistical differences between the records taken in leaves of branches with fruits (F+) and branches without fruits (F–). Still, P_{pmin} values were higher in F+ than in F– at certain moments along the recorded period: at the end of period 2, at the beginning of the period in between P2 and P3, three days after the sudden pick of VPD on DOY 249, and on the central days of period 3. Both in the P2 and P3 periods, relative P_{pmin} values increased from 20%, or less, at the beginning of both periods, to over 60% in P2 and around 80% in P3. In between both periods relative P_{pmin} values decreased to below 20%, except on days in which, either the interruption of irrigation (DOY 208) or peak VPD values (around DOY 249), cause sudden increases on P_{pmin} (Fig. 1). Moreover, there were no differences neither among trees nor between treatments (i.e. among the 24 ZIM sensors) in the shape of the daily turgor related measurements (daily P_p curves) along the whole experimental season (Fig.S1, supplementary material).

3.2. Relationship between maximum turgor and environmental variables

The seasonal courses of P_{pmin}, for both F+ and F– treatments, was plotted against main environmental variables (Fig.1). Irrigation was enough to keep REW values close to 1 for most of the irrigation season, except after DOY 300, when irrigation supplies were reduced and even withheld because of the autumn rains (Fig. 1C). The PCA analysis helped us to evaluate the plant-water relations and, basically, the effect of the environmental variables on P_{pmin}. With this approach we assessed the effect of the environmental variables shown in Fig. 1, for periods P2 and P3, as well as for in between P2 and P3. Results are shown in Table 1. The main variability was further explained by first principal component (PC1) of the PCA than the second one (PC2) for the three periods studied. Those PC1 and PC2 were also renamed depending on which variable had a greater impact on P_{pmin}. Thus, in all of cases PC1 was renamed as *maximum atmospheric demand* and PC2 as *water availability*. Although the maximum wind-speed (u_{max}) belonged to the PC2 in period 2 and in between periods, we considered renaming PC2 as water availability because of the high effect of the irrigation amounts and REW on the variance. On period 3, both precipitation (P) and u_{max} belonged to PC1 instead of PC2, because of their effect on the *atmospheric demand*.

To test the influence of both the *maximum atmospheric demand* and *water availability* on P_{pmin} for both treatments (F+ and F–), we performed linear models with P_{pmin} and those components of the PCA for each treatment and interval period (Table 2). For both treatments, the most important factor that explained the P_{pmin} daily fluctuations in period 2 (DOY 169–201), was the *maximum atmospheric demand*, followed by the *water availability*. In between periods (DOY 202–286), the adjustment between PC1 and PC2 with P_{pmin} was greater than in period 2. Nevertheless, in period 3 (DOY 287–313) no

influence of *water availability* was found, although the irrigation water supply was withheld due to rainy events. In this case, the *maximum atmospheric demand* (including u_{max} and P) was the main explanatory variable and the adjustment was lower than in between periods, as occurred in period 2.

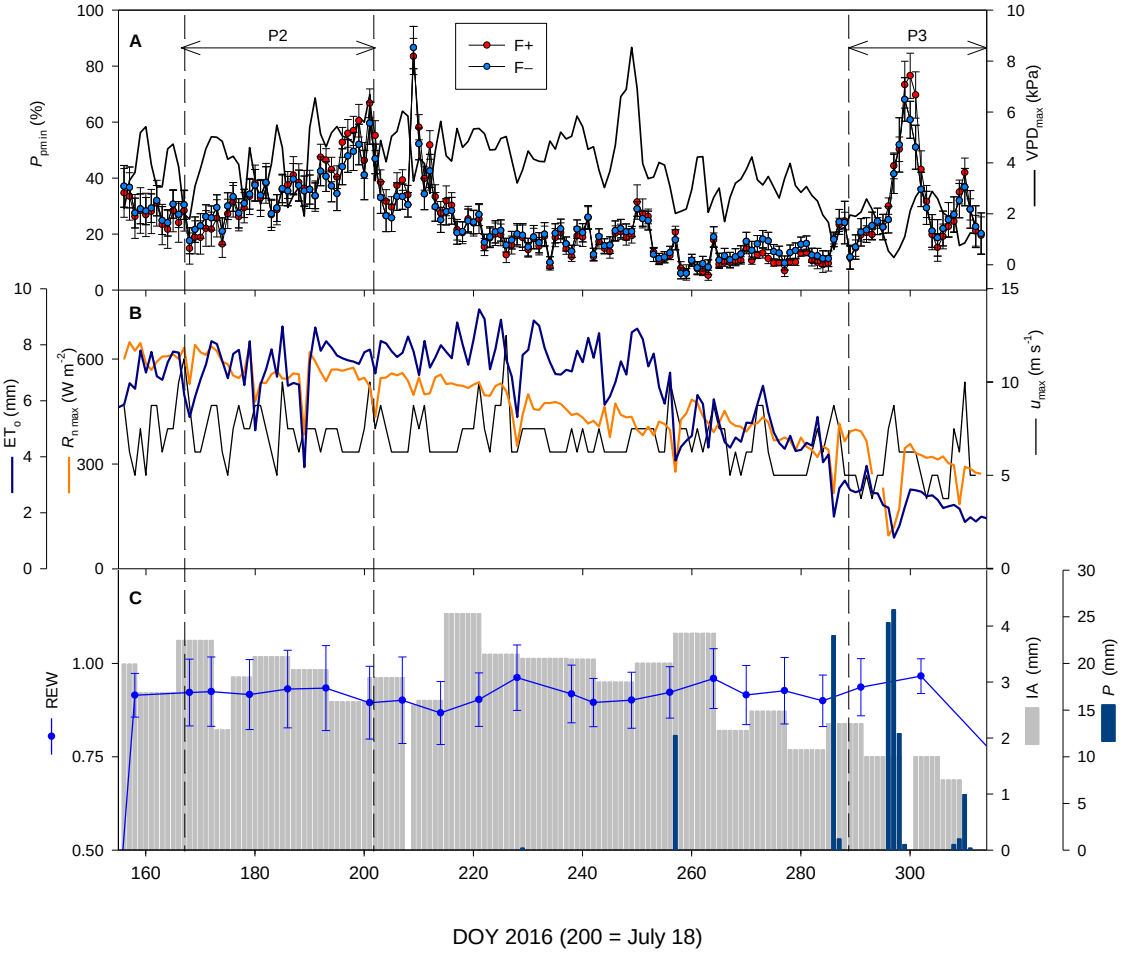

Fig. 1 Seasonal courses of maximum vapour pressure deficit (VPD_{max}), calculated from weather records at the experimental orchard, and of the relative maximum daily turgor (P_{pmin}; avg ± SE) recorded on leaves both close to a cluster of fruits (F+ treatment) and far from them (F– treatment) (see text for details on the treatments). Differences on P_{pmin} between treatments were never significant ($P \leq 0.05$) (**A**). Seasonal courses of potential evapotranspiration (ET_o) in the area, maximum net radiation (R_{nmax}) and maximum wind speed (u_{max}) (**B**). The seasonal course of relative extractable water (REW; avg ± SE) and values of both precipitation (P) collected in the orchard and irrigation amounts (IA) supplied to the experimental trees (**C**). P2 and P3 accounts for periods 2 and 3 in which olive is most sensitive to water stress (Fernández et al., 2013; Fernández et al., 2014a). DOY = day of year.

Table 1. Results from the principal component analysis (PCA) based on the main environmental variables that could have affected plant performance in every interval of fruit development along the experimental season. PC1 and PC2 are the results of the first and second component of PCA which explain most of the variability in P_{pmin}. PC1 and PC2 were renamed according to the main daily environmental variables of each group, which appear in bold. Precipitation was removed from the analysis of period 2, since there was no rain in that period. Proportion of the variance is the interval adjustment of the variance which is explained by each component of the PCA, whereas the total variance of the analysis is explained by the cumulative proportion. VPD_{max} = daily maximum vapour pressure deficit; P = precipitation; u_{max} = maximum daily wind speed; ET_o = reference evapotranspiration; IA = irrigation amount; REW = relative extractable water; DOY = day of year. All variables except ET_o were

	Period 2		In between periods		Period 3	
	DOY 169 – 201		DOY 202 – 286		DOY 287 – 313	
	PC1	PC2	PC1	PC2	PC1	PC2
Environmental variables	Atmospheric demand	Water availability	Atmospheric demand	Water availability	Atmospheric demand	Water availability
VPD_{max} (kPa)	**0.558**	0.06	**-0.467**	0.164	**0.473**	-0.002
P (mm)			0.154	**-0.465**	**-0.448**	0.380
u_{max} (m s^{-1})	-0.200	**0.428**	-0.240	**-0.551**	**-0.371**	0.105
R_{nmax} (W m^{-2})	**0.443**	0.347	**-0.494**	0.085	**0.455**	-0.141
ET_o (mm)	**0.528**	0.369	**-0.550**	-0.030	**0.433**	0.213
IA (mm)	-0.362	**0.518**	-0.296	**-0.509**	0.151	**0.632**
REW	-0.206	**0.534**	0.254	**-0.431**	0.142	**0.615**
Proportion of variance	0.409	0.220	0.426	0.282	0.489	0.233
Cumulative Proportion		0.630		0.611		0.722

Table 2. Results, for each treatment (F+ and F–) and interval of fruit development along the whole experimental year of the linear models fitted to the principal component analyses (PCA) for the main environmental daily variables that affects P_{pmin}, the response variable. Each interval was selected according to the main periods of water sensitivity in olive trees (Fernández et al. 2013, Fernández 2014a). PC1 and PC2 are the results of the first and second component of PCA which explain most of the variability in the response variable. PC1 and PC2 were renamed according to the group of environmental daily variables with more weight on P_{pmin}. F+ is when the sampled leaf was close to a cluster of fruits and F– is when the sample leaf was far from a cluster of fruits (see text for details). DOY = day of year.

	Period 2			In between periods			Period 3		
	DOY 169 – 201			DOY 202 – 286			DOY 287 – 313		
		PC1	PC2		PC1	PC2		PC1	PC2
		Atmospheric demand	Water availability		Water availability	Atmospheric demand		Atmospheric demand	Water availability
	R^2	*P* value	*P* value	R^2	*P* value	*P* value	R^2	*P* value	*P* value
F+	0.24	0.04	0.03	0.37	< 0.01	< 0.01	0.19	0.03	0.73
F–	0.25	0.06	0.02	0.37	< 0.01	< 0.01	0.28	< 0.01	0.53

3.3. Relationship between of maximum turgor and fruit development

Our results show that the time courses of fruit growth, measured as the rate of fruit dry weight, exhibit a double-sigmoid pattern (Fig. 2). The first phase of rapid growth occurred from ca. DOY 168 till DOY 208, i.e. on the P2 period, the maximum rate of pit hardening. The second phase of fast growth was from ca. DOY 294 to 313, i.e. on period P3, when most changes in fruit colour index occurred, the fruits going from light green and yellowish to purple. Those two phases of maximum rate of pit hardening and veraison agreed with an increment on P_{pmin} in both treatments (Fig. 2A).

Both for F+ and F–, the increment in P_{pmin} was linearly correlated, in P2, with fruit dry weight (R^2 = 0.77, P < 0.0001; Fig. 3A). In P3, however, we found no correlation between both variables (Fig. 3B). This is not surprising because the number of sampling days for both fruit dry weight and fruit colour index was very low in comparison with the high variability of P_{pmin} on that period (Fig. 2).

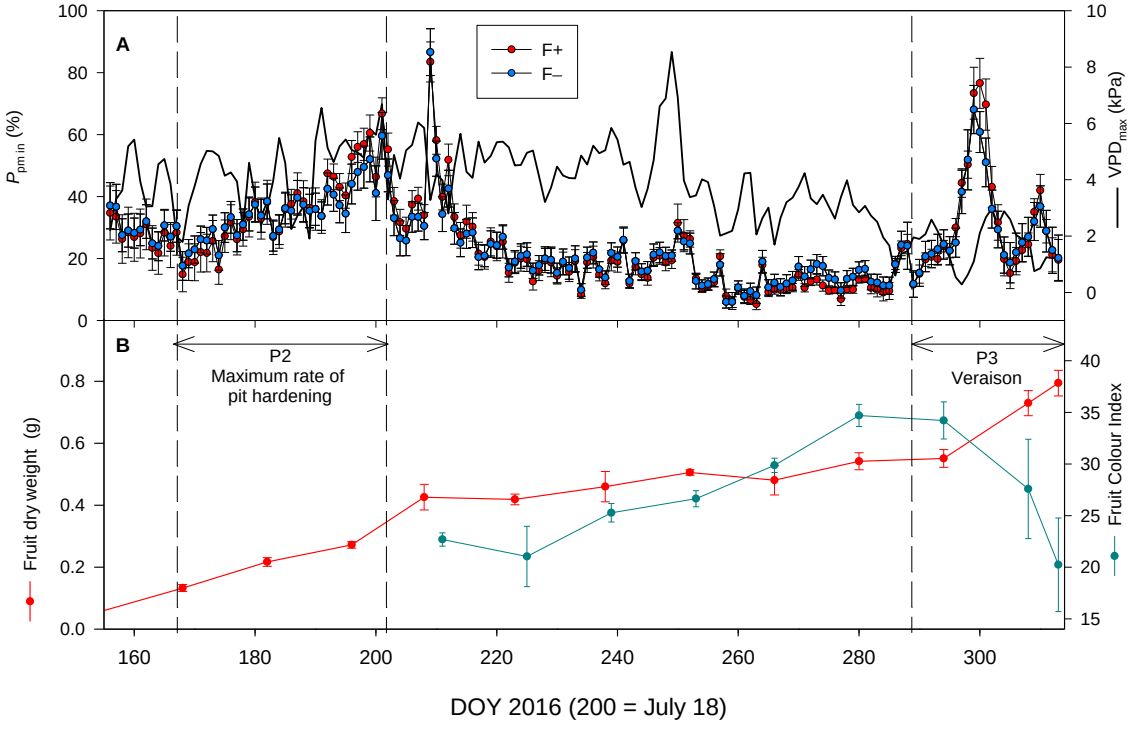

Fig. 2 Seasonal courses of maximum vapour pressure deficit (VPD_{max}), calculated from weather records at the experimental orchard, and of the relative maximum daily turgor (P_{pmin}; avg ± SE) recorded on leaves both close to a cluster of fruits (F+ treatment) and far from them (F– treatment) (see text for details on the treatments). Differences on P_{pmin} between treatments were never significant ($P \leq 0.05$) (**A**). Seasonal courses of fruit dry weight (n = 6) and fruit colour index (n = 25) measured along the whole experimental season. The shown values are avg ± SE (**B**). P2 and P3 accounts for periods 2 and 3 in which olive is most sensitive to water stress (Fernández et al., 2013; Fernández et al., 2014a). In 2016, the experimental year, P3 agreed with veraison. DOY = day of year.

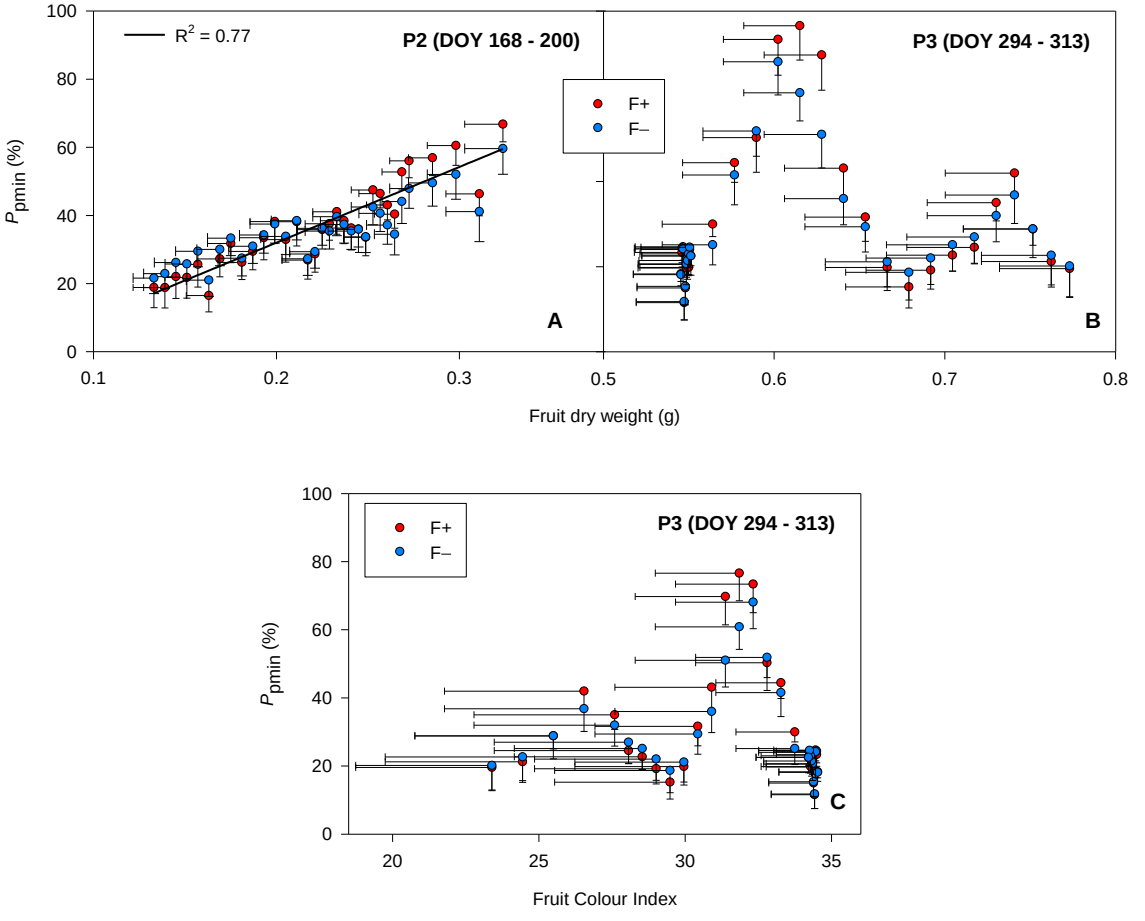

Fig. 3 Relationship between fruit dry weight (avg – SE) and relative maximum daily turgor (P_{pmin}; avg – SE) for periods P2 (**A**) and P3 (**B**). Relationship between fruit colour index (avg – SE) and the relative maximum daily turgor (P_{pmin}; avg – SE) (**C**). P_{pmin} values were recorded on leaves both close to a cluster of fruits (F+ treatment) and far from them (F– treatment) (see text for details on the treatments). All correlations were made on the average of both treatments and were significant at least as $P \leq 0.05$. P2 and P3 correspond to the periods 2 and 3 in which olive is most sensitive to water stress (Fernández et al., 2013; Fernández et al., 2014a). DOY = day of year.

3.4. Leaf-water relations and the influence of fruit presence

Significant differences ($P \leq 0.05$) between the F+ and the F– treatments were found for maximum daily net CO_2 assimilation ($A_{N,max}$) around the beginning of period 2 (DOY 166 and 169), .No differences were found, hoewver, for maximum daily stomatal conductance ($g_{s,max}$), predawn leaf water potential (Ψ_{pd}) and predawn leaf relative water content (RWC_{pd}) (Fig. 4B–D). For the rest of the experimental season there were no statistical differences between treatments, for any of the variables. The time courses of $A_{N,max}$ and $g_{s,max}$ (Fig. 4B,C) were affected by events of high VPD_{max} (Fig. 4A), such as the peak VPD values recorded around DOY 249. At the end pf P3, both gas exchange variables decreased, likely due to those days in November being cold and dark (Fig.1B). The Ψ_{pd} values suggest a lack of overnight recovery of the trees water status in mid-summer (in between periods 2 and 3), since values lower than -0.5 MPa, the threshold for satisfactory recovery (Fernández et al., 2014a) were often recorded (Fig. 4D). Likely the high values of VPD on those days (Fig. 4A) were responsible for that. On period 3, however, when VPD values were lower, the trees were able to rehydrate properly during the night. These findings agree with the time course of RWC_{pd} (Fig.4E). Around DOY 253, when a marked peak of VPD occurred, $g_{s,max}$, $A_{N,max}$ and RWC_{pd} decreased, as corresponded.

The results of the calculations derived from the pressure-volume (P-V) curves performed for each sampled day are given in Fig. 5. The seasonal courses showed a non-stationary trend for all the calculated variables. Less negative values were attained for F+ treatment compared with F–, for both π_o and the leaf water potential at turgor loss point (Ψ_{tlp}) (Fig. 5B and C), although the high variability of the values led to non-significant differences. A marked decrease on the osmotic potential at full turgor (π_o) there was observed on DOY 211 as the response to the interruption of irrigation on DOY 208. However, in period 3 there were significant differences (P values ≤ 0.05) between both F+ and F– treatments. In the case of the absolute capacitance at full turgor (C_{FT}) there were statistical differences only on DOY 202 being higher for F+ than F–.

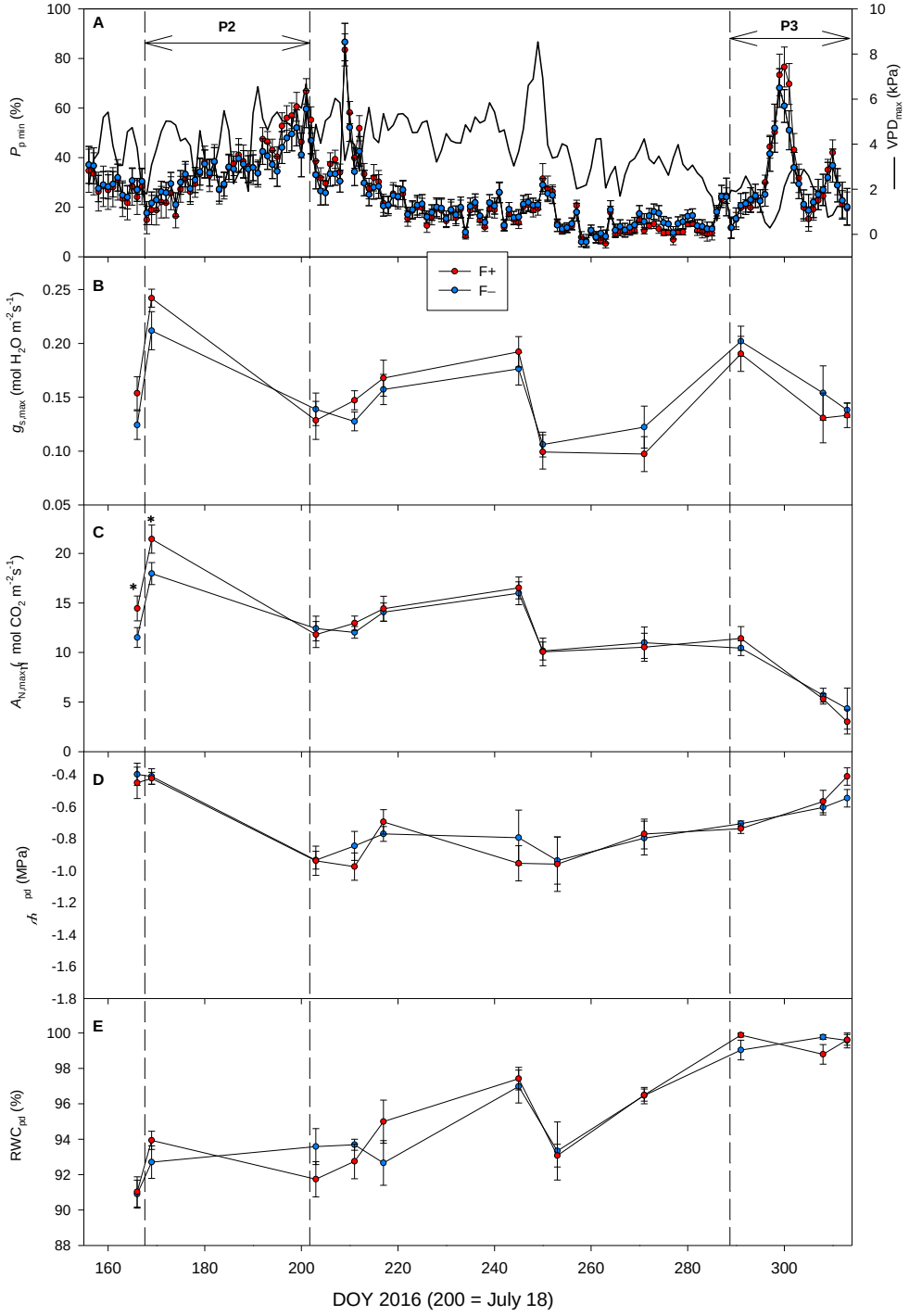

Fig. 4 Seasonal courses of maximum vapour pressure deficit (VPD_{max}), calculated from weather records at the experimental orchard, and of the relative maximum daily turgor (P_{pmin}; avg ± SE) recorded on leaves both close to a cluster of fruits (F+ treatment) and far from them (F– treatment) (see text for details on the treatments). Differences on P_{pmin} between treatments were never significant ($P < 0.05$) (**A**). Seasonal courses of maximum daily stomatal conductance (g_{smax}) (**B**), CO_2 net assimilation (A_{max}) (**C**), predawn water potential (Ψ_{pd}) (**D**) and relative water content (RWC_{pd}) (**E**). All values, except VPD, are represented as avg ± SE. Asterisks indicate significant differences between treatments, at $P \leq 0.05$. Asterisks are not shown when no differences were found. P2 and P3 accounts for periods 2 and 3 in which olive is most sensitive to water stress (Fernández et al., 2013; Fernández et al., 2014a). DOY = day of year.

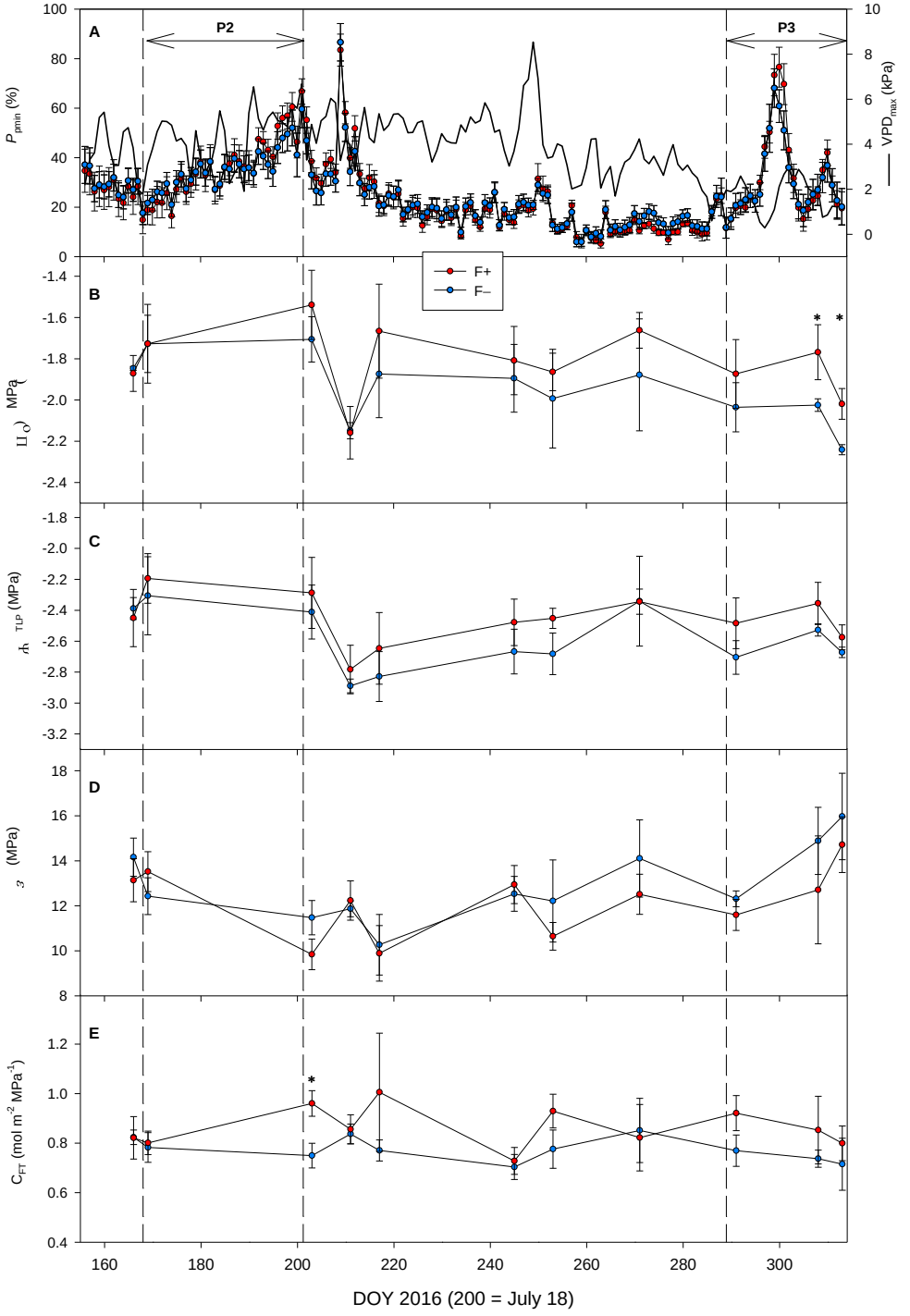

Fig. 5 Seasonal courses of maximum vapour pressure deficit (VPD_{max}), calculated from weather records at the experimental orchard, and of the relative maximum daily turgor (P_{pmin}; avg ± SE) recorded on leaves both close to a cluster of fruits (F+ treatment) and far from them (F– treatment) (see text for details on the treatments). Differences on P_{pmin} between treatments were never significant ($P \leq 0.05$) (**A**). Seasonal courses of osmotic potential at full turgor (π_o; avg ± SE) (**B**), water potential at turgor loss point (Ψ_{TLP}; avg ± SE) (**C**), elastic modulus (ε; avg ± SE) (**D**), and absolute capacitance at full turgor (C_{FT}; avg ± SE) (**E**). The parameters were derived from six pressure-volume curves per treatment and day. Red dots indicated parameters recorded on leaves that were close to a cluster of fruits (F+) treatment and blue dots relatively far from them (F–) treatment (see text for details). Asterisks indicate significant differences between treatments, at $P < 0.05$. Asterisks are not shown when no differences were found. P2 and P3 accounts for periods 2 and 3 in which olive is most sensitive to water stress (Fernández et al., 2013; Fernández et al., 2014a). DOY = day of year.

4. DISCUSSION

4.1. Daily variations on maximum turgor: environmental components

The objective of this study was to unravel the mechanisms behind the relative maximum daily turgor (P_{pmin}) behavior as an indicator of plant-water stress and its potential for irrigation scheduling in olive orchards (Zimmerman et al., 2008; Fernández et al., 2011; Bramley et al., 2013; Aissaoui et al., 2016; Marino et al., 2016). Although it is demonstrated that irrigation in a super-high density olive orchard can be scheduled from turgor related measurements, particularly from the shape of the daily P_p curves (Padilla-Díaz et al., 2016, 2018), there are still gaps on our understanding of the physiological meaning of the ZIM probes readings (Fernández, 2014b). Findings by other authors (Lee et al., 2012; Aissaoui et al., 2016; Marino et al., 2016) on the influence of main environmental variables that can affect the plant-water status (e.g. changes in the air water vapor pressure deficit, VPD), do not provide enough information on the response of P_{pmin} to the environment. In addition, Fernández et al. (2011) and Padilla-Díaz et al. (2016), among others, reported different P_p values at the beginning than at the end of the irrigation season, for trees with similar water status. All these lack of consitency took us towards to develop the experiment presented here. As mentioned above, the current experiment was built under full irrigation conditions, to avoid events of severe water stress in which the ZIM probes became useless to properly assess the leaf turgor, because of the air accumulation in between mesophyll cells (Ehrenberger et al., 2012).

Our results suggest that, under non-limiting soil water conditions, P_{pmin} was mainly driven by the previous daily values of the *atmospheric demand*, followed by *water availability* in the soil (Fig. 1, Table 2). This is not surprising, since in those two variables are known to have a key influence on plant water status and transpiration (see the review by Fernández et al., 2014a, for olive). Thus, the plant transpiration (E) depends on the water potential gradient ($\Delta\Psi$) between the soil (Ψ_{soil}) and the leaves (Ψ_{leaf}) and the hydraulic conductance (K) of the plant. Under non-limiting soil water conditions, K usually remains constant and close to its maximum, because of low, if any, xylem embolism. Thus, in trees under full irrigation the *atmospheric demand*, which is conformed mainly by VPD and net radiation, becomes the main variable affecting P_{pmin}. This agrees with our results in Fig. 1 and Table 2. Our findings also agree with results previously reported for *Arabidopsis thaliana*, for which P_p was closely related to the degree of plant transpiration (Ache et al., 2010). For olive, the findings of Rodriguez-Dominguez et al. (2012), in the same orchard as our experiment and under a control, fully irrigated treatment, show that the P_p values yielded information about the development of tension in xylem through a positive correlation between stem sap flow and P_p. Also, recent results found by Aissaoui et al. (2016) in well-watered trees of two Tunisian cultivars, show a tight relationship (ca. R^2 = 0.8) between P_p and VPD along a single day measurements.

Nevertheless, our results show that, for similar values of *maximum atmospheric demand* and *water availability*, the daily pattern of P_{pmin} depended on the fruit development stage (Figs. 2 and 3). Other authors (Lee et al., 2012) found in tomato plants, also under well-watered conditions, a marked effect of the atmospheric demand on turgor values. However, they also found that there were an incompletely recovery of turgor during night, which could not be explained and did not agree with the soil water availability. Our results, and those reported by Lee et al. (2012), point out the fact that not all the variability of P_{pmin} could be explained by the prevailing environmental conditions, and that other factors, so far unidentified, should cause an apparent loss of turgor even under well-watered conditions.

4.2. Seasonal variations on maximum turgor: fruit influences

Our results show no differences on P_{pmin} for leaves that were close (F+) or far (F–) from a cluster of fruits (Fig. 1A). Still, and despite the lack of significant differences, we found greater P_{pmin} values in F+ than in F–, both at the period of maximum rate of pit hardening (P2) and during veraison (P3). But these differences were not enough to suggests that the proximity of fruits, acting as sinks of water and carbon (Matthews and Shackel, 2005) have an effect on the ZIM records. Our data, in fact, show no influence of the sampled leaf being close or far to a fruit cluster. This could be due to the experimental trees being under non-limiting soil water conditions, which avoided significant water stress in the trees and allowed for all its leaves to be hydraulically connected (Fernández et al., 2011) and thus with a similar water status (Fig. 4). Doubts remain on whether different findings could be expected under water stress conditions. In fact, at the beginning of the experiment, when the soil water was still bellow field capacity (Fig. 1C), low values of gas exchange and RWC were observed, with significant differences between treatments in maximum net photosynthesis at midday (Fig. 4). The low available water caused stomata closing to avoid excessive water loses and xylem embolism formation (Sperry and Tyree, 1988; McDowell et al., 2008), with consequence in photosynthesis (Flexas and Medrano, 2002; Flexas et al., 2004). This agrees with findings by other authors (Chaves et al., 2003, 2010; Medrano et al., 2016) where drought stress is directly affecting plant and fruit growth through associated imbalances in water and carbon transport from the plant to the fruit. Indeed, the carbon transport from the leaves to the fruits will be affected by drought because there is a tight relationship between xylem and phloem by sharing water potential (Diaz-Espejo and Hernandez-Santana, 2017).

Fruit growth, understood as accumulated dry weight (Fig.2B), had the well-known sigmoidal pattern that commonly occurs for olive trees (Lavee, 1986). In our case, the first phase of high rate of fruit growth overlapped with P2, and was coincident with a constant increment on P_{pmin} (Fig. 3A). The increment on P_{pmin} could not be attributed either to soil water availability or to *maximum atmospheric demand*, because both of them explained ca. 24% only of such increase (Table 2). At predawn, when P_{pmin} values occurred, the plant water status is in equilibrium with that of the soil, such that Ψ_{pd} can be assumed equal to

Ψ_{soil}. Therefore, we can assume that changes observed in Ψ_{pd} along the experimental season were mainly due to changes in Ψ_{soil}. On the other hand, Ψ_{pd} is equal to the sum of P_{pmin} and the osmotic potential. In our case, and because of the applied full irrigation, that osmotic potential can be considered osmotic potential at full turgor (π_o). Taken into account that P2 agreed with the rate of maximum pit hardening, when ninety per cent of the endocarp growth occurs and oil accumulation begins (Rapoport et al., 2004), we can assume fruits acting as a sink of carbon. Assimilates, therefore, would be exported from the leaf, through the phloem, to the fruit, leading to π_o values less negative than in other phases of fruit growth (Fig. 5B). This could explain the increasing P_{pmin} values along the P2 period. In P3, however, there was no correlation between fruit growth and P_{pmin} (Fig. 3B). Likely, and as mentioned above, the number of measurements of fruit growth made on P3 was not enough for a proper comparison with the highly variable P_{pmin} values. Bustan et al. (2011), looking for an effect of the reserves of carbon on the alternate-bearing in olive, found that during fruit development the resources of carbon changed according to the dynamics of source-sink relationships along the season, supporting our assumption of the reduction in P_{pmin} by carbon translocation. Another hint to explain the explain the response of P_{pmin} values to carbon translocation is that the hydrolysis of starch granules to glucose and sucrose and translocation from the leaf to other plant organs occurs mainly during the night (Stiit and Zeeman, 2012)

On the other hand, $\Psi_{fruit} - \Psi_{leaf}$ causes the main driving forces of water and sugar transport and integrate the overall plant functioning (Génard et al., 2007). For olive, the relationships between water potential in fruits (Ψ_{fruit}) and leaves (Ψ_{leaf}) have been studied by other authors, such as Sylvertsen and Albrigo (1980) and Dell'Amico et al. (2012). They found, for different olive cultivars under non-water stress conditions, that most of the time the water potential in the fruits (Ψ_{fruit}) was lower than Ψ_{leaf}, suggesting that the fluxes of water were primarily to supply fruits than leaves. These conclusions are in concordance with our results on the leaf capacitance at full turgor being usually higher for F+ than F- just after the P2 period (Fig. 5E). In fact, leaves closer to fruits could have a greater capacity to store water, i.e. a greater capacitance, to better serve the demands from the fruits. This indicates that a water flux in the direction leaf-fruit was more apparent in the leaves that were closer to a cluster of fruits. Hence, our results suggest that water and carbon fluxes between the fruit and the rest of the plant are effective on ensuring fruit development and, consequently, reproductive success.

Several studies reported leaf structural and mechanical changes in olive during leaf aging (Chartzoulakis et al., 1999; Centritto, 2002; Bacelar et al., 2004; Marchi et al., 2008). Those changes have an impact on the elastic modulus (ε), as a proxy of leaf cell wall stiffness, which tends to increase with leaf age (Bongi and Palliotti, 1994) and drought (Dichio et al., 2003). This agrees with our results (Fig. 5D). Moreover, the tendency of ε was to increase and be more variable at the end of the experiment (P3) point out that, as reported by the previously cited authors, as the leaf aged tends to be more rigid but not with the same rate for all the leaves. Other authors (Diaz-Espejo et al. 2018) suggested that

changes in both ε and osmotic potential (π) helped to avoid marked decreased in the leaf relative water content (RWC). Our results, in fact, shows greater values of RWC at the end of the season than at the beginning (Fig. 4E) likely because of the mentioned mechanisms occurring in the leaves of our experimental trees. In any case, our data show no differences on any of the recorded variables between the F+ than in F–treatments.

4.3. Future challenges

Our results suggest that, in trees with heavy fruit load, similar records can be expected by the ZIM probes independently of they being clamped in leaves close or far from fruits. This support suggestions by Fernández et al. (2011) and Padilla-Díaz et al. (2016) on a single ZIM probe per tree being enough to reliably assess plant-water status and to schedule irrigation. Our results also show that P_{pmin} values are affected by fruit growth and fruit changes during ripening, but more experiments are needed to disentangle those effects. Special attention should be paid on the periods when the olive tree is more sensitive to water stress, because of the complex interactions going on between leaves and fruits.

5. CONCLUSIONS

Our results confirm that, in olive trees growing under non-limiting soil water conditions, relative maximum daily turgor (P_{pmin}) was mainly driven by the previous daily values of *atmospheric demand*, followed by *water availability*. However, under similar values of *atmospheric demand* and *water availability*, the daily pattern of P_{pmin} changed depending on the fruit development stage. Moreover, the evidences of the good adjustment between the accumulated growth in the fruit and P_{pmin}, as well as the tent of the decrease in the maximum osmotic potential in the leaf, during the period of maximum rate of pit hardening and fruit growth (P2), suggested a seasonal influence of the fruit on P_{pmin}, as a result of compensating the carbon allocation from the leaves to the fruits under an equilibrium between water potential in the soil and leaf water potential. Phenomenon that likewise occurred in P3, however other processes implicated like changes in pathways of oil synthesis together with fruit growth were likely interacting with each other. Moreover, the increase on the elastic modulus with leaf aging did not have an influence on $P_{pmin.}$ For the clamping of the ZIM probes, our results show that it can be made in any leaf, regardless of being close or far from a cluster of fruits. Finally, the observed effects of main fruit development stages on P_{pmin} suggest that, after understanding the mechanisms below, this water stress indicator can become more useful to schedule irrigation on those periods when the plant water status may have a marked effect on fruit production.

6. SUPPLEMENTARY MATERIAL

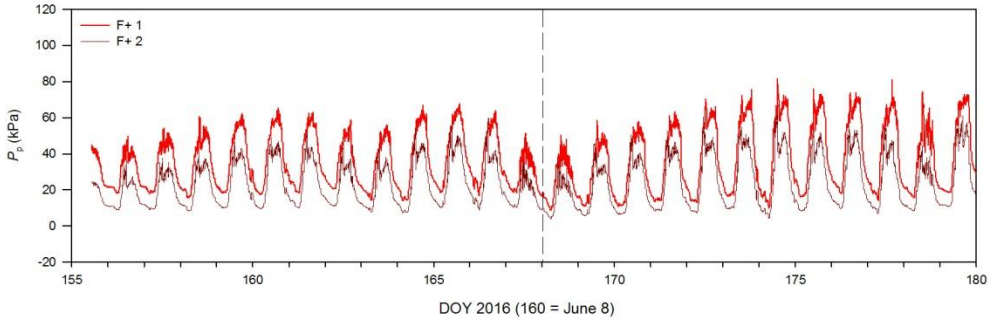

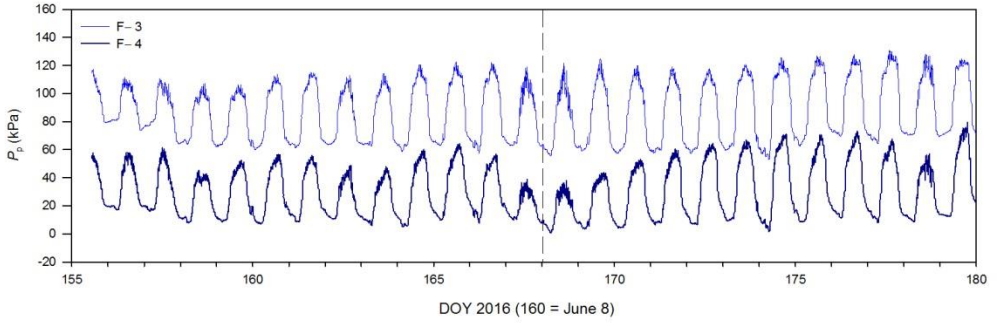

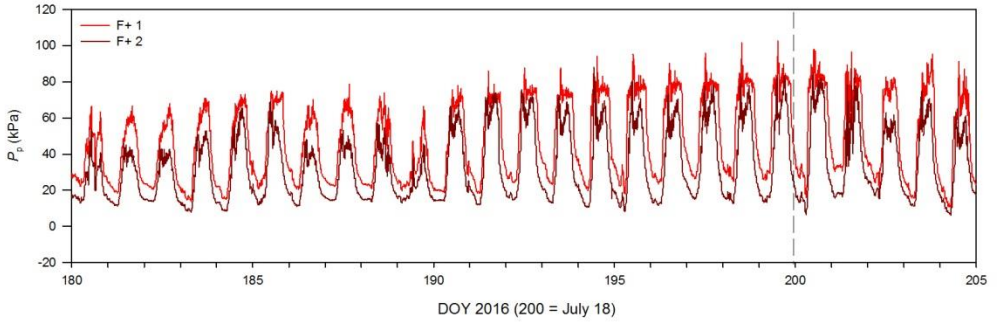

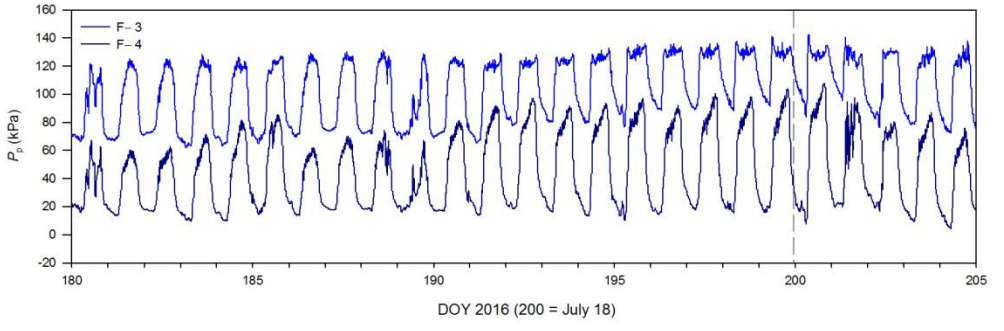

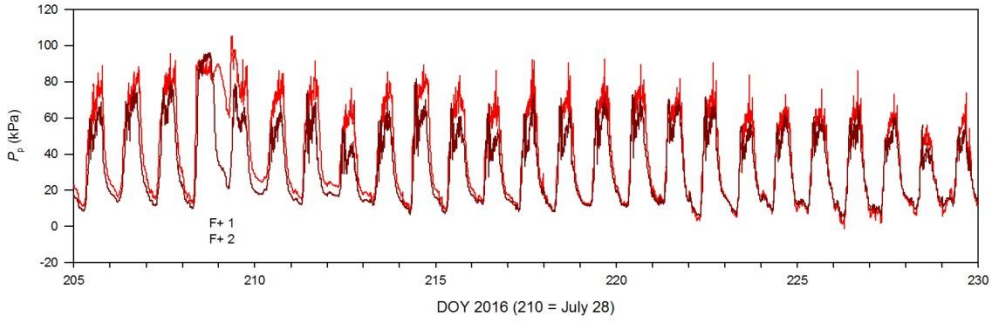
P_p (kPa)
F+ 1
F+ 2
DOY 2016 (210 = July 28)

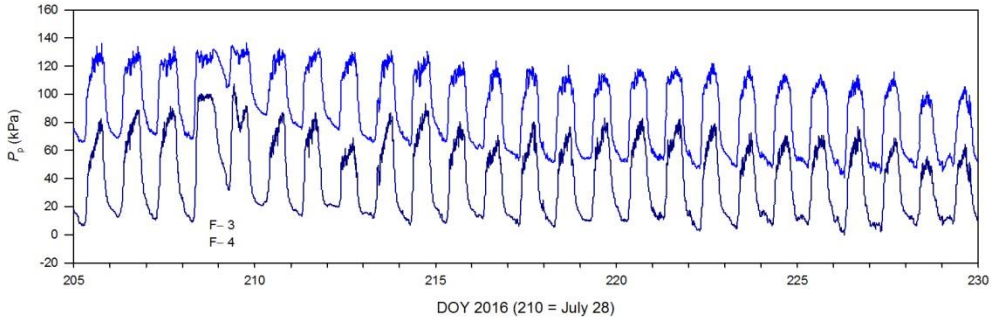
P_p (kPa)
F– 3
F– 4
DOY 2016 (210 = July 28)

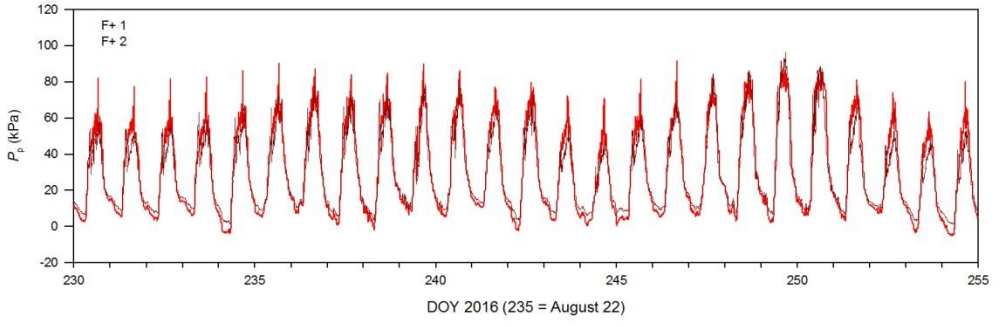
P_p (kPa)
F+ 1
F+ 2
DOY 2016 (235 = August 22)

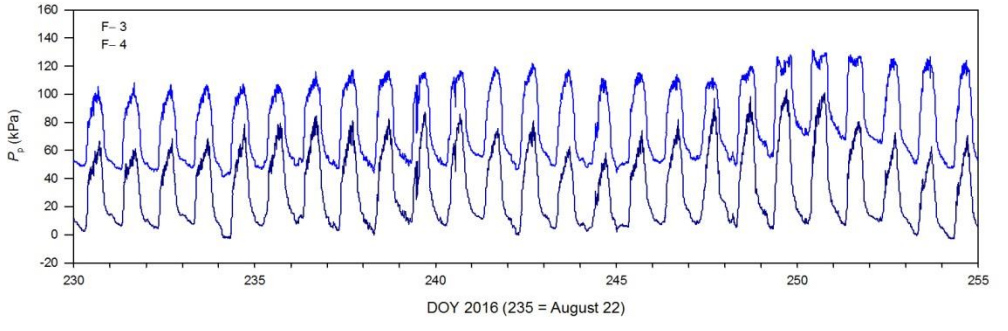
P_p (kPa)
F– 3
F– 4
DOY 2016 (235 = August 22)

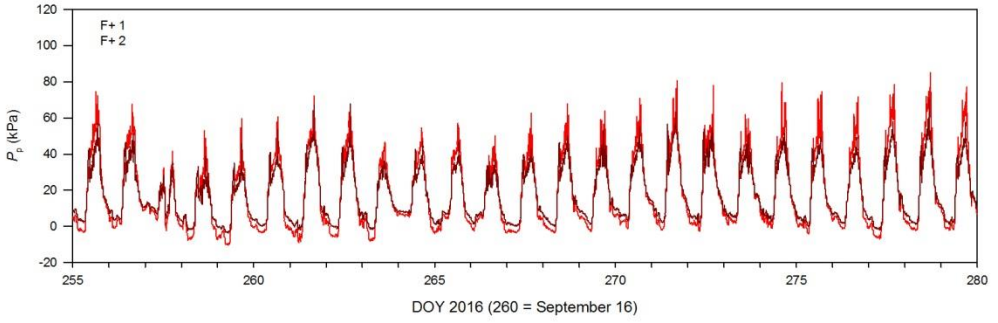
F+ 1
F+ 2
P_p (kPa)
DOY 2016 (260 = September 16)

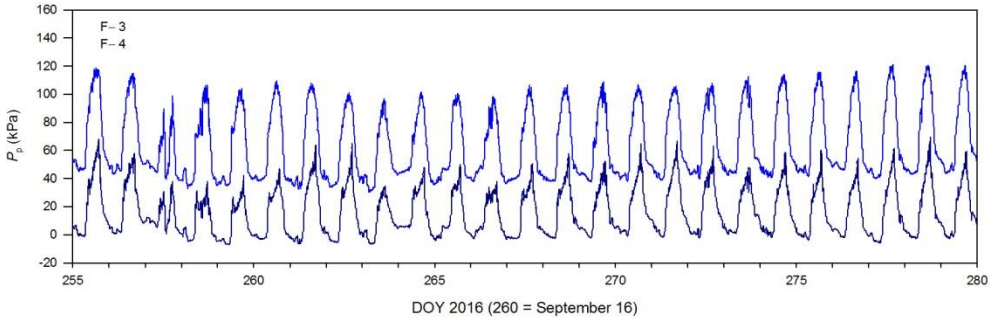
F– 3
F– 4
P_p (kPa)
DOY 2016 (260 = September 16)

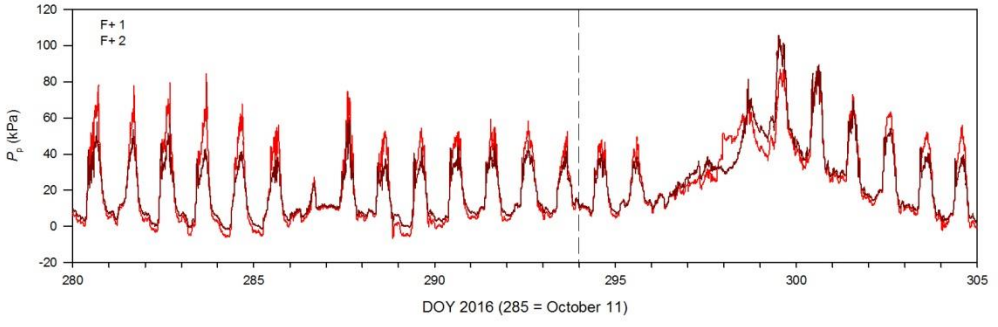
F+ 1
F+ 2
P_p (kPa)
DOY 2016 (285 = October 11)

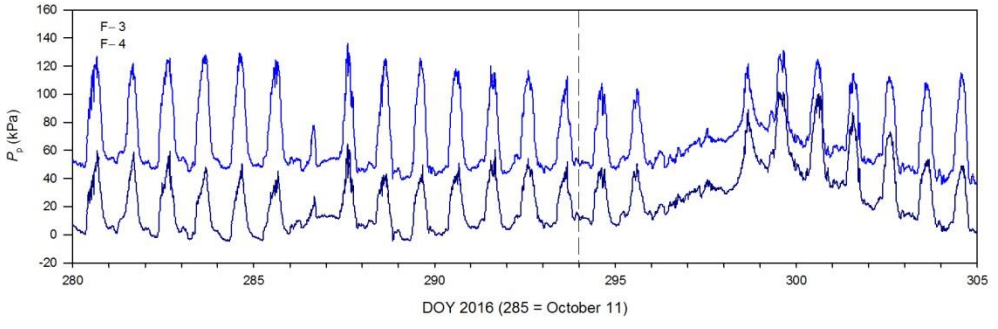
F– 3
F– 4
P_p (kPa)
DOY 2016 (285 = October 11)

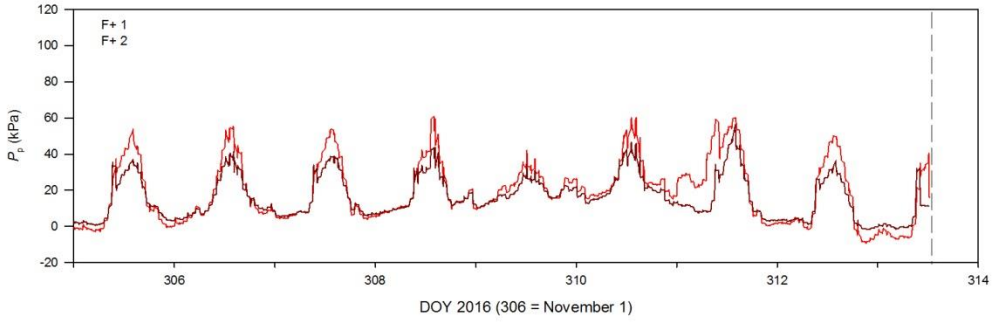
F+ 1
F+ 2
P_p (kPa)
120
100
80
60
40
20
0
-20
306
308
310
312
314
DOY 2016 (306 = November 1)

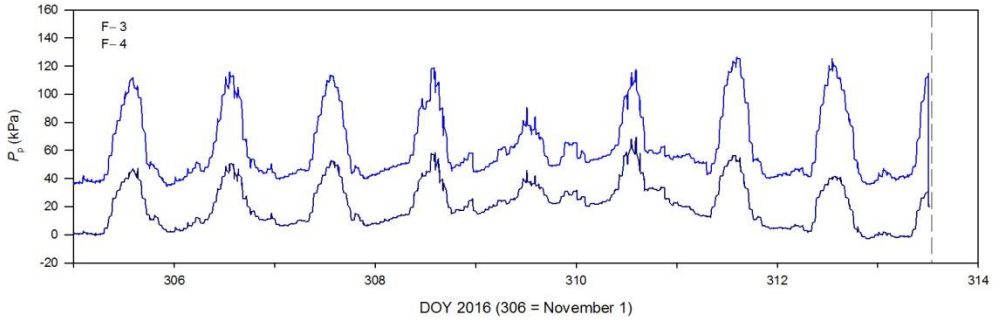
F– 3
F– 4
P_p (kPa)
160
140
120
100
80
60
40
20
0
-20
306
308
310
312
314
DOY 2016 (306 = November 1)

Chapter 5

Leaf turgor and leaf thickness under drought stress in olive

1. INTRODUCTION

In the last decades, the knowledge and awareness for a precise use of water in areas of scarcity has allowed the development of new sensors for monitoring plant water status. Among them, those relying on plant-based measurements have the advantage of informing on the plant response to the soil and atmospheric water status (Jones, 2004). The data collected with those sensors, however, are not always easy to interpret, due to the complexity of the soil-water-plant-atmosphere relationships (Jones, 2007; Fernández et al., 2014, 2018) and the adaptive responses to drought stress. Therefore, a greater understanding of the actual meaning of plant-based measurements for assessing water stress is needed for an efficient implementation of the sensors and related systems in commercial orchards.

For an irrigation user, the best plant-based sensors are those which allow monitoring the plant water status from non-destructive, automatic and continuous measurements, easy to install and maintain, and implemented with transmission systems for easy access to the collected data through the internet (Fernández 2014b). Among the wide variety of available plant-based methods (Jones, 2004; Fernández 2014b; Fernández 2017), a few rely on the measurements in the leaf. This is the case of the LeafSen sensor (hereafter LS sensor; Sharon and Bravdo, 2001) which measures the diel variations of leaf thickness, and the leaf patch clamp pressure probe or ZIM probe (Zimmerman et al., 2008), that measures a variable inversely related to the cell turgor pressure (P_p; kPa) (Ehrenberger et al., 2012). When the trees have enough water, the daily Pp curves show maximum values around midday, when the daily leaf turgor is minimum due to water loses by transpiration. At night, however, Pp values are closer to zero, in correspondence with greater leaf turgor pressure. When the sampled trees are under water stress conditions, the shape of the daily P_p curve changes. For moderate water stress, half-inversed P_p curves are collected. If the water stress increases, completely inversed P_p curves appears (more details in Fernández et al., 2011, and Ehrenberguer et al., 2012). Fernández et al. (2011) and Ehrenberger et al. (2012) stablished the relationship those three shapes or "States" derived from the daily P_p curves with the plant water status in olive trees. They reported that the State 1 was usually corresponded with a negligible water stress ($\Psi_{stem} > -1.2$ MPa), the State 2 with a moderate stress (within the interval between -1.2 MPa $< \Psi_{stem} < -1.7$ MPa) and the State 3 with severity levels of water stress ($\Psi_{stem} < -1.7$ MPa).

The two mentioned leaf sensors have been proposed for irrigation scheduling (Sharon et al., 2001; Pardossi and Incrocci, 2011; Cirillo et al., 2013; Fernández et al., 2011a; Bramley et al., 2013, Fernández, 2014b; Padilla-Díaz et al., 2016; Marino et al., 2016; Martínez-Gimeno et al., 2017). The LS was tested as indicator for irrigation scheduling, for the first time, by Seelig et al. (2012), but under greenhouse conditions. The ZIM probe, however, has proved to have a potential to schedule irrigation in commercial orchards, i.e. under field conditions. Padilla-Díaz et al. (2016), for instance, were able to schedule irrigation in commercial hedgerow olive orchard from the shape of daily Pp curves derived

from ZIM-probe readings. Both sensors, in fact, proved useful to schedule deficit irrigation strategies with which 45% and 55% of water savings, by LS and ZIM probes, respectively, were achieved (Seelig et al., 2012; Padilla-Díaz et al. 2016, 2018).

Although the close correspondence between daily P_p curves and the water potential (Ψ) in the stem (Fernández et al., 2011; Ehrenberger et al., 2012), there are still gaps in our understanding on the actual turgor fluctuations and the turgor measured by ZIM probes. In the case of the leaf thickness measurements, it is known that daily fluctuations of this variable are related to transpiration (Tyree and Cameron, 1977; Seelig et al. 2012). Also, decreasing Ψ values promote leaf shrinkage due to dehydration (Sylversten and Levy, 1982; Burquez, 1987; Sancho-Knapik et al, 2010, 2011), as well as a reduction in the relative water content of the leaf (Afzal et al., 2017). Furthermore, the relationship between leaf thickness and turgor pressure have been estimated (Scoffoni et al.; 2013;Seelig et al.; 2015) but never measured with a sensor on a leaf. Hence, understanding how both leaf thickness and turgor processes are coupled is complex and far from being completely understood.

It is known that a decrease in leaf turgor is a main driver of stomatal closure (Brodribb & Holbrook, 2003; Rodriguez-Dominguez et. al., 2016), causing an inhibition of photosynthesis (Lawlor & Cornic 2002; Brodribb and Holbrook 2003; Bartlett et al. 2012) and plant growth (Frensch and Hsiao, 1994). But the specific role of leaf turgor as a possible driver of other processes is still poorly understood. Cell turgor is recognized as a main driver of cell growth, being responsible for changes in cell wall properties (Lockhart et al., 1965; Cosgrove 1987, 2005, 2016; Kroeger et al. 2011). It is also involved in other processes such as water and carbon transport (Fatichi et al., 2014). A major scientific breakthrough would be the comprehension of diel and seasonal patterns in leaf turgor, which ultimately translates into growth processes (Steppe et al., 2015).

The aim of this study was to determine, from the combined use of ZIM probes and LS sensors, the threshold level of leaf turgor that is driving leaf thickness growth and changes in cell wall properties using pressure-volume curves. We also aimed at determining the threshold levels of water-environmental drivers of leaf turgor, and leaf turgor as a driver of leaf growth. We hypothesized that soil water limitation constrains cell growth in leaves. To this purpose, we carried out a greenhouse experiment using the olive tree as a plant model. Several studies have been recently made on this species, involving turgor measurements (Aissaoui et al. 2016; Marino et al. 2016; Padilla-Díaz et al., 2016, 2018, Rodriguez-Dominguez et al; 2016; Fernandes et al.; 2017). We had well-irrigated trees and trees under drought-stress and recovery. For insight into the mechanisms that drive leaf turgor and thickness, we also studied the relationships between plant water potential (leaf water potential at predawn, Ψ_{pd}; midday leaf water potential, $\Psi_{leaf,}$ and stem water potential, Ψ_{stem}), relative leaf maximum water content (RWC_{leaf}) at predawn and maximum leaf osmotic potential (π_{max}) at midday.

2. MATERIALS AND METHODS

2.1. Plant material and experimental setup

The experiment was carried out with 2-year old olive seedlings (*Olea europaea* L. cv. Arbequina). Plants were grown at Seville, south-west Spain, and in February 2016 were sent to the greenhouse facilities at the Institute for Agricultural and Fisheries Research (ILVO) in Melle, Belgium (50° 59' 35.8" N, 3° 47' 03.1" E). Each plant was transplanted to 35-L pots, with a substratum for Mediterranean plants (AGROFINO, Peltracom, Overpelt, Belgium) which consisted in a soil mixture of peat litter (10% organic material), clay, lava and calcium-magnesium based slow-released fertilizers (NPK 14-14-18, 1.2 kg m^{-3}). The irrigation doses were estimated from the daily cumulated plant-water consumption, assessed with Dynagage sap flow sensors (stem heat balance method, Dynamax, 2005) connected to a CR-1000 datalogger. They were estimated once every two weeks and input in an irrigation controller. Water was applied daily by a drip irrigation system providing one 2 L h^{-1} dripper per plant. At the beginning of the experiment, six trees of similar height and stem diameter (1.24 ± 0.03 m; 8.32 ± 0.17 mm, avg. ± sd, respectively) were selected. Three of them were maintained under well-watered soil conditions (control treatment, each tree was named as C1, C2, C3) during the whole experiment, and the other three trees were under water stress conditions(stress treatment, with trees named as S4, S5, S6). The experiment started on April 18th, when all trees presented similar values for midday stem water potential (Ψ_{stem} = -1.40 ± 0.16 MPa, avg ± sd). The stress period in the stress treatment lasted from April 22^{sd} to May 17th, a period in which the irrigation was withheld. From May 17th to 29th, we had daily irrigation with the same amount of water as the control treatment, from the recovery of the stress.

2.2. Soil and meteorological measurements

The volumetric water content (VWC; %) was monitored along the whole experimental period with one EC5 soil moisture sensor (EC5, Decagon, Pullman, WA-US) per tree. The EC5 sensors were calibrated following the manufacturer's instructions. At the same time that the calibration was carried out under soil rehydration, soil water potential (Ψ_{soil}) was measured with two tensiometers (TensioTrans, model TT 1531, Bambach GbR Tensio-Technik, Geisenheim, Germany). A water retention curve was fitted to the values recorded during calibration.

Meteorological conditions in the greenhouse simulating Mediterranean climate were fixed, and controlled by a MT/MTV sensor unit (HortiMaX). Moreover, a meteorological station was placed in between trees for measuring continuously air temperature (T_a; ºC), relative humidity (RH; %) and photosynthetically active radiation (PAR; µmol $m^{-2}s^{-1}$). T_a in the greenhouse was measured by a copper-constantan thermocouple (Omega, Amstelveen, The Netherlands) and ranged between 20 − 36 ºC. RH was measured with a capacitive RH sensor (Type HIH-3610, Honeywell, Morristown, NJ,

USA), and ranged from 15% to 85.5%. Vapour Pressure Deficit (VPD; kPa) was calculated from T_a and RH records, with values going from 0.6 to 4.93 kPa. PAR was measured with a quantum sensor (Li-190S, LiCOR, Lincoln, NE, USA) and ranged between 0 and1570 μmol m^{-2} s^{-1}. Both soil and meteorological measurements were recorded by a datalogger (CR-1000, Campbell Scientific Inc., Logan, Utah, USA) and uploaded to the PhytoSense cloud service (Phyto-IT BVBA, Mariakerke, Belgium) for its storage and processing. Sensor signals were logged every three seconds and averaged every five minutes for its storage.

2.3. Turgor and leaf thickness measurements

Healthy and fully developed current-year leaves were selected to monitor turgor (from P_p values; kPa) and leaf thickness variations (μm). Sampled leaves were the 5th or 6th leaf from the apex and from the middle of the canopy. One ZIM probe (Yara Water-Sensors, YARA ZIM Plant Technology GmbH, Hennigsdorf, Germany) per tree was clamped to monitor P_p values (n = 3) . In the opposite leaf, a leaf clip sensor (LS, LeafSen, Netafim, Tel Aviv, Israel) was installed to monitor the leaf thickness (n = 3). In all cases, the central nerve of the leaf was avoided during sensor installation. The sensors were installed on March 31, 2017, early in the morning (4.00 – 5.00 GMT) when both leaf turgor and thickness were around their maximum. The recorded P_p values were sent every 5 min from the Yara ZIM-lab transmitter by USB wire to a local computer for their storage. Leaf thickness values were recorded and stored following the same methodology as detailed for the soil and meteorological measurements (Section 2.2). All sensors worked properly and none of them were reclamped. Still, we had P_p data missing from May 8 to May 15 due to a problem with the data storage in the greenhouse computer.

The P_p values were normalized for comparison between treatments, according to the equation:

$$P_p\ (\%) = \frac{P_p' - P_{pmin}}{P_{pmax} - P_{pmin}}\ x\ 100 \quad , \qquad (1)$$

where P_p' is the current P_p value, P_{pmin} and P_{pmax} are the minimum and maximum P_p values, respectively, recorded during the experimental period.

The correlation between leaf thickness variations along and air temperature, was explored after Lauriks et al. (2017). Basically, both before and after the experiment, the LS sensors were installed in an aluminium plate of 0.5 mm thickness, in the greenhouse facilities, during 4 days to be under temperature conditions similar as those during the experimental period. The aluminium plate was assumed to be thickness constant and the variations registered by the LS sensors were used to correct for their temperature dependency. The first day of the experimental period, the leaf thickness outputs were adjusted to zero in all trees, for recording relative thickness variations (μm).

2.4. Plant-water relations and concomitant measurements

Measurements of leaf water potential at predawn (Ψ_{pd}; MPa; 2.30 – 4.00 GMT) and at midday (Ψ_{leaf}; MPa; 12.00 – 16.00 GMT), and of stem water potential at midday (Ψ_{stem}; MPa; 12.00 – 16.00 GMT), were made every week, with a Scholander-type pressure chamber (PMS Instrument Company, Albany, Oregon, USA). One leaf per tree, of the same type as described in Section 2.3, was sampled each time. For midday stem water potential we choose leaves close to the main stem, from the inner part of the canopy, and wrapped them at least 2 hours prior to the measurements in plastic bags covered with aluminium foil.

Leaf relative water content (RWC_{leaf}; %) was calculated for one leaf per tree, in the 6 trees sampled trees and on the same days as Ψ_{pd}. Leaves were taken just after the Ψ_{pd} measurements (03.00 – 04.00 GMT). Again, the leaves were sampled as described in section 2.3. The leaves were immediately introduced in opaque plastic tubes, stored in darkness and taken to the laboratory for determining their fresh weight (FW; g) with a digital balance (DK 6200 with 10^{-3} g accuracy, Henk Maas, Veen, The Netherlands). Later, the leaves were rehydrated by immersing the petiole in distilled water at 4 ºC during 24 h, in darkness. After rehydration, the excess of water was removed by a soft cloth, and the leaves were weighted for the well-watered weight (WW; g). Then, the leaves were oven dried until dehydration (48 h at 70 ºC) and weighted for the dry weight (DW; g). RWC_{leaf} was calculated as:

$$RWC_{leaf}\ (\%) = \frac{FW - DW}{WW - DW}\ x\ 100 \quad . \qquad (2)$$

The time courses of the maximum adjustment of leaf osmotic potential (π_{max}; MPa) were derived from two leaves per tree, sampled at midday (12.00 – 14.00 GMT) from the same days as described in Section 2.3. The leaves were cleaned with a damp paper towel, packed in aluminium foil and immediately submerged in liquid nitrogen. Then they were stored at -20 ºC until analysis with a thermocouple psychrometer with standard C-52 chambers (Wescor inc., Logan, UT, USA) connected to a datalogger (PSYPRO, Wescor Inc.). Two discs were punched from each leaf, avoiding the central nerve, and measured under constant temperature for at least 45 min, for sample equilibrium inside the chamber. The data recorded were averaged firstly by leaf and secondly by tree.

Both during the stress period and at the end of the recovery period, the maximum stomatal resistance was measured with a porometer (AP4, Delta-T, Cambridge, UK) in the two treatments. One leaf per tree was sampled at 08.00 – 09.00 GMT, with the same criteria as described in Section 2.3. That is when maximum leaf gas exchange occurs in olive (Fernández et al., 1997). Moreover, at the end of the experiment the leaf area of each tree was measured with a LICOR 3100 leaf area meter (LI-COR, Lincoln, NE, USA).

2.5. Pressure-volume curves

Again, a leaf with the same characteristics as reported in Section 2.3 was sampled at predawn, on the same days as the other physiological variables mentioned above. Just after cutting, the leaves were rehydrated as mentioned above. Each rehydrated leaf was the used to make pressure-volume (P-V) curves, i.e. to calculate parameters derived from the relationship between the loss of leaf water potential (Ψ_{leaf}) with the loss of water volume (g; later transformed into RWC_{leaf}) along the leaf dehydration. For this purpose, Ψ_{leaf} (MPa) was measured periodically with a Scholander-type pressure chamber till ca. −4 MPa, at the same time that the loss of weight was determined with a digital balance. Later, the leaf area (S; m^2) was calculated using the ImageJ software (Schneider et al.; 2012), from images scanned with a Canon CanoScan Lide 120 scanner, Finally, the leaves were oven-dried during at least 48 h at 70 ºC, to obtain their DW (g). For calculations, we followed the protocol published by Sack et al. (2011). The first interception point of the linear relationship $-1/\Psi_{leaf}$ (Y axis) vs the RWC_{leaf} (%) (X axis) curve determined the leaf water potential at turgor loss point (Ψ_{tlp}; MPa). As a consequence, the osmotic potential at full turgor (π_o; MPa) was given by the intercept of that linear relationship with the Y axis. In addition, the elastic modulus (ε; MPa) corresponded with the slope of the relationship $-1/\Psi_{leaf}$ vs RWC from full turgor till turgor loss point. The absolute capacitance at full turgor (C_{FT}; mol m^{-2} MPa^{-1}) was estimated till Ψ_{tlp} with the following equation (Blackman and Brodribb, 2011):

$$C_{FT}\,(mol\,m^{-2}\,MPa^{-1}) = \frac{\partial RWC_{leaf}}{\partial \Psi_{leaf}} \left(\frac{DW}{S}\right)\left(\frac{WW}{DW}\right)\frac{1}{M} \quad . \qquad (3)$$

The parameters derived from the P-V curves were averaged by treatment.

2.6. Statistical analysis

We fitted generalized additive models (GAM) using environmental variables and internal leaf water relations as explanatory variables to predict leaf thickness and P_p. For a better understanding of the relationship between RWC_{leaf} and P_p values, Ψ_{pd} and π_{max}, we also performed GAM. All the cases integrated smoothness estimation and were performed using the "mgcv" package (Wood, 2006) under a Gaussian family distribution with $P \leq 0.05$ as significant level. Smooth terms were represented using cubic splines with smoothing parameters selected by generalised cross-validation (GCV). We used the coefficient of determination (R^2) to explain the goodness of fit of the observed values vs. predicted values of the models. To analyse the differences between treatments and dates in the parameters of the internal water-relations derived from the P-V curves, we tested with a Shapiro-Wilk the normality and the homoscedasticity of the variance with a Levene's test prior to Student's t-Test taken a $P \leq 0.05$ as significant level. All the statistical analyses were made using R software (RStudio v.1.1.383; RStudio Inc., Boston, MA, USA).

3. RESULTS

3.1. Tree water deficit induced changes in leaf thickness and turgor measurements

A similar behaviour of leaf thickness and P_p was observed in all trees of the same treatment (Fig. 1). Along the experiment, the variability of leaf thickness increased in both treatments, being more patent in control treatment than in the stress. This variability was due to C2 and C3 trees that increased its thickness differently but higher than C1. In the stress treatment, the maximum leaf thickness decreased slightly till about May 8th (i.e. 15 days after irrigation was withheld). From that day the maximum leaf thickness decreased abruptly. A similar pattern was shown by the amplitude of the leaf daily shrinkage, being wider at the end of the stress period (Fig. 1b and 2c) than at the beginning. The P_p values were less variable than leaf thickness, for both treatments, along the whole experiment, except for the stress treatment during the stress period. On April 25th, the minimum daily value of P_p was increasing, the difference between P_p maximum and P_p minimum started to decrease on 4th of May. State 2 appeared, for the first time, on May 8th (Fig. 2d), and State 3 on May 10th. After the beginning of the recovery period in the stress treatment (from 18th of May till the end of the experiment), both leaf thickness and P_p curves responded in less than 24 hours to the water applied. During the second night of the recovery period, two trees went from State 3 to State 1, and the minimum values of P_p and the maximum values of leaf thickness were similar to the values of May 4 (Fig. 1). Along the recovery period both maximum leaf thickness and the minimum P_p values were closer to the values recorded at the beginning of the experiment. However, the amplitude of the daily leaf shrinkage and the amplitude on the P_p curve were lower compared with the control treatment (Figs. 1 and 2).

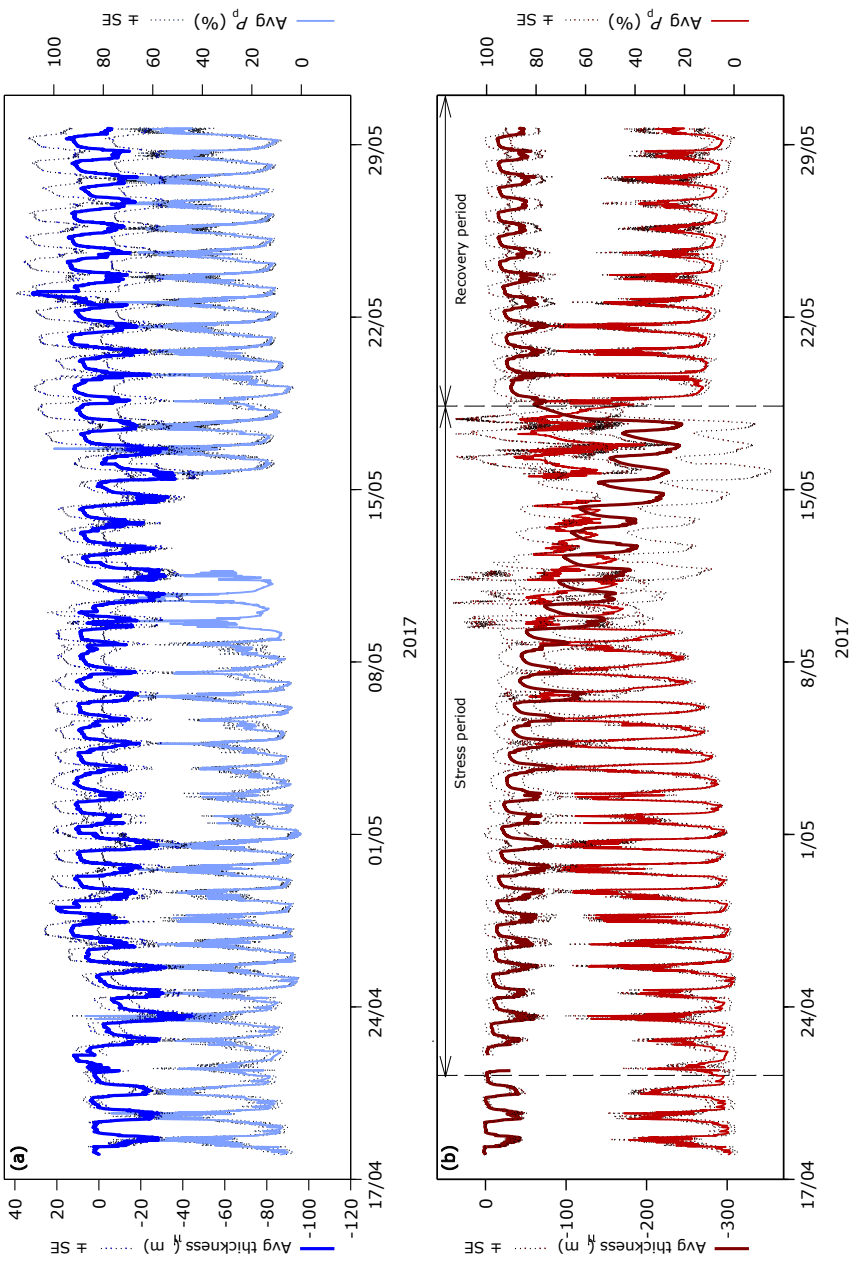

Fig. 1 Time courses of the leaf thickness (µm; avg. ± SE) and P_p (%; avg. ± SE) readings by leaf clip sensors and ZIM probes along the whole greenhouse experiment in 2017 under (a) control and (b) stress treatments. In the stress treatment, in between the long-dashed vertical lines the irrigation was withheld (stress period), from the last vertical line to the end of the experimental period the irrigation was restarted (recovery period) (b). Three trees per treatment were monitored.

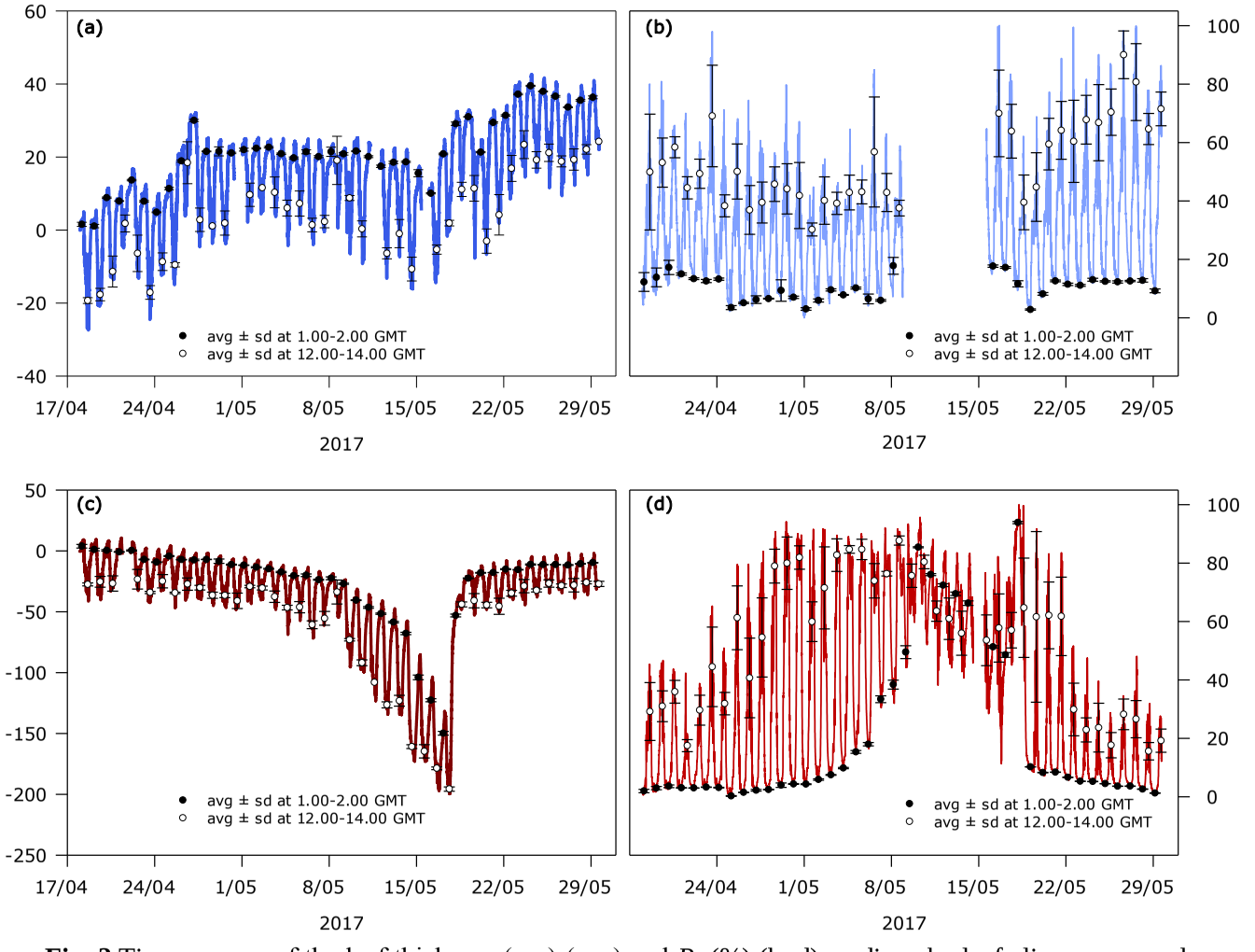

Fig. 2 Time courses of the leaf thickness (µm) (a, c) and P_p (%) (b, d) readings by leaf clip sensors and ZIM probes along the whole greenhouse experiment in 2017 for the one tree of the control treatment (a, b; tree C3) and its opposite tree in the stress treatment (c, d; tree S6). Black dots correspond with the predawn (avg ± sd) of the readings in the period of time between 1.00 – 2.00 GMT. White dots are the midday (avg ± sd) of the readings in the period of time between 12.00 – 14.00 GMT.

The minimum and the maximum for both leaf thickness and P_p were taken as the averaged values before predawn interval, 1.00 to 2.00 GMT (3:00−4:00 a.m., local time), and midday interval, ranged between 12.00 to 14.00 GMT (2:00−4:00 p.m., local time) (Fig. 2). For both treatments and variables, the averaged night values showed a better goodness of fit with a low standard deviation. In the case of the averaged diurnal values, the dispersion of the data was higher than those of the night. These results are not surprising, since the environmental variability at midday influenced both leaf turgor and leaf shrinkage. The successive calculations shown in this work were made with these average values for the night (predawn) and day (midday). We chose those averaged values because important leaf water processes happen in those periods (e.g. the minimum night values are implicated in the plant water recover during night, as well as midday values are related with maximum plant water consumption).

Results of stomatal resistance at midday showed significant differences between treatments, at the end of the stress period (control: 496.59 ± 245.69 s m^{-1}; stress: 2249.67 ± 616.49 s m^{-1}; avg ± sd respectively, P value < 0.05). Nevertheless, at the end of the experiment there were no significant differences between both treatments (control: 824.60 ± 371.74 s m^{-1}; stress: 819.75 ± 376.76 s m^{-1}; avg ± sd, $P > 0.05$).

3.2. Environmental drivers of turgor, leaf thickness and plant water status

Figure 3 shows the relationships between volumetric soil water content (VWC; %) and vapour pressure deficit (VPD; kPa) with P_p and leaf thickness, for each experimental tree and all along the experimental period. The threshold values for VWC were obtained from the estimated pF curve (R^2 = 0.96, supplementary material). The pF curve showed that field capacity occurred at 26.71% of VWC, and the permanent wilting point (PWP) was reached at 14.95% of VWC. Although we are aware that the estimation of the pF curve with measurements derived from soil sensors were not very accurate (e.g. lower values Ψ_{soil} measured with tensiometers), and together with the high variability that soils present, we considered this pF estimation as a good proxy to understand the limits of soil moisture that are affecting plant performance. In fact, the values of PWP fitted very well with the behaviour of P_p values and leaf thickness in the stress treatment, which suffered exponential changes, for both variables. From FC to PWP (Fig. 3a and c) in the control treatment, the C1 tree was close to the limit of FC. This indicates that tree C1 was suffering some water stress in comparison with the other trees of the control treatment. All control trees received the same amounts of water, but the C1 trees was the one with the greatest leaf area (C1 = 9352.2 cm^2; C2 = 7919.6 cm^2, C3 = 6934.4 cm^2. Values obtained at the end of the experiment). Leave thickness increased in C2 and C3, but not in C1. This is in agreement with the moderate level of water stress suffered by that tree, already commented (Fig. 3c). In the case of P_p values, a 20% of P_p was the threshold limit because higher value of the control treatment appeared at this point at predawn (Fig. 3a, b), moment in which the tree is in equilibrium with the soil water status. Exceeded the limit of FC, both predawn and midday values increased abruptly in the case of P_p values (Fig.3a) and

decreased also abruptly for leaf thickness (Fig.3c). On the contrary, the response to VPD, in the control treatment, was linear for both P_p for midday values (Fig.3b). In the stress treatment we found no relationship, neither for leaf thickness nor forP_p, with VPD and VWC (Fig. 3b, d).

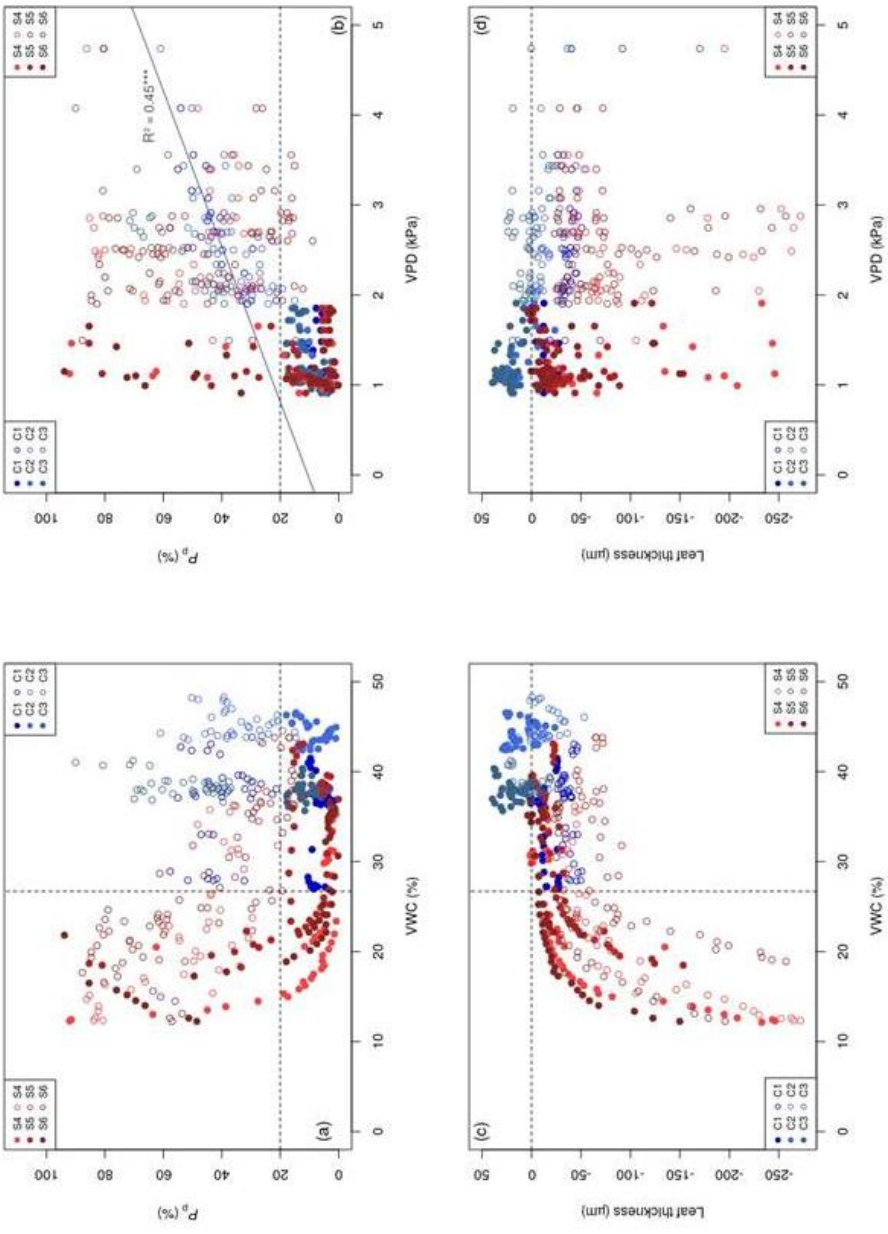

Fig. 3 Relationships between soil volumetric water content (VWC; %) and air vapour pressure deficit (VPD; kPa) with P_p (%) (a, b), and leaf thickness (µm) (c,d) along the whole experiment. Group of blue dots correspond with control treatment and group of red dots with the stress treatment. Each different dot colour belongs to one tree monitored in the experiment, where the trees C1, C2 and C3 were control trees and S4, S5, S6 were stress trees. Filled dots represent the average of predawn values and opened dots the average of midday values (see Fig. 2 to identify those averaged values). P_p threshold (a, b) was selected as the lowest predawn values for control treatment whilst leaf thickness threshold (c, d) was the zero line, both of cases those thresholds are represented as straight horizontal lines. The threshold of VWC represents the soil field capacity, showed as vertical black dashed lines (a, c). Grey strait lines represent the fitted generalized additive models to all dataset and the goodness of fit is represented by the coefficient of determination (R^2), *** $P < 0.001$. No grey lines mean non-significant relationship.

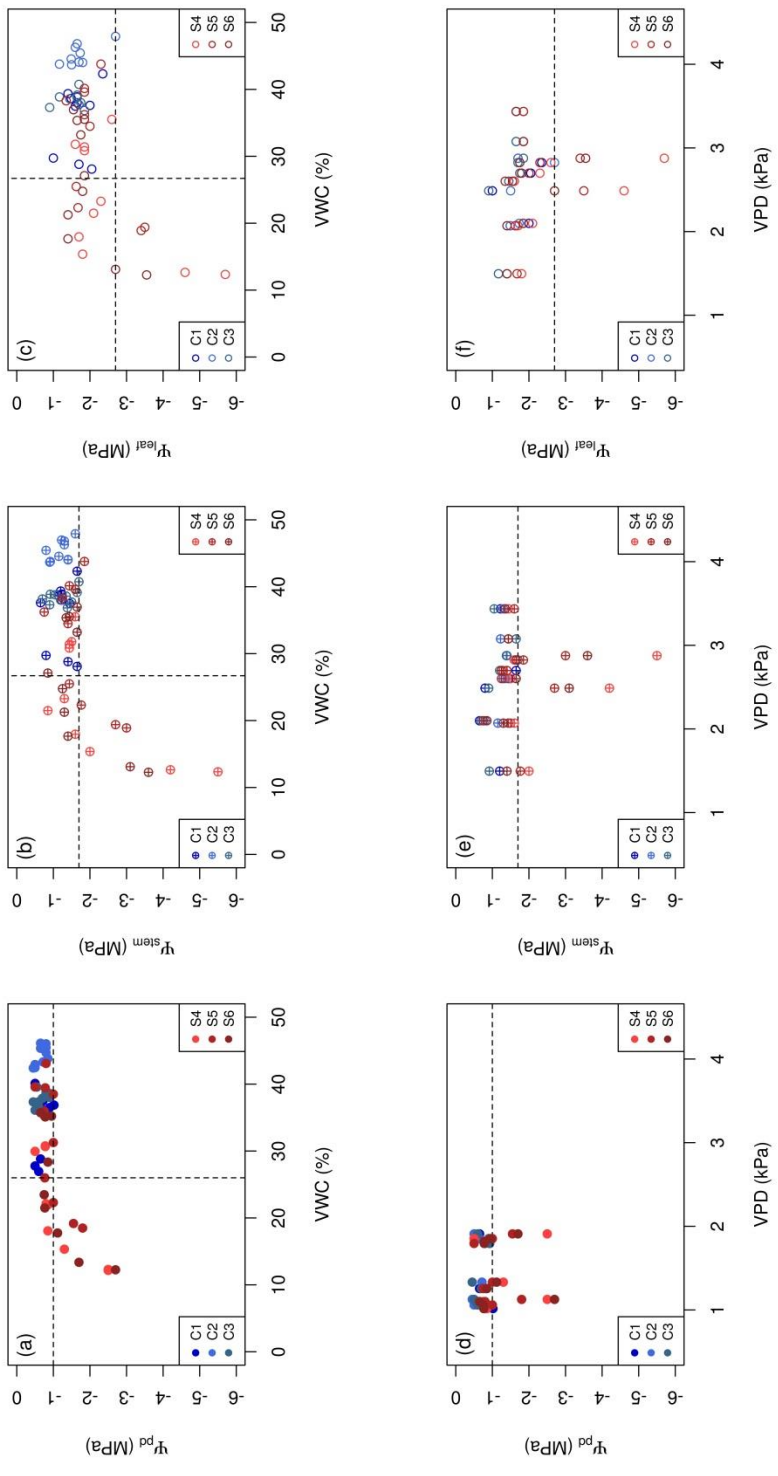

Fig. 4 Relationships between soil volumetric water content (VWC; %) and air vapour pressure deficit (VPD; kPa) with predawn water potential (Ψ_{pd}; MPa) (a, d), stem water potential (Ψ_{stem}; MPa) (b, e) and leaf water potential at midday (Ψ_{leaf}; MPa) (c, f) along the whole experimental period. Group of blue dots correspond with control treatment and group of red dots with the stress treatment. Each different dot colour belongs to one tree monitored in the experiment, where the trees C1, C2 and C3 were control trees and S4, S5, S6 were stress trees. Filled dots represent the values at Ψ_{stem} and environmental parameters at predawn (a, d), dots with cross represent environmental parameters at midday compared with Ψ_{stem} (b, e), and opened dots represent environmental parameters at midday compared with Ψ_{leaf} (c, f). The Ψ threshold values fit with the lowest values found for the control treatment, being $\Psi_{pd} = -1.4$ MPa, $\Psi_{stem} = -1.7$ MPa and $\Psi_{leaf} = -2.7$ MPa, all of them are shown in the graphs as horizontal dashed lines. The threshold of VWC represents the soil field capacity, showed as vertical black dashed lines (a, b, c).

The VWC and VPD relationships with plant water status are shown in Fig. 4. The threshold values stablished for water potentials followed the same criterion as for Fig. 3, were the lowest values for the control treatment were chosen as the limit for well-watered trees. Figs. 4a to 4c suggest that the values of $\Psi_{pd} = -1$ MPa, $\Psi_{stem} = -1.7$ MPa, $\Psi_{leaf} = -2.7$ MPa are thresholds for field capacity conditions. As expected, there was no relationship between VPD and plant water status, either for predawn or midday measurements, for both treatments (Figs. 4d, e, f).

3.3. Plant water relations as drivers of turgor and leaf thickness

Leaf thickness showed a significant, non-linear relationship between water potentials at predawn and at midday (Fig. 5a, b, c) in contrast to P_p values (Fig. 5d, e, f). In Fig. 6 is represented an approach of the classical Höfler diagram, being in this case constructed from concomitant measurements in both treatments along the whole experimental period. This diagram shows changes in leaf relative water content (RWC_{leaf}; %) together with changes in P_p values at predawn, Ψ_{pd} and maximum values of osmotic potential (π_{max}; MPa). These concomitant measurements were fitted using generalized additive models with integrated smoothness estimation, and the results showed significant relationships at $P < 0.001$. As expected, when the water stress appeared all variables declined, expected P_p values that increased. The relationship between RWC_{leaf} and π_{max} was always linear. For the rest of variables, it become linear from 70-80% of RWC_{leaf}, suggesting the point of turgor loss point could be around this interval. By contrast, towards full turgor (i.e. over the threshold of 20% for P_p and over the 94% of RWC_{leaf} taken as threshold, as it is the lowest value found for control treatment) there were high variability including in the control treatment for all the variables measured.

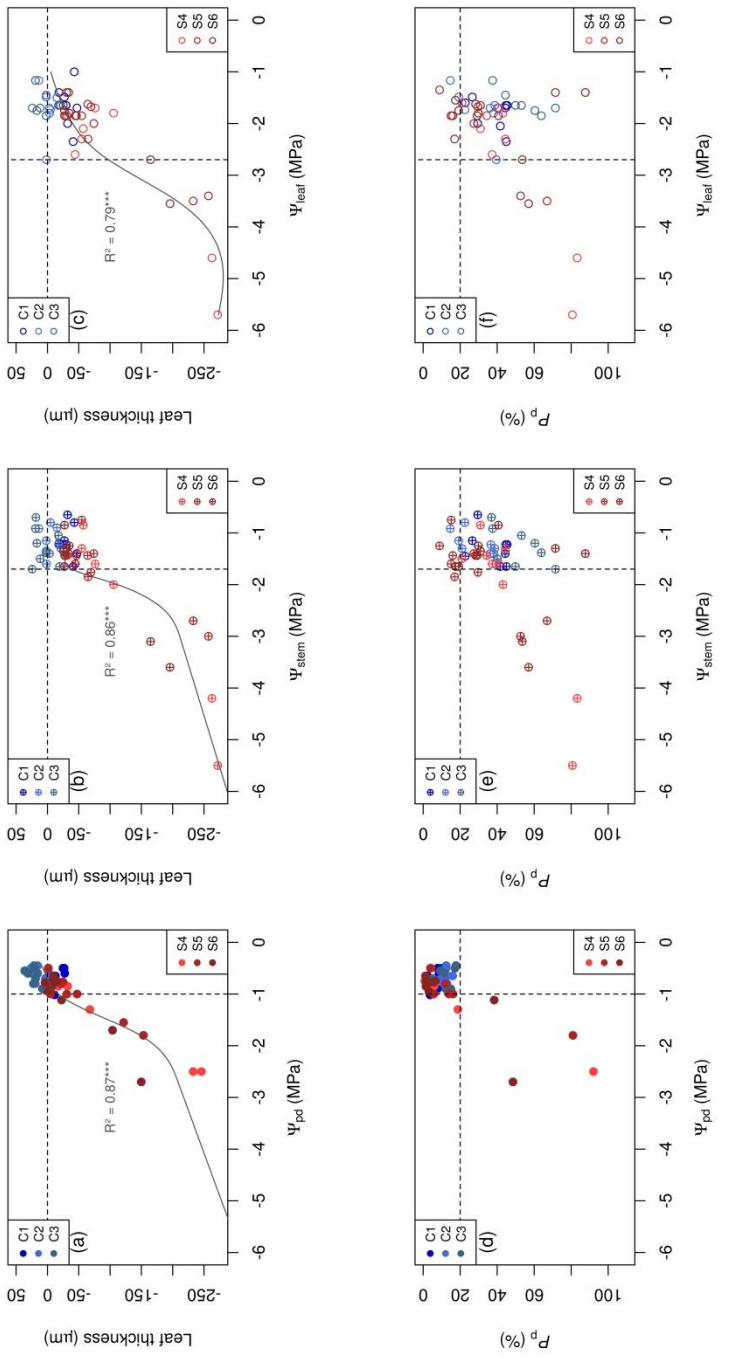

Fig. 5 Relationships between leaf thickness (µm) and P_p values and predawn water potential (Ψ_{pd}; MPa) (a, d), stem water potential (Ψ_{stem}; MPa) (b, e) and leaf water potential at midday (Ψ_{leaf}; MPa) (c, f). Values of P_p and leaf thickness were taken at the same time as Ψ measurements, see Fig. 2 to identify those dial values along the whole experimental period. Group of blue dots correspond with control treatment and group of red dots with the stress treatment. Each different dot colour belongs to one tree monitored in the experiment, where the trees C1, C2 and C3 were control trees and S4, S5, S6 were stress trees. Filled dots represent the values at Ψ_{stem} and environmental parameters at predawn (a, d), dots with cross represent environmental parameters at midday compared with Ψ_{stem} (b, e), and opened dots represent environmental parameters at midday compared with Ψ_{leaf} (c, f). The Ψ threshold values fit with the lowest values found for the control treatment, being $\Psi_{pd} = -1$ MPa; $\Psi_{stem} = -1.7$ MPa and $\Psi_{leaf} = -2.7$ MPa, all of them are shown in the graphs as vertical dashed lines. Leaf thickness threshold (a, b, c) was the zero line whilst P_p threshold (a, b) value that was selected as the lowest predawn values for control (d, e, f) both of cases those thresholds are represented as horizontal dashed lines. Grey strait lines represent the fitted generalized additive models to all dataset and the goodness of fit is represented by the coefficient of determination (R^2), *** $P < 0.001$. No grey lines mean non-significant relationship.

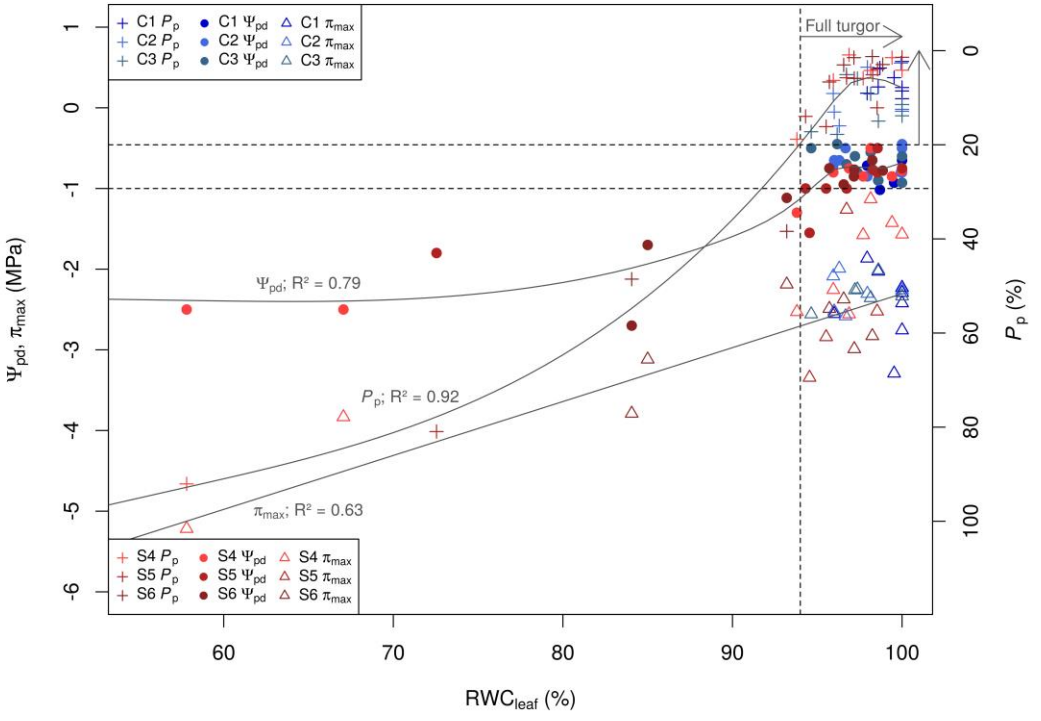

Fig. 6 A Höfler diagram approach showing the relationship between the leaf water potential at predawn (Ψ_{pd}; MPa), inversely related leaf turgor pressure (P_p; %) derived from the ZIM probes readings, the maximum osmotic potential taken at midday (π_{max}; MPa) for the variation of the leaf relative water content (RWC_{leaf}) taken at predawn. The concomitant measurements were taken from different leaves and treatments along the whole experimental period. Group of blue symbols correspond with control treatment and group of red symbols with the stress treatment. Each different group symbol colour belongs to one tree monitored in the experiment, where the trees C1, C2 and C3 were control trees and S4, S5, S6 were stress trees. Crosses corresponded with P_p values, dots with values of Ψ_{pd}, whereas triangles were π_{max}. Dashed lines corresponded with the threshold values selected as the las value for the control treatment in all variables measured except π_{max}, being Ψ_{pd} = – 1 MPa; P_p = 20 % and RWC_{leaf} = 94%. Grey strait lines represent the fitted generalized additive models to each variable measured and the goodness of fit is represented by the coefficient of determination (R^2), *** $P < 0.001$.

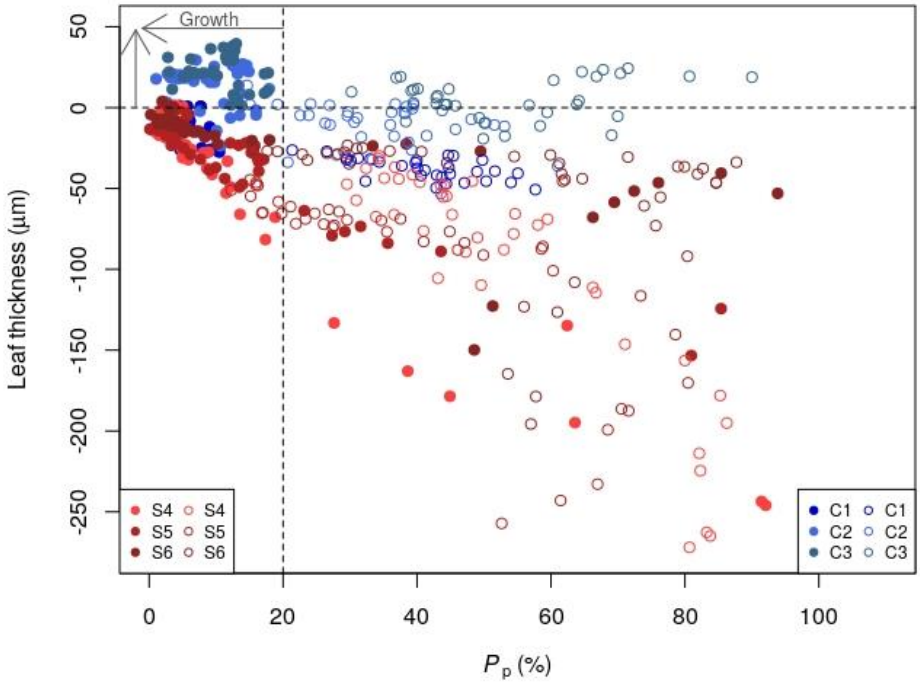

Fig. 7 Relation between leaf thickness (µm) and P_p (%) for predawn (filled dots) and midday (opened dots). Group of blue dots correspond with control treatment and group of red dots with the stress treatment. Each different dot colour belongs to one tree monitored in the experiment, where the trees C1, C2 and C3 were control trees and S4, S5, S6 were stress trees. Horizontal dashed line represents the threshold value for leaf thickness growth whereas vertical dashed line was the minimum threshold of P_p values.

The Figure 7 shows the relationship between midday and predawn values for P_p and leaf thickness. This graph suggests that leaf growth in thickness occurred mainly at predawn and, as explained in Section 3.2, under the 20% as P_p threshold value leaf growth only occurred for two out of the tree control trees. When the stress became more severe, there were linear relationships between predawn and midday values for the stress treatment, relationships that not were found for the control treatment. In other to understand if growth were due to changes in the cell walls of the leaves, we constructed pressure-volume (P-V) curves at the beginning and at the end of the experiment. These results appear in Table 1. All the variables derived from the P-V curves are concordant with the values showed in the Höfler diagram approach (Fig. 6). At the beginning of the experiment, and for both treatments, there were not significant differences in any of the variables derived from the P-V curves (Table 1). By contrast, at the end of the experiment there were significant differences between treatments. In the stress treatment occurred an increase in the relative water content at turgor loss point (RWC_{tlp}; %) and in the elastic modulus (ε; MPa), conversely the absolute capacitance at full turgor (C_{FT}; mol m^{-2} MPa^{-1}) that decreased. There were non-significant differences for both treatments for the osmotic pressure at full turgor (π_o; MPa) and water potential at turgor loss point (Ψ_{tlp}), along the whole experiment.

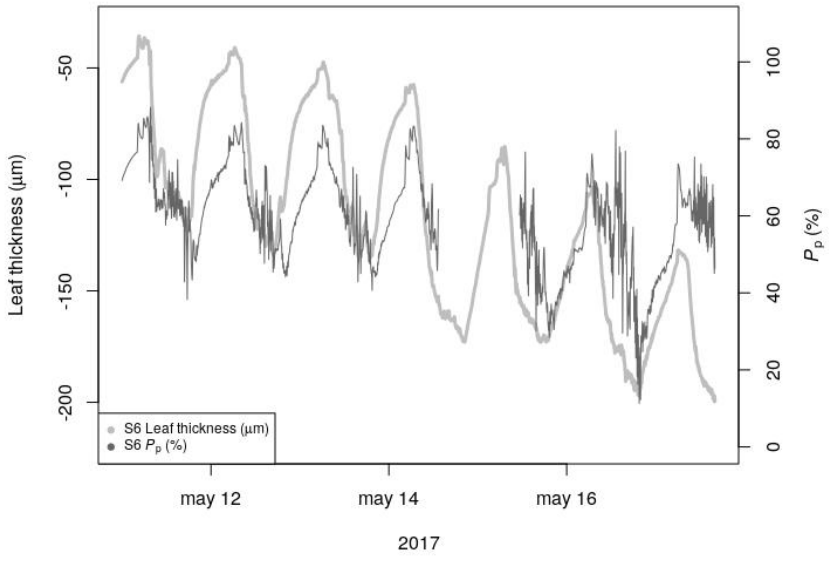

Fig. 8 Time courses of the daily P_p (kPa) values and daily leaf thickness (µm) that occurred under severe drought in the drought stress period. P_p shows the typical inversion of the daily curve that normally occurs under severe drought stress whereas the leaf thickness shows the typical shrinkage pattern. It is shown only one sensor (S6) due to a problem in the computer of the greenhouse.

The dynamics of the P_p and leaf thickness values recorded on some days in the drought stress period are shown in Fig. 8. Data for the S6 tree only are shown, because we had a problem with the computer and some values recorded on the stress period were lost. The figure shows that the daily variations of the P_p values were similar to those of leaf thickness.

4. DISCUSSION

This is the first time that threshold levels of turgor, as a driver of leaf thickness in olive, were derived from the combined used of ZIM probes and LS sensors, together with the analysis of changes in cell wall properties derived from pressure-volume curves. We also determined the threshold levels of water-environmental drivers of turgor and their influence on growth processes in combination with additional measurements of plant water status, both under well-watered and drought conditions.

4.1. Environmental drivers of leaf growth and turgor

Our results showed that, under well-watered conditions, the behaviour of both turgor and leaf thickness along the day was mainly influenced by VPD (Fig. 3b and d). However, when water in the soil decreased below field capacity, the main driving variable was soil water availability (Fig. 3a and c). Thus, below field capacity soil water availability started to play a major role on plant performance, being the plant response ensuring its survival by maintaining hydraulic conductivity mainly by closing stomata among other processes. These results agree with recent findings by Rodriguez-Dominguez et al. (2016), who found that the observed decline in stomatal conductance was 87% driven by turgor signals. It is well known that one of the first responses to water scarcity is stomata closing, which limits transpiration and water loss, being also a major limitation to photosynthesis (Flexas and Medrano, 2002; Flexas et al. 2004). However, olive has the ability to conduct photosynthesis under low values of water potential (Ψ) (paper Alfonso, paper Moriana, fotosíntesis con estrés; Padilla-Díaz et al., 2018). Also, the 50% of loss conductivity (P50) in olive is organ dependent (Rodriguez-Dominguez et al. 2018), presenting the roots the largest resistance for taking up water from drying soils. Also, stem P50 values is ca. Ψ_{stem} = –6 MPa for olive (Torres-Ruiz et al. 2017; Rodriguez-Dominguez et al. 2018; Padilla-Díaz et al., *in preparation*), which is in agreement with its marked resistance to drought. This low P50 value is one of the features for maximizing photosynthesis under drought stress.

Leaf growth, however, did not occurred below field capacity (Fig. 3c, Fig. 7). Although photosynthesis could occur under drying soils conditions, either the rate of CO_2 net assimilation was not enough to promote growth or the assimilates are used for other processes, such as fruit growth or oil accumulation, but not for leaf growth. Other authors

have also observed that growth is affected earlier and more markedly than photosynthesis (Fatichi et al. 2013; Boyer, 1970; Hsiao, 1973; Muller et al., 2011; Tardieu et al., 2011).

Our results, on Ψ_{stem} = – 1.7 MPa being a threshold for water stress, supports previous findings by Fernández et al. (2011) and Ehrenberguer et al. (2012), on Ψ_{stem} = – 1.7 MPa value being a limit for the change from state 2 to state 3 (Fernández et al. 2011, Fernández 2014b). Notwithstanding, Marino et al. (2016), for other olive varieties, found lower threshold values for Ψ_{stem} and its relationship with the indicators derived from the shape of the daily P_p curves. They attributed these differences to some variability between cultivars and meteorological conditions of the orchards. Thus, they suggested minimum values of P_p, which normally occur at predawn, as an alternative indicator for irrigation scheduling.

Our findings show that the relationship between leaf growth in thickness and maximum turgor processes (minimum values of P_p) took place at predawn (Fig.2, 7). For growing processes, P_p values necessary have to be in the interval below 20% of maximum daily values, and Ψ_{pd} values must be over –1 MPa. Therefore, the threshold of Ψ_{pd} = –1 MPa and the limit of 20% of turgor loss at predawn could be used as indicators for irrigation scheduling purposes when maximum plant performance is pursued. Below the field capacity threshold, where no leaf thickness growth processes will take place (Fig. 3c), there is still a safety margin for irrigation scheduling of olive orchards (Fig.4a, b), because olive can keep significant plant performance under harsh conditions of water stress (Fernández et al. 2014b). We further address leaf thickness growth, turgor and plant-water relations in Section 4.3.

4.2. Internal plant water relations as drivers of turgor

The classical Höfler diagram shows the extent at which changes in cell volume (measured as relative water content, RWC) are related with the water potential (Ψ), turgor pressure (P_c) and osmotic pressure (π) components in cellular water relations. diagram is showed how water potential (Ψ) and turgor pressure (P) decrease as osmotic pressure (π) increases when the relative water content (RWC) drops till incipient plasmolysis. Then, in this point, the turgor is lost and equal to zero ($\Psi_{tlp} = \pi$), moment in which the decreases in Ψ are equal to π as RWC decreases due to the symplastic water in the cell. In this study, the daily variations in leaf turgor considered as P_p values from the ZIM probes readings in different moments along the day and degree of plant-water status (measured as Ψ) were not apparently related (Fig. 5d, e, f). Although the water relations including P in cells are well known by Höfler diagrams, measurements of leaf turgor taken with ZIM probes seems that there were a not obvious relationship between Ψ and P_p (Fig. 5d, e, f), especially when the inversion of the curve appears (State 3). To understand this behaviour, we could attribute by some possible explanations not mutually exclusive, which are explained in the subsequent paragraphs.

On one hand, the accumulation of the air in the leaf tissues during dehydration (Ehrenberger et al., 2012), avoid any possible relation between stem Ψ values lower than –1.7 MPa and P_p readings. When this phenomenon of air accumulation occurs, the inversion of the daily P_p curve (State 3) appears. And even at lower stress values, i.e. during state 2, there are moments during the day at which there is no correlation between P_p and the actual water status of the plant. Taken into account other leaf Ψ such as at predawn and midday stablished as threshold values (Fig. 5d, e, f), the inversion of the curve also could occur, but only in the stress treatment. Our results from the P-V curves (Table 1) showed that Ψ_{tlp} fell into the same range for both treatments as we found as threshold value for midday leaf Ψ (Fig. 5f; Ψ_{leaf} = – 2.7 MPa) in the same moment as the Ψ_{stem} (Fig. 5e; = – 1.7 MPa). These results suggest that, for our olive trees cv. Arbequina, the response of the inversion of the curve could be related with a loss of leaf turgor.

However, in control trees never appeared an inversion of the P_p curve although the Ψ_{leaf} taken as threshold at midday (Fig. 5) was similar as Ψ_{tlp} from the results of the P-V curves (ca. Ψ_{tlp} = –2.5 MPa). If we take into account the Höfler diagram, during increasing water stress there were changes in the leaf water relations (Table 1, Fig. 6), to maintain the leaf water and the Ψ before the Ψ_{tlp}. Our results showed that there was osmotic adjustment in both control and stressed plants (Fig. 6), as well as a significant increment of the elastic modulus (ε) only in the stress treatment (Table 1). Thus, the response to water scarcity in the soil by the leaves in the stress treatment was to rise ε, which is related with a stiffness of the leaves. The results of Barlett et al. (2012) showed that the leaves stiffness through sclerophylly and elastic adjustments gives to the leaves the ability of retaining more water, to better tolerate severe drought stress conditions. This tolerance was explained by the combination of changes in ε and the increment in the leaf relative water content at turgor loss point (RWC_{tlp}), equal as we found for olive trees under drought stress (Table 1). Although we obtained an increment $RWC_{tlp,}$ we also found a decrease in the capacitance at full turgor (C_{FT}), which means that the capacity to release water to other tissues would be reduced. This could be an effective mechanism to avoid the loss of turgor to maintain the stomatal open and to maximize photosynthesis under extreme drought conditions (Moriana et al. X; Perez-Martin et al X).

Moreover, if we bear in mind that leaves are composed by multiple and different cells coordinated, our results about the inversion of the curve could not be attributed only to loss of turgor nor changes in ε. The different types of tissues that conform the leaves as well as other structures (e.g. trichomes) are also implicated in maintaining the leaf water status before the turgor loss point (Nguyen et al.; 2017). Such that different cell structures, changes in stiffness of the cell walls, an osmotic adjustment, and perhaps the accumulation of air in the mesophyll cells, are responses that olive leaves have to avoid water losses. Their interactions could be implicated in the response of the inversion of the P_p curve.

Moreover, other biological processes occurring in the leaves, that are poorly understood, could have an influence on the P_p response. For example, the influence of the

phloem on turgor processes in the leaves seems to be important, since xylem and phloem share their water potentials (Diaz-Espejo and Hernandez-Santana, 2017). Also, there are possible influences of the fruits, since water and photoassimilates are exported from the leaves to the sinks (fruits) (Padilla-Díaz et al, *unpublished*). All of these complex interactions, together with those explained in the previous paragraphs, illustrates the difficulty of explaining the inversion of the P_p curve, phenomenon that occurs only under drought stress.

Going a step forward in this work, during the inversion of the P_p curve the daily dynamic of the curve was practically similar to the daily behaviour of the relative leaf thickness (Fig. 8). However, due to a problem with the computer in the greenhouse, unfortunately we had lost a great fraction of that behaviour for most of inversions of P_p curves. Still, the data set that we could conserve (Fig. 8) shows similar daily dynamics of leaf turgor and leaf thickness, although for P_p values there was more variability during the day than for leaf thickness. At night, however, both sets of readings were similar. This could be explained by changes in plant transpiration occurring during the day, that were registered by the ZIM probes but did not affect the LS sensor readings. This behaviour is also observed in Fig. 7, where leaf thickness and P_p values were related at night but not during the day, when leaf turgor pressure was low and the leaves were shrinking. Nevertheless, Fig. 7 shows a high tree-to-tree variability. Scoffoni et al. (2013) pointed out that, along leaf dehydration, the accumulation of intracellular air space was a consequence of the leaf shrinkage. This was in detriment to mesophyll hydraulic conductance in order to prevent xylem cavitation during daily transpiration. They reported a partial reversibility of the leaf shrinkage. In our case, our results on leaf thickness and the inversion of the P_p curves from living leaves showed a complete recovery (Fig. 1 and 2). Hence, we should conduct a more in-depth drought-stress study, in combination with leaf anatomy and hydraulic conductivity, to unravel the mechanistic processes that are underling the inversion of the P_p curve and its relationship with the leaf thickness.

4.3. Meaning of turgor in the plant water relations as drivers of growth

Organ growth depends on cell division and cell enlargement (Cosgrove et al., 2005). Cell differentiation could also be considered as a process associated with growth, and it is subjected to complex genetic regulations. Plant growth is widely studied in pollen, being this cell type used as an organism model given its easy manipulation for experimentation and for mathematical modelling (Kroeger et al, 2017; + more references). When growth is considered at the organ level (e.g. leaf thickness growth), it has to be taken into account that the cells from the tissues in an organ are tightly regulated. That means that different kinds of tissues have differentiated cell structures, each contributing differently to leaf water relations (Nguyen et al.; 2017) and growth. Most studies on leaf thickness refer to shrinkage under drought stress, the importance novel aspect of our experimental study is that we also the leaf thickness growth.

In this work, we presented an approach to Höfler diagram being the first time that it was applied to ZIM probes to measure turgor. All the parameters of this approach were measured at predawn, with the exception of π that was taken at midday, when the values were maximum (π_{max}). The parameters at predawn, when leaf thickness reached its maximum, were indicative of growth (Fig. 7). This agrees with main growth processes taking place at night, when the starch is hydrolysed to glucose serving as fuel for growth (Furze et al.; 2018). We are aware that this Höfler approach is not suitable to represent the plant water status under drought, because, as was explained in the previous section, the P_p values are not reliable under drought stress. Nevertheless, this Höfler approach is still perfectly adequate to understand the mechanisms underlying growth processes and water relations.

Our results demonstrate that 20% of P_p value (i.e. less than 80% in turgor) was a turgor threshold from which leaf thickness did not increase (Fig. 7), mainly due to low soil water availability (Fig. 3c). This result is in agreement with findings reported by Lockhart (1965), who reported a threshold limit of turgor for P_c = 0.9 MPa as a minimum turgor value for growth processes, which account for water limitation to growth. Moreover, according to Cosgrove (1987, 2005, 2017), turgor is fundamental for growth processes and requires a well-hydrated leaf. In the case of olive, less than 80% in turgor would be conditioned to $\Psi = -1$ MPa and RWC_{leaf} = 94% as thresholds at predawn (Fig. 6). In this well-hydrated state, the high RWC in the cells and the high turgor pressure exerted over the cell walls trigger mechanisms that weaken the cell wall by the movement of microfibres (Cosgrove, 2005, 2017). This weaken by a loose of the cell wall promotes a drop in turgor pressure through the pressure that the wall exerts over the cell. As a result, there is an increase of π allowing water flows into the cell for restoring turgor, which promotes a cell wall enlargement and the subsequent growth (Schopfer, 2006). Although the cell wall expansion and the synthesis of the new cell wall are independent processes, both are well coupled.

Our results support the hypothesis of growth proposed by Cosgrove (2005, 2017) and Schopfer (2006), because within the interval of 94% < RWC_{leaf} < 100% the P_p values were variable towards full turgor (i.e. P_p from 20 to 0%) as well as π_{max} (Fig. 6).Growth is determined by inelastic changes in the cell wall (Cosgrove, 2005, 2016, 2017), which are a result of the irreversible changes in cell volume and surface area (Schopfer, 2006). These irreversible changes showed by two trees in the control treatment (i.e. C2 and C3, Fig.3c and Fig. 7) of this experiment could be defined as inelastic or plastic growth. By contrast, the recovery of the shrinkage from the drought stress to the initial thickness value (Fig. 1b, Fig. 3c, and Fig. 7) could be understood as elastic or reversible growth due to changes in leaf water relations only. Therefore, could we confirm that the leaf thickness growth was not due to an increase of the stiffness of the cell walls of the leaves? The parameters derived from the P-V curves (Table 1) showed that there were non-significant differences for ε since the beginning till the end of the experimental period for the control treatment. This demonstrates that there was neither an increment of the leaves stiffness nor the leaves

became thicker were de determinant of the values recorded by LS sensors in control treatment, attributing finally those chances to leaf thickness growth.

4.4. Future perspectives

The thresholds stablished in this study open new perspectives to stablish the limits or thresholds in the biological processes related with turgor and its interactions with the environment. These limits can be used not only for stablishing new indicators for irrigation scheduling. Combined with models (Steppe et al., 2006; De Swaef and Steppe; 2010), offer new opportunities for both precision irrigation and the fundamental understanding of processes governing fluxes of water and carbon in plants. The new mechanistic approaches for modelling parameters are difficult or impossible to measure (Steppe et al. X), will be accurately determined by the use of those thresholds and would be implemented even also in ecological models for dynamic global vegetation (DGVMs; Cox et al., 2000; Sitch et al., 2008; Leuzinger et al. 2013). However, before its implementation for irrigation scheduling, field experiments using the methodology presented in this work together with experiments of fruit influences as carbon sinks, will certainly be the new lines of precision irrigation research in the context of climate change.

5. CONCLUSIONS

The present study demonstrates the hydraulic processes that evolve leaf turgor, thickness and plant water status along the continuum soil-plant-atmosphere are dependent of the field capacity as a threshold of soil water availability. Under drought stress the inversion of the P_p curve could not been only attributed to a loss of turgor responses but also to other processes such as an osmotic adjustment, an increase in the stiffness of the cell walls as well as other interactions that also could promote the accumulation of air in the mesophyll cells to avoid water losses. These interactions processes are poorly understood in the leaves. However, during the inversion of the P_p curve the daily dynamic of the curve was similar to the daily behaviour of the relative leaf thickness. This suggests that ZIM probe measure a variable related with leaf thickness during the inversion of the P_p curve, opening a new door for irrigation scheduling at lower values of water potential. In addition, under non-limiting soil water conditions, there was an irreversible growth in leaf thickness mediated by turgor that occurred only exceeded by threshold values of P_p > 20%, Ψ = –1 MPa and RWC_{leaf} = 94%. These limits offer new opportunities for both precision irrigation and modelling about the fundamental understanding growth processes.

6. SUPPLEMENTARY MATERIAL

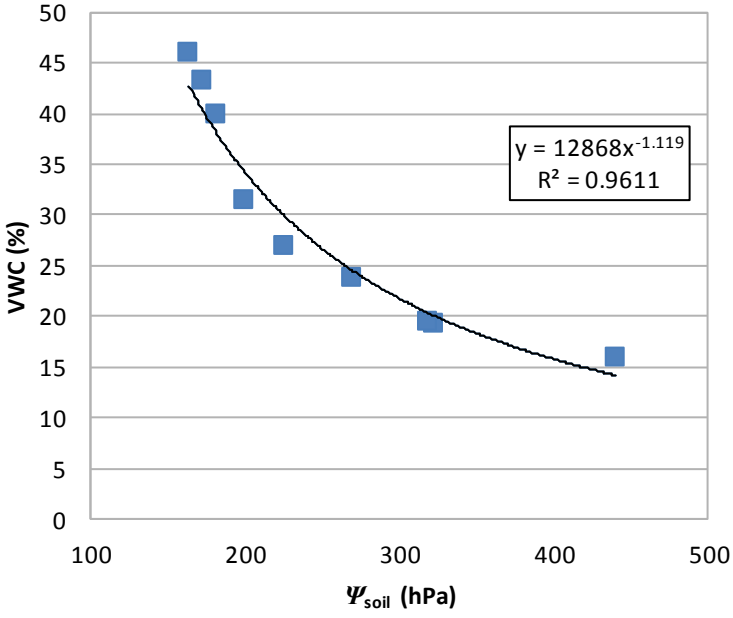

Fig. S1. Adjustment of a pF curve using a power function.

Table S1. Determination of the soil water availability from the fitted pF curve (Fig. S1).

	pF (hPa)	VWC (%)
Saturation	100	74.45
Field capacity	250	26.71
Dry	290	22.62
Wilting point	420	14.95

Chapter 6

General discussion

The main purpose of this PhD was to validate of the use of the indicators for irrigation scheduling derived from the turgor related measurements in a commercial olive orchard as well as to get deeper in the fundamental understanding of the interaction between the environmental and plant mechanisms that drive these turgor measurements.

In the Chapters 2 and 3, the user-friendly of water stress indicator for irrigation scheduling was firstly tested and validated in a regulated deficit irrigation strategy compared with a traditionally scheduled using the crop coefficient approach. The use of these indicators derived just on the visual analysis from the shape of the leaf turgor related measurements from the ZIM probe readings were concluded as the most promising plant-based method for automatic and continuous monitoring of water stress and its use for irrigation scheduling, in periods when the olive tree is most sensitive to water stress, in commercial olive orchards. The impact on crop performance was similar along two years under the same irrigation scheduling approach. Not only was similar in between years, but also was between the crop coefficient approach and to the 100% treatment in which were replaced a 100% of the irrigation needs. The plant water status under the use of the methodology proposed here along the whole experimental years was similar to the crop coefficient approach and similar to the control treatment in periods of high crop sensitivity to water stress. This pointed out the capacity of this methodology to supply the crop water needs in this moments of high sensitivity. Moreover, the vegetative growth was reduced, facilitating the mechanical harvesting as well as a better light interception by the canopy, ensuring a longer productive life of the orchard. In these two chapters is remarkable the 55% of water savings that we obtained following the methodology proposed in this PhD compared with the replacement of the 100% of the irrigation needs. Additionally, this method could be combined with remote sensing which allow a differential irrigation doses and frequencies depending on the water requirements identified in the orchard, contributing to the potential rational use of water for precision irrigation in super high density olive orchards.

However, our irrigation scheduling approach has several limitations. On one hand, the 120% of the increment of the irrigation amounts at the beginning of the periods, during 1 to 3 days, in which the olive tree is most sensitive to water stress have never been contrasted with the crop physiology nor crop performance. Moreover, although could be reasonable the changes in the 15% of the irrigation amounts and its relation with the coefficient of variation of our orchard, this 15% might be tested in another different orchard conditions, even if our results showed that those irrigation amounts seems to be adequate for keeping non-limiting soil water conditions. Secondly, Marino et al. (2016) found for Sicilian olives different intervals of plant water status and its correspondence with the shape of the visual daily curves identified by Fernández et al. (2011). These authors attributed those intervals fundamentally to the different genotypes and the different environmental characteristics of the orchards and they proposed a new indicator for irrigation scheduling in commercial olive orchards based on the minimum values of turgor related measurements. This new indicator was explored in the Chapter 4 and 5. And thirdly, ZIM probe does not work properly beyond a certain level of water stress which, in

our case, was reported to be that occurring at ca. $\Psi_{stem} < -1.7$ MPa and the shape of the daily curve suffer an inversion. This behaviour limits the use of the ZIM probes for irrigation scheduling in periods in which the crop can reach high levels of water stress. Nevertheless, the physiological mechanisms that underlie such behaviour with turgor readings were explored in the Chapter 5.

The study of other indicators derived from the ZIM probes readings such as the maximum daily turgor would be fundamental to a better comprehension about the responses under the variations of the environmental changes on the plant water status. In the Chapter 4, the environmental variables were explored as well as the proximity of fruits and changes in the elastic modulus on the maximum turgor readings. In this PhD was concluded that, under non-water limiting soil conditions, there were a daily pattern on the maximum turgor resulting from the influence of the atmospheric conditions (mainly driven by the vapour pressure deficit) and, on second place, by the water availability in the soil. The daily behaviour of maximum turgor measurements was complemented with a seasonal pattern that was explained as a result of compensating the carbon allocation from the leaves to the fruits under an equilibrium between water potential in the soil and leaf water potential. This result suggest that, after understanding the mechanisms below, this water stress indicator can become more useful to schedule irrigation on those periods when the plant water status may have a marked effect on fruit production. Also, the increase on the elastic modulus with leaf aging did not have an influence on the maximum turgor as well as the location of the leaf being close or far to the fruits. From these results, we concluded that the ZIM probes could be clamped in any leaf, regardless of being close or far from a cluster of fruits.

As was mentioned above, ZIM probe does not work properly when certain level of water stress is reached, being $\Psi_{stem} < -1.7$ MPa in our case, where the shape of the daily curve suffer an inversion. To unravel the mechanisms that underline that behaviour, as well as the maximum turgor under drought stress and its environmental drivers, in the Chapter 5 was described an experiment under greenhouse conditions with a control treatment, in which the plant water needs was replaced, and a stress treatment with a period in which the irrigation was withhold and a later recovery. Also, the turgor related measurements were complemented with the exploration of the continuous leaf thickness measurements. In this PhD was found that, under non-limiting soil water conditions, there was an irreversible growth in leaf thickness mediated by turgor that occurred only exceeded by threshold values of the maximum turgor at $P_p > 20\%$, $\Psi = -1$ MPa and $RWC_{leaf} = 94\%$. To unravel if those mechanisms attributed to growth were determined by the stiffness of the cell walls of the leaves, pressure-volume curves were performed and showed that only in the stress treatment the leaves changed its elasticity in order to tolerate lower values of water stress. These thresholds mentioned offer new opportunities for both precision irrigation and modelling about the fundamental understanding growth processes.

In the Chapter 5 also was found that the soil water availability was the main driver of the hydraulic processes that evolve leaf turgor, thickness and plant water status along the continuum soil-plant-atmosphere, as was stablished in the Chapter 4. However the novelty here was that water at field capacity as a threshold of soil water availability was the main turning point as determinant of such processes in the leaves. Under drought stress, exceeded this threshold, the inversion of the daily curve appeared and as a result of the combination of turgor loss responses with other processes such as an osmotic adjustment, an increase in the stiffness of the cell walls and other interactions that could promote the accumulation of air in the mesophyll cells to avoid water losses. Nevertheless, during the inversion of the curve the daily dynamic of the curve was similar to the daily behaviour of the relative leaf thickness which suggests that ZIM probe measure a variable related with leaf thickness during the inversion of the P_p curve. This advance opens a new door for irrigation scheduling at lower values of water potentials and, in the case of regulated deficit irrigation, in periods when the olive tree can tolerate severe conditions of water stress.

Chapter 7

Conclusions

- The irrigation scheduling approach proposed in this doctoral thesis, based on the visual analysis from the P_p curves of the ZIM system and the three days weather forecast, allowed for an effective application of regulated deficit irrigation in a hedgerow olive orchard with high plant density.
- Our irrigation scheduling approach can be used by farmers without specific training, since it is based on the State shown by the outputs from the ZIM sensors.
- Two years under our irrigation scheduling approach showed a crop performance as good as the crop coefficient approach, where also no differences were found for both approaches on growth, plant water status and gas exchange.
- Using our irrigation scheduling approach ca. 50% of water savings could be reached and an increment of the water productivity respect to a full irrigated treatment.
- The 120% of the irrigation needs and changing by 15% the irrigation amounts applied for the rest of each period seem to be adequate for keeping non-limiting soil water conditions on those periods when we used our irrigation scheduling approach.
- Under non-limiting soil water conditions, relative maximum daily turgor (P_{pmin}) was mainly driven by the previous daily values of *atmospheric demand*, followed by *water availability*.
- There were no influence of the proximity of fruits on P_{pmin} records, suggesting that P_{pmin} readings can be made in any leaf regardless of being close or far from a cluster of fruits.
- The increase on the elastic modulus with leaf ageing did not have an influence on P_{pmin}.
- The pattern of P_{pmin} changed depending on the fruit developmental stage. Two stages were found to have a clearer influence: maximum rate of pit hardening and rapid fruit growth after the midsummer period.
- P_{pmin} could be a sensitive and reliable water stress indicator on those periods when the plant water status may have a marked effect on fruit production.
- Leaf turgor, thickness and plant water status along the continuum soil-plant-atmosphere were dependent on field capacity, as a threshold of soil water availability and, to a lesser extent, on the vapour pressure deficit of the air.
- Under severe drought stress, the properties of the cell walls changes and the similar dynamics of the inversion of the daily P_p curve as the leaf thickness measurements suggests that the ZIM probe measures a variable related to

leaf thickness during the inversion of the daily P_p curve. This finding opens new possibilities for improving irrigation scheduling in periods when the olive tree is less sensitive to drought stress.

CONCLUSIONES

- La estrategia de programación del riego propuesta en esta tesis doctoral, basada en el análisis visual de las curvas P_p de los sistemas ZIM y con las predicciones meteorológicas a tres días vista, permitió una aplicación efectiva del riego deficitario controlado en el olivar en seto de alta densidad.
- La estrategia de programación del riego puede ser usada por agricultores sin que sea necesario ningún tipo de entrenamiento específico previo, únicamente basándose en el cambio de estado mostrado por las lecturas de las sondas ZIM.
- Dos años bajo la programación del riego con la estrategia propuesta en esta tesis doctoral mostraron un buen funcionamiento de la planta tan bueno como el del coeficiente del cultivo, donde tampoco se encontraron diferencias para ambas estrategias en el crecimiento, estado hídrico de la planta ni en el intercambio de gases.
- Con la estrategia de programación del riego se consiguieron ahorros de agua más de un 50% y un incremento de la productividad del agua respecto al tratamiento bien regado.
- La aplicación de un 120% de las necesidades de riego y los cambios en el 15% en las cantidades aplicadas para el resto de cada periodo parece ser adecuado para mantener al suelo en unas condiciones no limitantes de agua. Estas condiciones son usadas para el riego en la estrategia de programación de esta tesis doctoral.
- Bajo condiciones no limitantes de agua en suelo, la turgencia máxima relativa ($P_{pmin)}$ fue principalmente determinada por la demanda atmosférica seguida por la disponibilidad hídrica del suelo.
- No hubo diferencias en la proximidad de los frutos en los registros P_{pmin} , lo que sugiere que estas lecturas pueden ser usadas en cualquier hoja independientemente de si se encuentra cerca o lejos de del fruto.
- El incremento del módulo de elasticidad debido al envejecimiento de la hoja no afecto al P_{pmin}.
- El patron de P_{pmin} cambió dependiendo del estadío de desarrollo del fruto. Se encontraron dos fases que tuvieron una clara influencia: la tasa máxima de endurecimiento del hueso y el de rápido crecimiento del fruto que se produce a fínales de la segunda mitad del verano.
- Nuestros datos apoyan al P_{pmin} como un indicador sensible y fiable del estrés hídrico en aquellos periodos en los que el estado hídrico de la planta puede tener una marcada influencia en la producción del fruto.

- Los procesos hidráulicos que envuelven la combinación de la turgencia de la hoja, el grosor de la misma y el estado hídrico de la planta a lo largo del continuo suelo-planta-atmósfera dependieron de la capacidad de campo, siendo esta última un umbral de la disponibilidad hídrica del suelo y, en menor medida, el déficit de presión de vapor del aire.
- Bajo estrés hídrico severo, las propiedades de las paredes celulares de la hoja cambiaron y tuvo lugar la inversión de la curva P_p diaria como las medidas registradas por el grosor de la hoja, sugiriendo que la sonda ZIM durante la inversión de la curva de P_p mide una variable relacionada con el grosor de la hoja. Estos resultados, por tanto, abren nuevas posibilidades para la mejora en la programación del riego en los periodos en los que el olivo es menos sensible al estrés hídrico.

REFERENCES

Ache, P., Baueer, H., Kollist, H., Al-Rasheid, K.A.S., Lautner, S., Hartung, W., Hedrich, R., 2010. Stomatal action directly feeds back on leaf turgor: new insights into the regulation of the plant water status from non-invasive pressure probe measurements. Plant J. 62, 1072–1082.

Ache, P., Bauer, H., Kollist, H., Al-Rasheid, K. A.S., Lautner, S., Hartung, W. and Hedrich, R., 2010. Stomatal action directly feeds back on leaf turgor: new insights into the regulation of the plant water status from non-invasive pressure probe measurements. Plant J., 62: 1072–1082.

Aissaoui, F., Chehab, H., Bader, B., Salem, A. Ben, M'barki, N., Laamari, S., Chihaoui, B., Mahjoub, Z., Boujnah, D. 2016. Early water stress detection on olive trees (*Olea europaea* L. cvs 'chemlali' and 'Chetoui') using the leaf patch clamp pressure probe. COMPUT ELECTRON AGR 131: 20–28.

Allen, R.G., Pereira, L.S., Raes, D., Smith, M., 1998. Crop evapotranspiration. Guidelines for computing crop water requirements. Irrigation and drainage paper 56. FAO, Rome, Italy

Bacelar, E.A., Correia, C.M., Moutinho-Pereira, J.M., Gonçalves, B.C., Lopes, J.I., Torres-Pereira, J.M.G., 2004. Sclerophylly and leaf anatomical traits of five field-grown olive cultivars growing under drought conditions. Tree Physiol. 24, 233–239.

Bacelar, E.A., Correia, C.M., Moutinho-Pereira, J.M., Gonçalves, B.C., Lopes, J.I., Torres-Pereira, J.M.G., 2004. Sclerophylly and leaf anatomical traits of five field-grown olive cultivars growing under drought conditions. Tree Physiol. 24, 233–239.

Baldoni L, Tosti N, Ricciolini C, Belaj A, Arcioni S, et al. 2006 Genetic structure of wild and cultivated olives in the central Mediterranean basin. Ann Bot 98: 935–942.

Bellvert, J., Marsal, J., Girona, J., Gonzalez-Dugo, V., Fereres, E., Ustin, S.L., and Zarco-Tejada, P.J., 2016. Airborne thermal imagery to detect the seasonal evolution of crop water status in peach, nectarine and Saturn peach orchards. Remote Sens. 8, 39. http://dx.doi.org/10.3390/rs8010039.

Ben-Gal, A., Kool, D., Agam, N., van Halsema, G.E., Yermiyahu, U., Yafe, A., Presnov, E., Erel, R., Majdop, A., Zipori, I., Segal, E., Rüger, S., Zimmermann, U., Cohen, Y., Alchanatis, V., Dag, A., 2010. Whole-tree water balance and indicators for short-term drought stress in non-bearing 'Barnea' olives. Agric- Water Manage. 98, 124–133.

Ben-Gal, A., Kool, D., Agam, N., van Halsema, G.E., Yermiyahu, U., Yafe, A., Presnov, E., Erel, R., Majdop, A., Zipori, I., Segal, E., Rüger, S., Zimmermann, U., Cohen, Y., Alchanatis, V., Dag, A.,2010. Whole-tree water balance and indicators for short-term drought stress in non-bearing 'Barnea' olives. Agric. Water Manage. 98, 124–133.

Ben-Gal, A., Kool, D., Agam, N., van Halsema, G.E., Yermiyahu, U., Yafe, A., Presnov, E., Erel, R., Majdop, A., Zipori, I., Segal, E., Rüger, S., Zimmermann, U., Cohen, Y.,

Alchanatis, V., Dag, A., 2010. Whole-tree water balance and indicators for short-term drought stress in non-bearing ‘Barnea’ olives. Agric. Water Manage. 98, 124–133.

Blackman, C.J., Brodribb, T.J. 2011 Two measures of leaf capacitance: insights into the water transport pathway and hydraulic conductance in leaves. Funct Plant Biol 38, 118–126.

Blackman, C.J., Brodribb, T.J. 2011 Two measures of leaf capacitance: insights into the water transport pathway and hydraulic conductance in leaves. Funct Plant Biol 38, 118–126.

Bongi, G., Palliotti, A., 1994. Olive. *In*: Schaffer, B., Andersen, P.C. (Eds.), Handbook of Environmental Physiology of Fruit Crops. Volume I: Temperate Crops. CRC Press, Inc., Boca Raton, Florida, USA, pp. 165–187.

Bongi, G., Palliotti, A., 1994. Olive. In: Schaffer, B., Andersen, P.C. (Eds.), Handbook of Environmental Physiology of Fruit Crops, Volume I. Temperate Crops. CRC Press, Inc., Boca Raton, Florida, USA, pp. 165–187.

Bramley, H., Ehrenberger, W., Zimmermann, U., Palta, J.A., Rüger, S., Siddique, K.H.M., 2013. Non-invasive pressure probes magnetically clamped to leaves to monitor the water status of wheat. Plant Soil 369:257–268

Bramley, H., Ehrenberger, W., Zimmermann, U., Palta, J.A., Rüger, S., Siddique, K.H.S., 2013. Non-invasive pressure probes magnetically clamped to leaves to monitor the water status of wheat. Plant Soil 369, 257–268.

Breton C, Tersac M, Bervillé A. 2006. Genetic diversity and gene flow between the wild olive (oleaster, *Olea europaea* L.) and the olive: several Plio-Pleistocene refuge zones in the Mediterranean basin suggested by simple sequence repeats analysis. J Biogeogr 33: 1916–1928.

Brodribb TJ, McAdam SAM. 2017. Evolution of the Stomatal Regulation of Plant Water Content. *Plant Physiology* 174: 639–649.

Bustan, A., Avni, A., Lavee, S., Zipori, I., Yeselson, Y., Schaffer, A.A., Riov, J., Dag, A., 2011. Role of carbohydrate reserves in yield production of intensively cultivated oil olive (*Olea europaea* L.) trees. Tree Physiol. 31(5), 519–530.

Cajias, E., Antunez, A., Román, L.F., 2016. Response to moderate water stress imposed after pit hardening in mature table olive orchard cv. Azapa. Agric. Water Manage. 173, 76–83.

Centritto, M., 2002. Interactive effects of elevated [CO2] and drought on peach seedlings. Plant Biosystems 5, 177–188.

Centritto, M., 2002. Interactive effects of elevated [CO2] and drought on peach seedlings. Plant Biosyst. 5, 177–188.

Chalmers, D.J., Mitchell, P.D., van Heek, L., 1981. Control of peach tree growth and productivity by regulated water supply, tree density and summer pruning. Journal of the J. Am. Soc. Hortic. Sci. 106, 307e312.

Chartzoulakis, K., Patakas, A., Bosabalidis, A.M., 1999. Changes in water relations, photosynthesis and leaf anatomy induced by intermittent drought in two olive cultivars. Environ. Exp. Bot. 42, 113–120.

Chartzoulakis, K., Patakas, A., Bosabalidis, A.M., 1999. Changes in water relations, photosynthesis and leaf anatomy induced by intermittent drought in two olive cultivars. Environ. Exp. Bot. 42, 113–120.

Chaves, M.M., Maroco, J.P., Pereira, J.S., 2003. Understanding plant responses to drought–from genes to the whole plant. Func Plant Biol. 30, 239–264.

Chaves, M.M., Zarrouk, O., Francisco, R., Costa, J. M., Santos, T., Regalado, A. P., Rodrigues, M.L., Lopes, C.M., 2010. Grapevine under deficit irrigation: hints from physiological and molecular data. Ann Bot. 105(5), 661–676.

Conejero, W., Alarcón, J.J., García-Orellana, Y., Nicolás, E., Torrecillas, A., 2007. Evaluation of sap flow and trunk diameter sensors for irrigation scheduling in early maturing peach trees. Tree Physiol. 27, 1753–1759.

Connor DJ (2005) Adaptation of olive (Olea europaea L.) to water-limited environments. Crop and pasture. Science 56(11):1181–1189.

Connor, D.J., Centeno, A., Gómez-del-Campo, M., 2009. Yield determination in olive hedgerow orchards. II. Analysis of radiation and fruting profiles. Crop Pasture Sci. 60, 443–452.

Connor, D.J., Fereres, E., 2005. The physisology of adaptation and yield expression in olive. Hort Rev 34, 155–229.

Connor, D.J., Gómez-del-Campo, M., Comas, J., 2012. Yield characteristics of N–S oriented olive hedgerow orchards, cv. Arbequina. Sci Hortic 133, 31–36.

Cuevas, M.V., Martín-Palomo, M.J., Diaz-Espejo, A., Torres-Ruiz, J.M., Rodriguez-Dominguez, C.M., Perez-Martin, A., Pino-Mejías, R, Fernández, J.E., 2013. Assessing water stress in a hedgerow olive orchard from sap flow and trunk diameter measurements. Irrig. Sci. 31, 729–746.

Cuevas, M.V., Martín-Palomo, M.J., Diaz-Espejo, A., Torres-Ruiz, J.M., Rodriguez-Dominguez, C.M., Perez-Martin, A., Pino-Mejías, R., Fernández, J.E., 2013. Assessing water stress in a hedgerow olive orchard from sap flow and trunk diameter measurements. Irrig. Sci. 31, 729–746.

Cuevas, M.V., Torres-Ruiz, J.M., Álvarez, R., Jiménez, M.D., Cuerva, J., Fernández, J.E., 2010. Assessment of trunk diameter variation derived indices as water stress indicators in mature olive trees. Agric. Water Manage. 97, 1293–1302.

Dell'Amico, J., Moriana, A., Corell, M., Girón, I.F., Morales, D., Torrecillas, A., Moreno, F., 2012. Low water stress conditions in table olive trees (*Olea europaea* L.) during pit hardening produced a different response of fruit and leaf water relations. Agric.Water Manage.114, 11–17.

Diaz-Espejo, A., Buckley, T.N., Sperry, J.S., Cuevas, M.V., de Cires, A., Elsayed-Farag, S., Martin-Palomo, M.J., Muriel, J.L., Perez-Martin, A., Rodriguez-Dominguez, C.M., Rubio-Casal, A. E., Torres-Ruiz, J.M., Fernández, J.E., 2012. Steps toward an improvement in process-based models of water use by fruit trees: A case study in olive. Agric. Water Manage. 114, 37–49.

Diaz-Espejo, A., Fernández, J.E., Torres-Ruiz, J.M., Rodriguez-Dominguez, C.M., Perez-Martin, A., Hernandez-Santana, V. 2018. The olive tree under wáter stress: fitting the pieces of response mechanisms in the crop performance puzzle. In: Water scarcity and

sustainable agriculture in semiarid environment. Elsevier Academic Press. pp. 439–479.

Diaz-Espejo, A., Hernandez-Santana, V., 2017. The phloem-xylem consortium: until death do them part. Tree Physiol. 37, 847–850.

Dichio, B., Xiloyannis, C., Angelopoulos, K., Nuzzo, V., Bufo, S.A., Celano, G., 2003. Drought-induced variations of water relations parameters in *Olea europea*. Plant Soil 257, 381–389.

Dichio, B., Xiloyannis, C., Angelopoulos, K., Nuzzo, V., Bufo, S.A., Celano, G., 2003.Drought-induced variations of water relations parameters in *Olea europaea*. Plant Soil 257, 381–389.

Dynamax, 2005. Dynagage Sap Flow Sensor User Manual. Houston, TX.

Egea, G., Fernández, J.E., Alcon, F., 2017. Financial assessment of adopting irrigation technology for plant-based regulated deficit irrigation scheduling in super high-density olive orchards. Agric. Water Manage. 187, 47–56.

Egea, G., Fernández, J.E., Alcon, F., 2017. Financial assessment of adopting irrigation technology for plant-based regulated deficit irrigation scheduling in super high-density olive orchards. Agric. Water Manage. 187, 47–56.

Ehrenberger, W., Rüger, S., Rodríguez-Domínguez, C.M., Díaz-Espejo, A., Fernández, J.E., Moreno, J., Zimmermann, D., Sukhorukov, V.L., Zimmermann, U., 2012. Leaf patch clamp pressure probe measurements on olive leaves in a nearly turgor less State. Plant Biol. 14 (4), 666–674.

FAO, 2009. High Level Expert Forum - How to Feed the World in 2050. Rome 12-13 October, 4 pp.

Fereres, E., Ruz, C., Castro, J., Gómez, J.A., Pastor, M., 1996. Recuperación del olivo después de una sequía extrema. In: Proceeings of the XIV Congreso Nacional de Riegos. Aguadulce, Almería, Spain, 11-13 June, 89–93.

Fereres, E., Soriano, M.A., 2007. Deficit irrigation for reducing agricultural water use. J Exp Bot 58,147–159.

Fernandes, R.D.M., Cuevas, M.V., Hernandez-Santana, V., Rodriguez-Dominguez, C.M., Padilla-Díaz, C.M., Fernández, J.E., 2017. Classification models for automatic identification of daily states from leaf turgor related measurements in olive. Comput Electron Agr. 142: 181–189.

Fernández, J.E., Rodriguez-Dominguez, C.M., Perez-Martin, A., Zimmermann, U., Rüger, S., Martín-Palomo, M.J., Torres-Ruiz, J.M., Cuevas, M.V., Sann, C., Ehrenberger, W., Diaz-Espejo, A., 2011. Online-monitoring of tree water stress in a hedgerow olive orchard using the leaf patch clamp pressure probe. Agric. Water Manage. 100, 25–35.

Fernández, .JE., 2014a. Understanding olive adaptation to abiotic stresses as a tool to increase crop performance. Environ. Exp. Bot. 103: 158-179.

Fernández, J.E., 2014b. Plant-based sensing to monitor water stress: Applicability to commercial orchards. Agric. Water Manage. 142: 99-109.

Fernández, J.E., 2017. Plant-Based Methods for Irrigation Scheduling of Woody Crops. Horticulturae, 3 (2), 35.

Fernández, J.E., Cuevas, M.V., 2010. Irrigation scheduling from stem diameter variations: a review. Agric. For. Meteorol. 150, 135–151.

Fernández, J.E., Diaz-Espejo, A., d'Andria, R., Sebastiani, L. & Tognetti, R., 2008b. Potential and limitations of improving olive orchard design and management through modelling. Plant Biosyst. 142 (1), 130–137.

Fernández, J.E., Diaz-Espejo, A., Romero, R., Hernandez-Santana, V., García, J.M., Padilla-Díaz, C.M., Cuevas, M.V., 2017. Precision irrigation in olive (*Olea europaea* L.) tree orchards. In: I.F. García-Tejero and V-H. Durán (Eds.), Water Scarcity and Sustainable Agriculture in Semiarid Environment: Tools, Strategies, and Challenges for Woody Crops. Elsevier, pp. 179-218.

Fernández, J.E., Green, S.R., Caspari, H.W., Diaz-Espejo, A., Cuevas, M.V., 2008. The use of sap flow measurements for scheduling irrigation in olive, apple and Asian pear trees and in grapevines. Plant Soil 305, 91–104.

Fernández, J.E., Moreno, F., Girón, I.F., Blázquez, O.M., 1997. Stomatal control of water use in olive tree leaves. Plant Soil. 190, 179–192.

Fernández, J.E., Perez-Martin, A., Torres-Ruiz, J.M., Cuevas, M.V., Rodriguez-Dominguez, C.M., Elsayed-Farag, S., Morales-Sillero, A., García, J.M., Hernandez-Santana, V., Diaz-Espejo, A., 2013. A regulated deficit irrigation strategy for hedgerow olive orchards with high plant density. Plant Soil 372:279-295.

Fernández, J.E., Perez-Martin, A., Torres-Ruiz, J.M., Cuevas, M.V., Rodriguez-Dominguez, C.M., Elsayed-Farag, S., Morales-Sillero, A., García, J.M., Hernandez-Santana, V., Diaz-Espejo, A., 2013. A regulated deficit irrigation strategy for hedgerow olive orchards with high plant density. Plant Soil. 372, 279–295.

Fernández, J.E., Perez-Martin, A., Torres-Ruiz, J.M., Cuevas, M.V., Rodriguez-Dominguez, C.M., Elsayed–Farag, S., Morales-Sillero, A., García, J.M., Hernandez-Santana, V., Diaz-Espejo, A., 2013. A regulated deficit irrigation strategy for hedgerow olive orchards with high plant density. Plant Soil 372, 279–295.

Fernández, J.E., Romero, R., Montaño, J.C., Diaz-Espejo, A., Muriel, J.L., Cuevas, M.V., Moreno, F., Girón, I.F., Palomo, M.J., 2008a. Design and testing of an automatic irrigation controller for fruit tree orchards, based on sap flow measurements. Aust. J. Agric. Res. 59, 589–598.

Flexas, J., and Medrano, H., 2002. Drought-inhibition of Photosynthesis in C3 Plants: Stomatal and Non-stomatal Limitations Revisited. Annals of Botany, 89(2), 183–189.

Flexas, J., Bota, J., Loreto, F., Cornic, Sharkey, T.D. 2004. Diffusive and Metabolic Limitations to Photosynthesis under Drought and Salinity in C3 Plants. Plant boil. 6(3), 269–279.

Gago, J., Douthe, C., Coopman, R.E., Gallego, P.P., Ribas-Carbo, M., Flexas, J., Escalona, J., Medrano, H. 2015. UAVs challenge to assess water stress for sustainable agriculture. Agric. Water Manage. 153, 9–19.

García, J.M., Cuevas, M.V., Fernández, J.E. 2013. Production and oil quality in 'Arbequina' olive (*Olea eurpoaea*, L.) trees under two deficit irrigation strategies.

García, J.M., Morales-Sillero, A., Pérez-Rubio, A.G., Diaz-Espejo, A., Montero, A., Fernández, J.E., 2017. Virgin olive oil quality of hedgerow 'Arbequina' olive trees under deficit irrigation. J Sci Food Agric 97 (3), 1018–1026.

Génard, M, Bertin, N., Borel, C., Bussières, P., Gautier, H., Habib, R., Léchaudel, M., Lecomte, A., Lescourret, F., Lobit, P., Quilot, B., 2007. Towards a virtual fruit focusing on quality: modelling features and potential uses. J Exp Bot. 58, 917–928.

Goldhamer, D.A., 1999. Regulated deficit irrigation for California canning olives. Acta Hortic. 474, 369e372.

Goldhamer, D.A., Fereres, E., 2004. Irrigation scheduling of almond trees with trunk diameter sensors. Irrig. Sci. 23, 11–19.

Gómez-del-Campo, M., 2013. Summer deficit–irrigation strategies in a hedgerow olive orchard cv. 'Arbequina': effect on fruit characteristics and yield. Irrig. Sci. 31 (3), 259–269.

Gómez-del-Campo, M., Centeno, A, Connor, D.J., 2009. Yield determination in olive hedgerow orchards. I. Yield and profiles of yield components in north–south and east–west oriented hedgerows. Crop & Pasture Sci. 60, 434–442.

Gomez-Rico, A., Salvador, M.D., Fregapane, G., 2009. Virgin olive oil and olive fruit minor constituents as affected by irrigation management based on SWP and TDF as compared to ETc in medium-density young olive orchards (*Olea europaea* L. cv. Cornicabra and Morisca). Food Res. Int. 42 (8), 1067–1076

Gonzalez-Dugo, V., Goldhamer, D.A., Zarco-Tejada, P.J., Fereres, E. 2015. Improving the precision of irrigation in a pistachio farm using an unmanned airborne thermal system. Irrig. Sci. 33, 43–52.

Gonzalez-Dugo, V., Zarco-Tejada, P., Nicolás, E., Nortes, P.A., Alarcón, J.J., Intrigliolo, D.S., Fereres, E., 2013. Using high resolution UAV thermal imagery to assess the variability in the water status of five fruit tree species withihn a commercial orchard. Precis. Agric. 14, 660–678.

Grattan, S.R., Berenguer, M.J., Connell, J.H., Polito, V.S., Vossen, P.M., 2006. Olive oil production as influenced by different quantities of applied water. Agric. Water Manag. 85, 133–140.

Gucci, R., Goldhamer, D.A., Fereres, E., 2012. Olive. In: Steduto, P., Hsiao, T.C., Fereres, E., Raes, D. (Eds.), Crop Yield Response to Water. Irrigation & Drainage Paper No. 66, FAO, Rome, Italy, pp. 298–313.

Hammami, S.B.M., Costagli, G., Rapoport, H.F., 2013. Cell and tissue dynamics of olive endocarp sclerification vary according to water availability. Physiol Plant 149, 571–582.

Hammami, S.B.M., Manrique, T., Rapoport, H.F., 2011. Cultivar-based fruit size in olive depends on different tissue and cellular processes throughout growth. Sci Hortic. 130, 445–451

Hernandez-Santana, V., Fernández, J. E., Rodriguez-Dominguez, C. M., Romero, R., & Diaz-Espejo, A. 2016. The dynamics of radial sap flux density reflects changes in stomatal conductance in response to soil and air water deficit. Agric For Meteorol, 218, 92-101.

Hernandez-Santana, V., Fernández, J.E., Cuevas, M.V., Perez-Martin, A., Diaz-Espejo, A., 2017. Photosynthetic limitations by water deficit: Effect on fruit and olive oil yield, leaf area and trunk diameter and its potential use to control vegetative growth of super-high density olive orchards. Agric. Water Manage. 184, 9–18.

Hernandez-Santana, V., Rodriguez-Dominguez, C.M., Fernández, J.E., Diaz-Espejo, A., 2016. Role of leaf hydraulic conductance in the regulation of stomatal conductance in almond and olive in response to water stress. Tree Physiol. 36 (6), 725–35.

Hothorn T., Bretz F., Westfall P., 2008. Simultaneous Inference in General Parametric Models. Biom. J. 50(3), 346—363.

Iniesta, F., Testi, L., Orgaz, F., Villalobos, F.J., 2009. The effects of regulated and continuous deficit irrigation on the water use, growth and yield of olive trees. Eur. J. Agro. 30, 258–265.

IPCC Climate Change 2007: The Physical Science Basis. Contribution of Working Group I to the Fourth Assessment Report of the Intergovernmental Panel on Climate Change. Cambridge Univ. Press.

IPCC. 2014. Core Writing Team, Pachauri, R.K., Meyer, L.A., eds. Climate Change 2014: Synthesis Report. Contribution of Working Groups I, II and III to the Fifth Assessment Report of the Intergovernmental Panel on Climate Change, IPCC. Geneva, Switzerland.

Jones HG. 2004. Irrigation scheduling: Advantages and pitfalls of plant-based methods. *Journal of Experimental Botany* 55: 2427–2436.

Jones, H.G., 2004. Irrigation scheduling: advantages and pitfalls of plant-based methods. J. Exp. Bot. 55, 2427-2436.

Jones, H.G., 2007. Monitoring plant and soil water status: established and novel methods revisited and their relevance to studies of drought tolerance. J. Exp. Bot. 58, 119–130.

Kaniewski D, Van Campo E, Boiy T, Terral J-FJF, Khadari B, Besnard G. 2012. Primary domestication and early uses of the emblematic olive tree: Palaeobotanical, historical and molecular evidence from the Middle East. Biol Rev. 87: 885–899.

Lavee, S., 1986. Olive. In: Monselise, S.P. (Ed.), CRC Handbook of Fruit Set and Development. CRC Press, Inc., Boca Raton, Florida, USA, pp. 261–276.

Lavee, S., Nashef, M., Wodner, M., Harshemesh, H., 1990. The effect of complementary irrigation added to old olive trees (*Olea europaea* L.) cv. Souri on fruit characteristics, yield and oil production. Adv. Hortic. Sci. 4, 135–138.

Lavee, S., Wodner, M., 1991. Factors affecting the nature of oil accumulation in fruit of olive (*Olea europaea* L.) cultivars. J. Hortic. Sci. 66, 583–591.

Lee, K.M., Driever, S.M., Heuvelink, Ep., Rüger S., Zimmermann, U., de Gelder, A., Marcelis, L.F.M., 2012. Evaluation of diel patterns of relative changes in cell turgor of tomato plants using leaf patch clamp pressure probes. Physiol Plant. 146, 439–447.

León, L., de la Rosa, R., Rallo, L., Guerrero, N. & Barranco, D., 2007. Influence of spacing on the initial production of hedgerow ‘Arbequina’ olive orchards. Span. J. Agric. Res. 5 (4), 554–558.

Marchi, S., Tognetti, R., Minocci, A., Borghi, M., Sebastiani, L., 2008. Variation in mesophyll anatomy and photosynthetic capacity during leaf development in a

deciduous mesophyte fruit tree (*Prunus persica*) and an evergreem sclerophyllous Mediterranean shrub (*Olea europaea*). Trees 22, 559–571.

Marino, G., Pernice, F., Marra, F.P., Caruso, T., 2016. Validation of an online system for the continuous monitoring of tree water status for sustainable irrigation managements in olive (*Olea europaea* L.). Agric. Water Manage. 177, 298–307.

Martinez, J.M., Muñoz, E., Alba, J., Lanzón, A., 1975. Report about the use of the "Abencor" analyzer. Grasas y Aceites 26, 379–385

Martínez-Gimeno, M.A., Castiella, M., Rüger, .S, Intrigliolo, D.S. & Ballester, C., 2017. Evaluating the usefulness of continuous leaf turgor pressure measurements for the assessment of Persimmon tree water status. Irrig. Sci. 35(2), 159–167.

Martín-Vertedor, A.I., Pérez Rodríguez, J.M., Prieto Losada, H., Fereres Castiel, E., 2011. Interactive responses to water deficits and crop load in olive (*Olea europaea* L., cv. Morisca) I. – Growth and water relations. Agric. Water Manage. 98, 941–949.

Matthews, M.A., Shackel, K.A., 2005. Growth and water transport in flexhy fruit. In: Holbrook, N.M., Zwieniecki, M.A. (Eds.), Vascular Transport in Plants. Elsevier, Boston, pp. 181–197.

McDowell, N., Pockman, W.T., Allen, C.D., Breshears, D.D., Cobb, N., Kolb, T., Plaut, J.,Sperry, J., West, A., Williams, D.G., 2008. Mechanisms of plant survival andmortality during drought: why do some plants survive while others succumbto drought? New Phytol. 178, 719–739.

Medrano, H., Perez-Peña, J., Prieto, J., Tomás, M., Franck, N., Escalona, J.M. 2016. Carbon balance in grapevine under a changing climate. In: Gerós, H., Chaves, M.M., Medrano, H., Delrot, S. Grapevine in a Changing Environment: A Molecular and Ecophysiological Perspective. John Wiley & Sons, Ltd.

Molden, D., Oweis, T., Steduto, P., Bindraban, P., Hanjra, M.A., and Kijne, J., 2010. Improving agricultural water productivity: Between optimism and caution. Agric. Water Manage. 97, 528–535.Moriana, A., Orgaz, F., Pastor, M., Fereres, E., 2003. Yield responses of a mature olive orchard to water deficits. J. Am. Soc. Hortic. Sci., 128 (3), 425–431.

Morales-Sillero, A., Jiménez, R., Fernández, J.E., Troncoso, G., Rejano, L., 2008. Effect of fertigation on the 'Manzanilla de Sevilla' table olive quality before and after "Spanish-style" green processing. Hortscience 43(1), 153–158.

Moriana, A., Girón, I.F., Martín-Palomo, M.J., Conejero, W., Ortuño, M.F., Torrecillas, A., Moreno, F., 2010. New approach for olive trees irrigation scheduling using trunk diameter sensors. Agric. Water Manage. 97, 1822–1828.

Moriana, A., Pérez-López, D., Prieto, M.H., Ramírez-Santa-Pau, M., Pérez-Rodríguez, J.M., 2012. Midday stem water potential as a useful tool for estimating irriagtion requirements in olive trees. Agric. Water Manage. 112, 43–54.

Naor, A., 2006. Irrigation scheduling and evaluation of tree water status in deciduous orchards. Hort Rev 32, 111–165.

Naor, A., Schneider, D., Ben-Gal, A., Zipori, I., Dag, A., Kerem, Z., Birger, R., Peres, M., Gal., Y., 2013. The effects of crop load and irrigation rate in the oil accumulation stage on oil yield and water relations of 'Koroneiki' olives. Irrig. Sci. 31, 781–791.

Orgaz F, Fereres E., 2001. Riego. In: Barranco D, Fernández–Escobar R, Rallo L (eds) El Cultivo del Olivo, 4th edn. Coedition. Mundi–Prensa and Junta de Andalucía, Madrid, pp 285–306

Ortuño, M.F., Conejero, W., Moreno, F., Moriana, A., Intrigliolo, D.S., Biel, C.A., Mellisho, C.A.D., Pérez-Pastor, A., Domingo, R., Ruiz-Sánchez, M.C.A., Casadesus, J., Bonany, J., Torrecillas, A., 2010. Could trunk diameter sensors be used in woody crops for irrigation scheduling? A review of current knowledge and future perspectives. Agric. Water Manage. 97, 1–11.

Padilla-Díaz, C.M., Rodriguez-Dominguez, C.M., Hernandez-Santana, V., Perez-Martin, A., Fernández, J.E., 2016. Scheduling regulated deficit irrigation in a hedgerow olive orchard from leaf turgor pressure related measurements. Agric. Water Manage. 164, 28–37.

Padilla-Díaz, C.M., Rodriguez-Dominguez, C.M., Hernandez-Santana, V., Perez-Martin, A., R.M.D., Fernandes, A., Montero, J.M., García, J.E., Fernández, 2018. Water status, gas exchange and crop performance in a super high density olive orchard under deficit irrigation scheduled from leaf turgor measurements. Agric. Water Manage. 202, 241–252.

Pastor, M., García-Vila, M., Soriano, M.A., Vega, V., Fereres, E., 2007-. Productivity of olive orchards in response to tree density. J. Hortic. Sci. Biotechnol. 82(4), 555–562.

Pérez-López, D., Moriana, A., Rapoport, H., Olmedilla, N., Ribas, F., 2008. New approach for using trunk growth rate and endocarp development in the irrigation scheduling of young olive orchards. Sci. Hortic. 115, 244–251.

Perez-Martin, A., Flexas, J., Ribas-Carbó, M., Bota, J., Tomás, M., Infante, J. M., Diaz-Espejo, A., 2009. Interactive effects of soil water deficit and air vapour pressure deficit on mesophyll conductance to CO_2 in *Vitis vinifera* and *Olea europaea*. J. Exp. Bot., 60 (8), 2391–2405.

Perry, C., 2011. Accounting for water use: Terminology and implications for saving water and increasing production. Agric. Water Manage. 98, 1840–1846.

Pinheiro J., Bates D., DebRoy S., Sarkar D., Team R.D.C., 2011. nlme: linear and nonlinear mixed effects models. R pack- age version 3.1–102. R Foundation for Statistical Computing, Vienna.

R Core Team 2017. R: A language and environment for statistical computing. R Foundation for Statistical Computing, Vienna, Austria. URL https://www.R-project.org/.

Rallo, L., Caruso, T., Díez, C.M., Campisi, G., 2016. Olive Growing in a Time of Change: From Empiricism to Genomics, In: E. Rugini et al. (Eds.), The Olive Tree Genome, Compendium of Plant Genomes. Springer, pp. 55–64.

Rallo, P., Rapoport, H.F., 2001. Early growth and development of the olive fruit mesocarp. J Hortic Sci Biotechnol 76, 408–412.

Ramos, A.F., Santos, F.L., 2009. Water use, transpiration, and crop coefficients for olives (cv. Cordovil), grown in orchards in Southern Portugal. Biosyst. Eng. 102, 321–333.

Rapoport, H.F., 2010. Botany and morphology. In: Barranco, D., Fernández-Escobar, R., Rallo, L. (Eds.), Olive Growing. RIRDC/AOA, Australia, pp. 33–57.

Rapoport, H.F., Costagli, G., Gucci, R., 2004. The effect of water deficit during earlyfruit development on olive fruit morphogenesis. J. Am. Soc. Hortic. Sci. 129,121–127.

Rapoport, H.F., Perez-Lopez, D., Hammami, S.B.M., Agüera, J., Moriana, A. 2013. Fruit pit hardening: physical measurement during olive fruit growth. Ann Appl Biol 163, 200–208

Rodriguez-Dominguez, C.M., Ehrenberger, W., Sann, C., Rüger, S., Sukhorukov, V., Martín-Palomo, M.J., Diaz-Espejo, A., Cuevas, M.V., Torres-Ruiz, J.M., Perez-Martin, A., Zimmermann, U., Fernández, J.E., 2012. Concomitant measurements of stem sap flow and leaf turgor pressure in olive trees using the leaf patch pressure probe. Agric. Water Manage. 114, 50–58.

Rosecrance, R.C., Krueger, W.H., Milliron, L., Bloese, J., Garcia, C., Mori, B., 2015. Moderate regulated deficit irrigation can increase olive oil yields and decrease tree growth in super high density 'Arbequina' olive orchards. Sci. Hortic. 190, 75–82.

Rousseaux, M.C., Figuerola, P.I., Correa-Tedesco, G., Searles, P.S., 2009. Seasonal variations in sap flow and soil evaporation in an olive (*Olea europaea* L.) grove under two irrigation regimes in an arid region of Argentina. Agric. Water Manage. 96, 1037–1044.

Rüger, S., Ehrenberger, W., Arend, M., Geßner, P., Zimmermann, G., Zimmermann, D., Bentrup, F.W., Nadler, A., Raveh, E., Sukhorukov, V.L., Zimmermann, U., 2010. Comparative monitoring of temporal and spatial changes in tree water status using the non-invasive leaf patch clamp pressure probe and the pressure bomb. Agric. Water Manage. 98, 232–290.

Ruiz-Sanchez, M.C., Domingo, R., Castel, J.R. 2010. Review. Deficit irrigation in fruit trees and vines in Spain. Span. J. Agric. Res. 8, S5–S20.

Sack, L., Pasquet-Kok, J., PrometheusWiki contributors. 2011. Leaf pressure-volume curve parameters. URL http://prometheuswiki.org/tiki-index.php?page=Leaf+pressure-volume+curve+parameters.

Sanzani, S.M., Schena, L., Nigro, F., Sergeeva, V., Ippolito, A., Salerno, M.G., 2012. Abiotic diseases of olive. J. Plant Pathol. 94(3), 469–491.

Sanz-Cortés, F., Martínez-Calvo, J., Badenes, M.L., Bleiholder, H., Hack, H., Llácer, G., Meier, U. 2002. Phenological growth stages of olive trees (*Olea europaea*). Ann. Appl. Biol. 140, 151–157.

Schneider, C.A., Rasband, W.S., Eliceiri, K.W., 2012. NIH Image to ImageJ: 25 years of image analysis. Nat. Methods 9(7), 671–675.

Schiermeier Q. 2010. The real holes in climate science. *Nature* 463: 284–287.

Seelig, H.D., Stoner, R.J., Linden, J.C., 2012. Irrigation control of cowpea plants using the measurement of leaf thickness under greenhouse conditions. Irrig Sci 30(4), 247–257.

Sharon, Y., Bravdo, B., 2001 A Fully–Automated Orchard Irrigation System Based on Continuous Monitoring of Turgor Potential with a Leaf Sensor. Acta Hort. 562, 55–61.

Sussmilch FC, Brodribb TJ, McAdam SAM. 2017. What are the evolutionary origins of stomatal responses to abscisic acid in land plants? *Journal of Integrative Plant Biology* 59: 240–260.

Sperry, J.S., Tyree, M.T., 1988. Mechanism of water stress-induced xylemembolism. Plant Physiol. 88, 581–587.

Stitt, M., Zeeman, S.C., 2012. Starch turnover: pathways, regulation and role in growth. Curr. Opin. Plant Biol., 15(3), 282–292.

Syvertsen, J.P., Albrigo, L.G., 1980. Seasonal and diurnal Citrus leaf and fruit water relations. Botanical Gazette 141, 440–446.

Torres-Ruiz, J.M., Diaz-Espejo, A., Morales-Sillero, A., Martín-Palomo, M.J., Mayr, S., Beikircher, B., Fernández, J.E., 2013. Shoot hydraulic characteristics, plant water status and stomatal response in olive trees under different soil water conditions. Plant Soil 373, 77–87.

Velez, J.E., Intrigliolo, D.S., Castel, J.R., 2007. Scheduling deficit irrigation of citrus trees with maximum daily trunk shrinkage. Agric. Water Manage. 90, 197–204.

Vossen, P.M., Connell, J.H., Klonsky, K.M., Livingston, P., 2004. Sample costs to establish a super-high- density olive orchard and productive olive oil – Sacramento Valley. University of California, Cooperative extension. Department of Agricultural and Resource Economics. Davis, CA

Vossen, P.M., Connell, J.H., Klonsky, K.M., Livingston, P., 2004. Sample Costs toEstablish a Super-High- Density Olive Orchard and Productive OliveOil—Sacramento Valley. University of California, Cooperative extension. Department of Agricultural and Resource Economics. Davis, CA.

Wood, S. N. (2006). Generalized Additive Models: An Introduction with R. Chapman and Hall/CRC.

Wood, S.N. (2013a) On p-values for smooth components of an extended generalized additive model. Biometrika 100:221-228.

Wood, S.N. (2013b) A simple test for random effects in regression models. Biometrika 100:1005-1010.

Zarco-Tejada, P.J., Berni, J.A.J., Suárez, L., Sepulcre-Cantó, G., Morales, F., Miller, J.R., 2009. Imaging chlorophyll fluorescence with an airborne narrow-band multispectral camera for vegetation stress detection. Remote Sens. Environ. 113, 1262–1275.

Zeileis, A., Grothendieck, G. 2005. zoo: S3 Infrastructure for Regular and Irregular Time Series. Journal of Statistical Software, 14(6), 1–27. doi:10.18637/jss.v014.i06

Zimmerman, D., Reuss, R., Westhoff, M., Geßner, P., Bauer, W., Bamberg, E., Bentrup, F-W., Zimmermann, U., 2008. A novel, non-invasive, online-monitoring, versatile and easy plant-based probe for measuring leaf water status. J. Exp. Bot. 59, 3157–3167.

Zimmermann, U., Bitter, R., Ribeiro Marchiori, P.E., Rüger. S., Ehrenberger, W., Sukhorukov, V.L., Schüttler, A., Ribeiro, R.F., 2013. A non-invasive plant-based

probe for continuous monitoring of water stress in real time: a new tool for irrigation scheduling and deeper insight into drought and salinity stress physiology. Theor. Exper. Plant Physiol. 25, 3–12.

Zohary D, Hopf M, Weiss E. 2012. Domestication of Plants in the Old World: The origin and spread of domesticated plants in Southwest Asia, Europe, and the Mediterranean Basin. Oxford University Press on Demand.

Cover design
Diseño de la portada
Sandra Sánchez
662023095

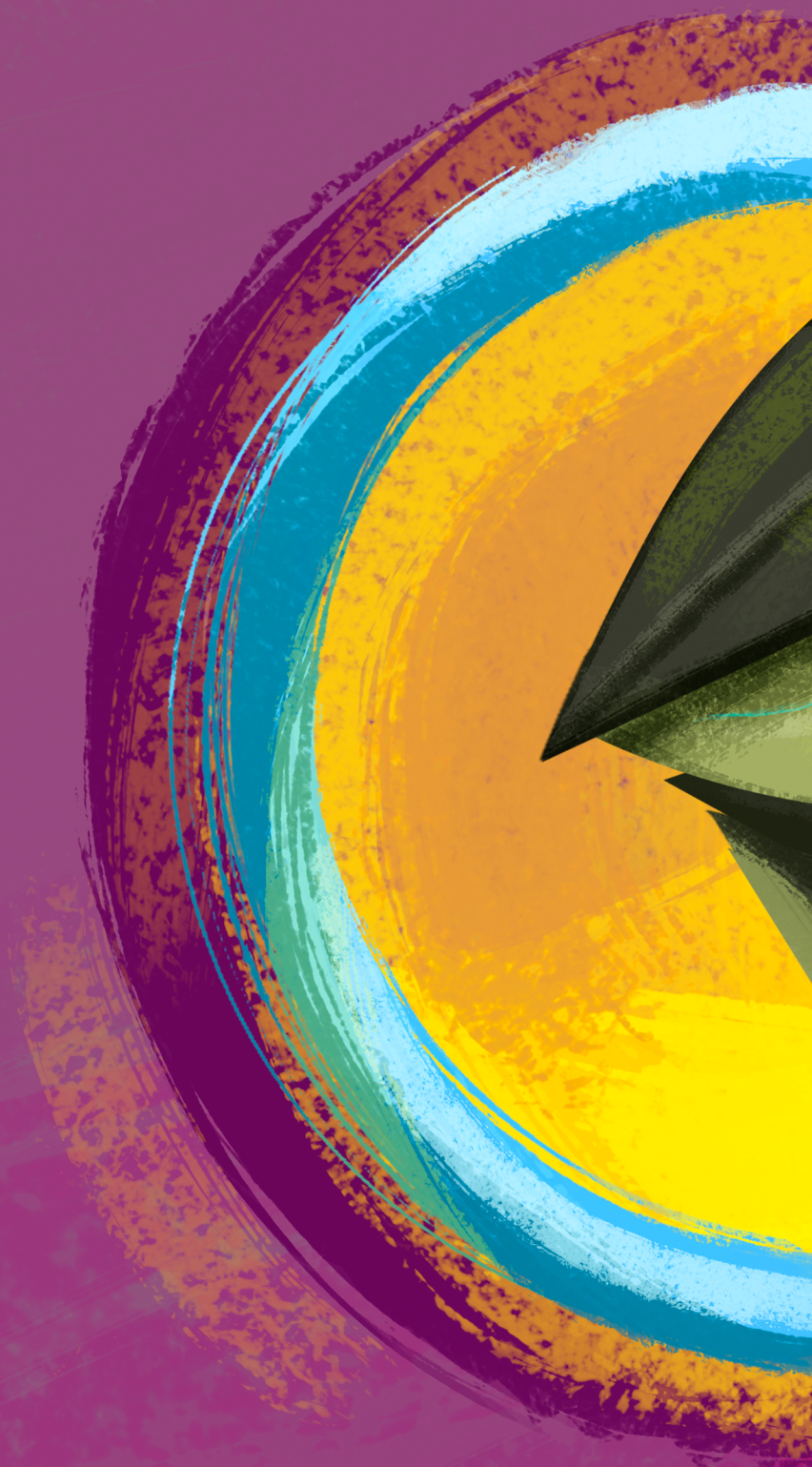

IRNAS

CSIC

UNIVERSIDAD DE SEVILLA